SCE-9001

SOUTHERN CALIFORNIA EDISON COMPANY

PWR REACTOR PHYSICS METHODOLOGY

USING

CASMO-3/SIMULATE-3

SEPTEMBER 1990

SCE-9001

SOUTHERN CALIFORNIA EDISON COMPANY

PWR REACTOR PHYSICS METHODOLOGY

USING

CASMO-3/SIMULATE-3

September 1990

Prepared By: R Y Chang 9/13/90
R. Y. Chang, Senior Engineer (Date)
Nuclear Fuel Analysis

Prepared By: CW Gabel 9/13/90
C. W. Gabel, Engineer (Date)
Nuclear Fuel Analysis

Approved By: OJ Thomsen 9/14/90
O. J. Thomsen, Supervisor (Date)
Nuclear Fuel Analysis

Approved By: PD Myers 9/19/90
P. D. Myers, Manager (Date)
Nuclear Fuel

Approved By: D.F. Pilmer 9/14/90
D. F. Pilmer, Consulting Engineer (Date)
Nuclear Engineering and Construction

Approved By: A. Evinay 9/14/90
A. Evinay (Date)
Nuclear Engineering Analysis

Approved By: Scott C Swoope 9-13-90
S. C. Swoope (Date)
Reactor Engineering, Station Technical

Southern California Edison Company
Nuclear Engineering Safety and Licensing
23 Parker Street
Irvine, California 92718

DISCLAIMER

This document was prepared by Southern California Edison Company for its own use. The use of information contained in this document by anyone other than Southern California Edison Company is not authorized, and in regard to unauthorized use neither Southern California Edison Company or any of its officers, directors, agents, or employees assumes any obligation, responsibility or liability, or makes any warranty or representation, with respect to the contents of this document, or its accuracy or completeness.

ABSTRACT

This report documents the validation and level of accuracy of the reactor core physics methodology used by Southern California Edison Company to perform steady-state analyses for Pressurized Water Reactors (PWR). The methodology is based on the CASMO-3/SIMULATE-3 computer program package. This methodology has been validated by an in-house benchmarking effort of CASMO-3/SIMULATE-3 predictions with measured data from power reactors and critical experiments. Based on the results from this benchmarking effort, a set of 95/95 tolerance limits has been calculated. Southern California Edison Company intends to use this methodology to perform PWR calculations including reload design, input to safety analyses, startup predictions, core physics databooks, and, reactor protection system and monitoring system setpoint updates.

TABLE OF CONTENTS

TABLE OF CONTENTS (continued)

LIST OF TABLES

LIST OF TABLES

LIST OF TABLES

LIST OF FIGURES

LIST OF FIGURES

ACKNOWLEDGEMENTS

The authors wish to acknowledge the individuals who assisted in the development of the CASMO-3/SIMULATE-3 PWR methodology. Many different people within Southern California Edison Company assisted. In particular, we would like to acknowledge D. Bose-Roy, P. Brashear, J. Judd, B. Park, S. Wu, and O. Thomsen. From the San Onofre Nuclear Generating Station engineering staff we thank A. Eckhart, D. Ramendick, S. Swoope, and M. McDevitt for conducting the startup testing and core surveillance programs which provided the physics data used in this benchmarking.

SECTION 1

INTRODUCTION, OVERVIEW, AND SUMMARY

1.0 INTRODUCTION

This report describes Southern California Edison (SCE) Company's reactor core physics methodology for Pressurized Water Reactor (PWR) analyses using the CASMO-3/SIMULATE-3 computer program package (References 1 through 6). Studsvik AB and Studsvik of America developed the CASMO-3/SIMULATE-3 computer program package. This package is widely accepted within the nuclear industry.

Yankee Atomic Electric Company (YAEC) provided the theoretical basis and validation of this computer program package to the NRC (References 7 and 8). In these reports YAEC provided detailed descriptions of the computer programs and a general methodology for performing reactor physics analyses.

The objective of this report is to demonstrate SCE's ability to use the CASMO-3/SIMULATE-3 computer program package. The report also documents the uncertainty factors determined through the benchmarking of key PWR physics parameters, presented in Table 1.1, with plant measurements.

1.1 OVERVIEW

The data demonstrating the applicability of SCE's methodology for PWR core physics analyses are documented in Sections 2 through 7 of this report.

Section 2, Description of Methodology, presents a brief description of the CASMO-3/SIMULATE-3 computer program package.

Section 3, Description of Reactors Used in the Benchmarking, describes the PWRs used in the benchmarks.

Section 4, Benchmark Comparisons, details the benchmarking of the key PWR core physics parameters listed in Table 1.1. For each parameter, the calculated data were compared with plant measurements, the sample mean and standard deviation were quantified, and a 95/95 tolerance limit (bias ± reliability factor) determined.

Section 5, Pin Peaking Factor Uncertainties, presents the derivation of the pin peaking factor 95/95 tolerance limits.

Section 6, Conclusions, presents the conclusions of this report and the range of applications for which SCE will use this methodology.

Section 7, References, presents documents referenced in this report.

1.2 SUMMARY

Table 1.2 summarizes the 95/95 tolerance limits calculated in Sections 4 and 5. The tolerance limits are such that, when applied to the CASMO-3/SIMULATE-3 results, there is a 95 percent probability, with a 95 percent confidence that the calculated values will conservatively bound the "true" values.

SCE concludes that this methodology is acceptable for the performance of all steady-state PWR core physics analyses including:

- Reload design,
- Safety analyses input,
- Startup predictions,
- Core physics databooks, and
- Reactor protection and monitoring system updates.

Table 1.1

List of Key PWR Physics Parameters

- Core Reactivity
  - Zero Power
  - Full Power
- Inverse Boron Worth
- Power Coefficient
- Isothermal Temperature Coefficient
- Control Rod Worth
- Axial Offset
- Assembly Power Peaking
  - F^s_Q
  - F^s_{XY}
  - F^s_R, $F^S_{\Delta H}$
- Pin Peaking
  - F_Q
  - F_{XY}
  - F_R, $F_{\Delta H}$

Table 1.2

List of 95/95 Tolerance Limits (Bias ± Reliability Factors)

Parameter		Bias	Reliability Factor	Units*
Core Reactivity (%Δk/k)				
Zero Power		-0.08	0.26	Absolute
Full Power		0.01	0.35	Absolute
Critical Boron (PPM)				
Zero Power		-7	26	Absolute
Full Power		2	34	Absolute
Inverse Boron Worth (PPM/%ΔK/K)		0.0	10%	Relative
Power Coefficient ($10^{-4}\Delta K/K/\%P$)		0.0	0.20	Absolute
Isothermal Temperature Coefficient ($10^{-4}\Delta K/K/^\circ F$)		0.05	0.24	Absolute
Control Rod Worth (%Δk/k)		1.2%	8.2%	Relative
Local Pin Power		0.0	2%	Relative
Axial Offset		-0.003	0.014	Absolute
Assembly Peaking	F_Q^s	0.0	4.17%	Relative
	F_{XY}^s	0.0	4.80%	Relative
	F_R^s	0.0	3.34%	Relative
Pin Peaking	F_Q	0.0	4.62%	Relative
	F_{XY}	0.0	5.20%	Relative
	F_R, $F_{\Delta H}$	0.0	3.89%	Relative

*For those parameters with differences expressed in relative units:

Predicted = Calculated * (1 - Bias ± Reliability Factor)

For parameters with differences in absolute units, the following equation applies:

Predicted = Calculated - Bias ± Reliability Factor

SECTION 2

DESCRIPTION OF METHODOLOGY

2.0 INTRODUCTION

This section provides a brief description of the CASMO-3/SIMULATE-3 methodology. Yankee Atomic Electric Company (YAEC) has already presented the theoretical bases and validation of CASMO-3 and SIMULATE-3 before the Nuclear Regulatory Commission (NRC). The computer program package has received NRC approval for use in core physics calculations (References 21 and 22).

2.1 COMPUTER PROGRAM DESCRIPTIONS

The CASMO-3/SIMULATE-3 computer program package (References 1 through 6) was developed by STUDSVIK AB, Nykoping, Sweden and their American subsidiary STUDSVIK OF AMERICA, Newton, Massachusetts. The computer program package consists of five computer programs:

- CASMO-3,
- CASLIB,
- MICBURN-3,
- MOVEROD-3, and,
- SIMULATE-3.

In addition, the Electric Power Research Institute's (EPRI) ESCORE computer program (Reference 9) was incorporated into the program sequence. The computer program sequence flow chart is shown in Figure 2.1.

These computer programs are briefly described below. Detailed information--theory, user manual, etc.--can be found in the referenced documents.

ESCORE

ESCORE (Reference 9) is a computer program for predicting best-estimate, steady-state fuel performance data for light water reactor fuel rods. This computer program has received NRC approval for use in calculating fuel rod temperatures for input to design and safety analyses (Reference 23). SCE uses this computer program to calculate the fuel temperature of the average rod as a function of burnup. Output from this computer program provides the burnup independent fuel pin temperature for use in

CASMO-3, and a burnup dependent fuel pin temperature for the SIMULATE-3 model.

CASMO-3

CASMO-3 is a multigroup, two-dimensional transport theory computer program (Reference 1). This computer program models cylindrical fuel rods of varying composition in a square pitch array. CASMO-3 can model fuel rods, fuel rods with integral burnable absorber, burnable absorber rods, control rods, guide tubes, in-core instruments, and water gaps.

CASMO-3 generates all cross-section data for SIMULATE-3. SCE uses CASMO-3 in a single assembly format with reflective boundary conditions. A 40-energy group cross-section library is used.

CASLIB

CASLIB (Reference 2) produces a binary neutron cross-section library for input to CASMO-3 from a card-image, formatted library. The card-image, formatted library, supplied with CASMO-3 from STUDSVIK, is based mainly on data from ENDF/B-IV with an update from ENDF/B-V and other sources. Both forty- and seventy-group cross-section data are available for nearly 100 materials.

MICBURN-3

MICBURN-3 (Reference 3) calculates the microscopic burnup in a fuel rod containing an initially homogeneously distributed strong burnable absorber such as gadolinia. It generates effective cross-sections as a function of the absorber number density to be used in CASMO-3.

MOVEROD-3

MOVEROD-3 (Reference 4) is a file editing program that creates a new CASMO-3 restart file from existing files by selecting and rearranging data for specified fuel pins. The new restart file can then be used for continued CASMO-3 calculations on a reconstituted fuel assembly.

TABLES-3

TABLES-3 (Reference 5) is a data processing program that links CASMO-3 to SIMULATE-3. The program processes the following types of data from CASMO-3:

- two-group cross-sections,
- discontinuity factors,

- fission product data,
- in-core instrument response data,
- pin power reconstruction data, and
- kinetics data.

TABLES-3 reads the CASMO-3 card image files and produces a master binary cross-section library for SIMULATE-3.

SIMULATE-3

SIMULATE-3 is a two- or three-dimensional (2-D or 3-D), two-group coarse mesh diffusion theory reactor simulator program (Reference 6). The program explicitly models the baffle/reflector region, eliminating the need to normalize to higher-order fine mesh calculations such as PDQ. Homogenized cross-sections and discontinuity factors are applied to the coarse mesh nodal model to solve the two-group diffusion equation using the QPANDA neutronics model. QPANDA employs fourth order polynomial representations of the intra-nodal flux distributions in both the fast and thermal groups.

The nodal thermal hydraulic properties are calculated based on the inlet temperature, RCS pressure, coolant mass flow rate, and the heat addition along the channels.

The pin-by-pin power distributions, on a 2-D or 3-D basis, are constructed from the inter- and intra-assembly information from the coarse mesh solution and the pin-wise assembly power distribution from CASMO-3.

The SIMULATE-3 program performs a macroscopic depletion. Individual Uranium, Plutonium, and lumped fission product isotope concentrations are not computed. However, microscopic depletion of Iodine, Xenon, Promethium, and Samarium is included to model typical reactor transients.

2.2 MODEL DESCRIPTIONS

CASMO-3 FUEL ASSEMBLY AND REFLECTOR MODELS

Each unique PWR fuel assembly type (defined by geometry, enrichment, and burnable poison pins) is separately modeled in CASMO-3 using octant symmetry. Enrichment zoning among fuel pins, burnable poison pins, and guide tubes are explicitly modeled. The water gap between assemblies in the reactor core is included in the CASMO-3 model. The spacer grids are also included. Design bases documents such as the updated Final Safety Analysis Report (FSAR), reload reports, and as-built drawings provide the necessary data to develop the CASMO-3 assembly models.

Three depletion cases are needed to generate each fuel assembly type's average cross-section data. First, the fuel assembly is depleted at hot full power, reactor average conditions. Moderator temperature, fuel temperature, and soluble boron concentration are set to constant average values for the complete depletion. The average fuel temperature at hot full power conditions is calculated with EPRI's ESCORE computer program (Reference 9). Next, the fuel assembly is depleted at a low moderator temperature, a few degrees below hot zero power conditions. However, the fuel temperature and the soluble boron concentration are kept at the constant hot full power, reactor average values. Last, the fuel assembly is again depleted at constant hot full power, reactor average conditions, but with a constant soluble boron concentration higher than is usually seen in normal operation. Restart files are saved from all three depletions. Each fuel assembly type is depleted to greater than 50 GWD/T assembly average burnup using the CASMO-3 default depletion steps.

Branch cases are performed to calculate instantaneous effects. Instantaneous effects are individually calculated and added together later to recreate the proper fuel assembly cross sections. The branch cases are executed from the hot full power, reactor average conditions restart file at typically 0, 5, 10, 20, 30, 40, and 50 GWD/T. Branch cases are run for off-normal moderator temperatures, fuel temperatures, soluble boron concentrations, and control rod insertions.

CASMO-3 also generates top, bottom, and radial reflector cross sections. The radial reflector consists of the stainless steel core baffle followed by about 15 centimeters (cm) of water. The top reflector extends from the top of the active fuel to the lower surface of the fuel assembly upper end fitting. The bottom reflector extends from the bottom of the active fuel to the lower surface of the core support plate. Reflector cross-sections are modeled as a function of soluble boron concentration and moderator temperature.

<u>TABLES-3 MODEL</u>

The TABLES-3 program generates two-dimensional reactor and cycle specific cross-section tables for SIMULATE-3. Data from the following CASMO-3 card image files are combined into binary cross-section libraries for input to SIMULATE-3:

- HFP Reactor Average Depletion + Branches,
  - Fuel Temperature Branches

- Moderator Temperature Branches
- Soluble Boron Concentration Branches
- Control Rod Insertion Branches

• Low Moderator Temperature Depletion,

• HFP High Soluble Boron Concentration Depletion,

• Bottom Reflector Data,

• Radial Reflector Data, and

• Top Reflector Data.

SIMULATE-3 MODEL

The SIMULATE-3 model divides the active fuel region into 20 axial and four radial nodes per assembly. A pseudo-assembly, consisting of reflector material, surrounds the core and is divided into one radial and 20 axial nodes. Axially, the fuel is divided into a single bottom reflector node, 20 nodes for the active fuel region, and a single top reflector node.

Additional model input data are the:

• Full core assembly serial number map,

• Quarter core fuel assembly type map,

• Fuel assembly axial zone definition, including reflectors,

• Asymmetric (radially) fuel assembly node definition,

• Control rod locations,

• Grouping of control rods into banks,

• Axial zone definitions for control rods, especially part length rods,

• In-core instrumentation locations,

• Fuel temperature versus power level and burnup correlation (ESCORE program),

• Core MW-thermal output at 100% power,

• Core pressure, power density, and coolant mass flow rate at 100% power conditions,

- Coolant inlet temperature versus power level,
- Input Restart files, and
- Output Restart file.

After the cycle base model is set up, the user can specify the percent power level, rod bank positions (percent withdrawn), output and edit options, and the type of calculation: depletion, xenon transient, coefficient calculation (e.g., ITC, IBW, FTC, etc).

Figure 2.1

Program Sequence Flow Chart

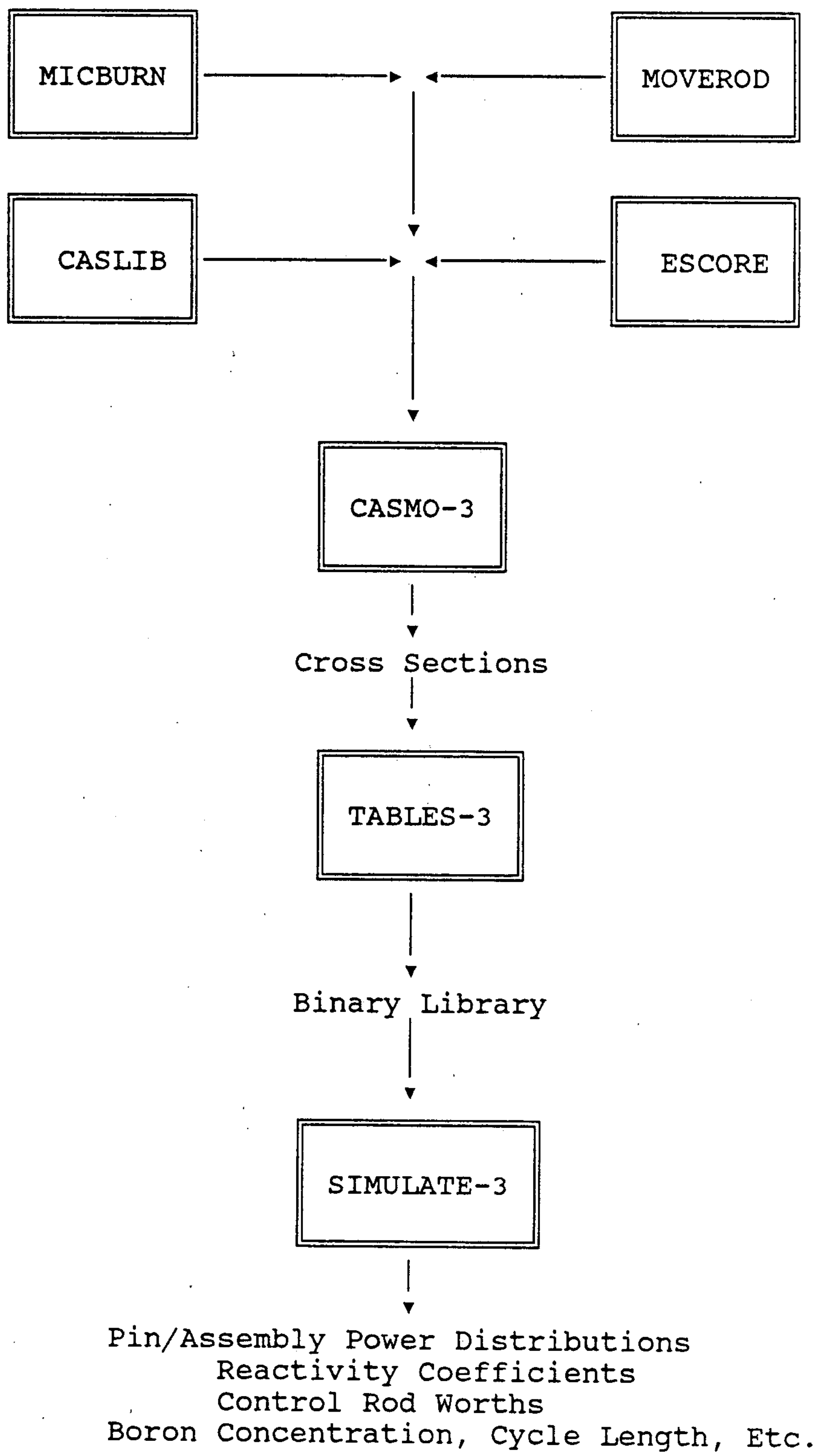

SECTION 3

DESCRIPTION OF THE REACTORS USED IN THE BENCHMARKING

3.0 INTRODUCTION

This report compares the CASMO-3/SIMULATE-3 predictions of key physics parameters against measured plant data. Data from four different reactor plants were used. The measurements were obtained during plant startup and normal operation. The reactor plants are:

- San Onofre Nuclear Generating Station Unit 1,
- San Onofre Nuclear Generating Station Unit 2,
- San Onofre Nuclear Generating Station Unit 3, and
- Arkansas Nuclear One - Unit 2.

The following sections provide brief descriptions of these reactor cores. Detailed information can be found in References 10, 11, and 12.

3.1 SAN ONOFRE NUCLEAR GENERATING STATION UNIT 1 (SONGS 1)

SONGS 1 is a commercial nuclear power plant. The unit began commercial operation in 1968 and has completed 10 cycles of operation. The plant is a Westinghouse three-loop PWR. The reactor core produces 1347 megawatts-thermal at 100% rated power.

The reactor core consists of 157 fuel assemblies arranged as shown in Figure 3.1. Both conventional and low leakage fuel management patterns have been used. Each fuel assembly consists of a 14 x 14 array of 180 fuel rods and 16 control rod guide thimbles. The fuel assembly cross-section is shown in Figure 3.2. Core, fuel assembly, and control rod data are summarized in Table 3.1.

The fuel rods consist of slightly enriched (3.15 to 4.0 weight percent U-235) uranium dioxide (UO_2) pellets with stainless steel cladding. The control rod guide thimbles are also stainless steel. Seven Inconel-718 grids are located along the length of the assembly.

The in-core instrumentation system for power distribution measurement consists of two moveable fission chambers. These instruments can be inserted into 30 core locations. The detector's neutron flux signal is processed off-line with the Westinghouse INCORE3 program (Reference 13). The 30 instrumented core locations are shown in Figure 3.3.

There are 45 full-length control rods, called rod cluster control assemblies (RCCA's). Each RCCA consists of 16 individual absorber rods fastened to a common hub. The RCCA's are not zoned. The single absorber material is Silver-Indium-Cadmium in stainless steel tubes. The RCCA's are moved in four symmetrically located banks. Banks #2 and #1 are called the Control Banks, and they are moved to control the reactor over the power range. The remaining RCCA's are called Shutdown Banks #1 and #2. Figure 3.1 shows the RCCA's locations.

The SONGS 1 reactor has two unique features which were modeled with CASMO-3/SIMULATE-3. The first unique feature modeled was the stainless steel fuel rod cladding. Most PWR cores use zircaloy cladding. The second unique feature was the use of mixed oxide (PuO_2 - UO_2) assemblies. In Cycles 2 and 3, four Edison Electric Institute (EEI) mixed oxide (PuO_2 - UO_2) demonstration assemblies were irradiated.

3.2 SAN ONOFRE NUCLEAR GENERATING STATION UNITS 2&3 (SONGS 2&3)

SONGS 2&3 are commercial nuclear power plants. SONGS 2 began commercial operation in 1983. SONGS 3 began commercial operation in 1984. Both units are in their fifth cycle of operation. SONGS 2&3 are Combustion Engineering two-loop PWRs. Each unit produces 3390 megawatts-thermal at 100% rated power.

Each reactor core consists of 217 fuel assemblies arranged as shown in Figure 3.4. Both conventional and low leakage fuel management patterns have been used. Each fuel assembly consists of a 16 x 16 array of 236 fuel/burnable absorber rods and 5 control rod guide tubes. A typical fuel assembly cross-section is shown in Figure 3.5. Core, fuel assembly, control rod, and burnable absorber data are summarized in Table 3.2.

The fuel rods consist of slightly enriched (1.87 to 4.05 weight percent U-235) UO_2 pellets clad in Zircaloy-4. The control rod guide tubes are also Zircaloy-4. Ten Zircaloy-4 grids and one Inconel-718 grid are located along the length of the assembly.

The in-core instrumentation system for power distribution measurement consists of 56 strings of fixed Rhodium detectors. Each detector string consists of five individual, 40 cm long, Rhodium detectors placed at about 10, 30, 50, 70, and 90 percent of active core height. The detector signals are processed off-line with the Combustion Engineering CECOR program (Reference 14) to determine the power distribution in the core. The 56 instrumented core locations are shown in Figure 3.6.

There are 83 full-length and eight part-length (PL) control rods, called control element assemblies (CEA's). Seventy-nine full-length CEA's have five identical individual absorber rods consisting of 1-1/8" Inconel nose cap, 12-1/2" Ag/In/Cd, and 136" of B_4C pellets. Four full-length CEA's located on the periphery of the core have four identical individual absorber rods consisting of 8-5/8" Inconel nose cap, 5" Ag/In/Cd, and 135-1/2" of B_4C pellets. The eight PLCEA's each have five identical absorber rods consisting of 75" of Inconel, 58" of water filled Inconel tube, and 16" of B_4C pellets. The cladding material is Inconel-625. The CEA's are moved in nine symmetrical groups: Regulating Groups 1 through 6, PLCEA, and Shutdown Groups A and B. Figure 3.4 shows the CEA locations.

Burnable absorber rods, consisting of B_4C-Al_2O_3 pellets in Zircaloy-4 cladding, were used in all cycles for both units. The burnable absorber rods have the same outer dimension as fuel rods and replace fuel rods when used.

The SONGS 2&3 reactors have several unique features. The outermost row of four assemblies does not line up with the next interior row of assemblies. The four-finger CEA inserted in the middle pair of these "off-set" assemblies has two fingers in one assembly and two fingers in the adjacent assembly. The burnable absorber rods in SONGS 2&3 do not extend the full length of the active fuel region and result in axially zoned fuel assemblies. Both units have been transitioned to 24-month fuel cycles with Cycle 5 being the second such cycle for each unit. Finally, the five control rod guide tubes per fuel assembly are large compared to Westinghouse and Babcock & Wilcox designs and displace four fuel rods each.

3.3 ARKANSAS NUCLEAR ONE - UNIT 2 (ANO-2)

ANO-2 is a commercial nuclear power plant operated by the Arkansas Power And Light Company. ANO-2 began commercial operation in 1980, and only data from the first cycle of operation are used in this report. The plant is a Combustion Engineering two-loop PWR. The reactor core produces 2815 megawatts - thermal at 100% rated power.

The reactor core consists of 177 fuel assemblies arranged as shown in Figure 3.7. Each fuel assembly consists of a 16 x 16 array of 236 fuel/burnable poison rods and five control rod guide tubes. A typical fuel assembly cross-section is shown in Figure 3.8. Core, fuel assembly, control rod, and burnable absorber data are summarized in Table 3.3.

The fuel rods consist of slightly enriched (1.93 to 2.94 weight percent U-235 in Cycle 1) UO_2 pellets with Zircaloy-4 cladding. The control rod guide tubes are also Zircaloy-4. Eleven Zircaloy-4 grids and one Inconel-625 grid are located along the length of the assembly.

The in-core instrumentation system for power distribution measurement consists of 44 strings of fixed Rhodium detectors. Each detector string consists of five individual, 40 cm long, Rhodium detectors placed at about 10, 30, 50, 70, and 90 percent of active core height. The detector signals are processed off-line with the CECOR program (Reference 14). The 44 instrumented core locations are shown in Figure 3.9.

There are 73 full-length and eight part-length (PL) control rods, called control element assemblies (CEA's). The full-length CEA's have dissimilar absorber rods. The four corner rods consist of an Inconel nose cap, 12-1/2" of Ag/In/Cd, and 135-1/2" of B_4C pellets. The center absorber rod uses solid Inconel plugs instead of Ag/In/Cd. The eight PLCEA's each have five identical absorber rods consisting of 75" of Inconel, 58" of water filled Inconel tube, and 16" of B_4C pellets. The cladding material is Inconel-625. The CEAs are moved in nine symmetrical groups: Regulating Groups 1 through 6, PLCEA, and Shutdown Groups A and B. Figure 3.7 shows the CEA locations.

Burnable absorber rods, consisting of $B_4C-Al_2O_3$ pellets in Zircaloy-4 cladding, are used. The burnable absorber rods have the same outer dimension as fuel rods and replace fuel rods when used.

Cycle 1 of ANO-2 has some unique features. The burnable absorber rods within some fuel assembly types are asymmetrically distributed (See Figure 3.9). Also the burnable absorber rods do not extend the full length of the active fuel region and result in axially zoned fuel assemblies. Finally, the five control rod guide tubes per fuel assembly are large compared to Westinghouse and Babcock & Wilcox designs and displace four fuel rods each.

Table 3.1

MECHANICAL DESIGN PARAMETERS

SONGS 1

Core description	
Power Level	1347 Megawatts-Thermal
Number of Assemblies	157
Number of Control Rods	45
Fuel Assembly Pitch	7.803 inches
Core area	67.1 Square Feet
Core Equivalent Diameter	110.9 inches
Fuel Assembly Description	
Fuel Rod Array	14 x 14
Fuel Rod Pitch	0.556 inches
Outside Dimension	7.76 inches
Number of Guide Tubes	16
Guide Tube I.D.	0.535 inches
Guide Tube O.D.	0.511 inches
Guide Tube Material	Stainless Steel
Fuel Rod Description	
Material	UO_2
Pellet % t.d. of 10.96 g/cm^3	95 nominal
Pellet Diameter	0.3835 inches
Clad Material	Stainless Steel
Clad I.D.	0.389 inches
Clad O.D.	0.422 inches
Clad Thickness	0.0165 inches
Active Fuel Length	120 inches
Full Length Control Rod	
Number	45 (16-Finger)
Clad Material	Stainless Steel
Clad Thickness	0.0185 inches
Clad O.D.	0.4315 inches
Absorber	
Material	Ag-In-Cd
Diameter	0.3905 inches
Length	133 inches

Table 3.1 (continued)

<u>EEI* Mixed Oxide Assemblies</u>	
Number of Assemblies	4
Fuel Rod Array	14 x 14
Outside Dimension	7.76 inches
Rod pitch	0.556 inches
Number of Guide Tubes	16
Guide Tube Material	Stainless Steel
<u>EEI Mixed Oxide Fuel Rods</u>	
Clad Material	Zircaloy-4
Outside Diameter	0.422 inches
Diametral Gap	0.0075 inches
Clad Thickness	0.0243 inches
Fuel Length	119.4 inches
<u>EEI Mixed Oxide Fuel Pellets</u>	
Diameter	0.3659 inches
Length	0.600 inches
Material	PuO_2 - UO_2
Density, % T. D.	91
Enrichment (w/o fissile Pu)	2.84 / 3.10 / 3.31
Pu Isotopics	
a/o Pu-239	80.6
a/o Pu-240	13.4
a/o Pu-241	5.2
a/o Pu-242	0.8

*EEI: Edison Electric Institute.

Table 3.2

MECHANICAL DESIGN PARAMETERS

SONGS 2&3

Core description	
Power Level	3390 Megawatts-Thermal
Number of Assemblies	217
Number of Control Rods	91
Fuel Assembly Pitch	8.180 inches
Core area	101.1 Square Feet
Core Equivalent Diameter	136 inches
Fuel Assembly Description	
Fuel Rod Array	16 x 16
Fuel Rod Pitch	0.506 inches
Outside Dimension	7.972 inches
Number of Guide Tubes	5
Guide Tube I.D.	0.90 inches
Guide Tube O.D.	0.98 inches
Guide Tube Material	Zircaloy-4
Fuel Rod Description	
Material	UO_2
Stack Height Density	10.061 g/cm^3
Pellet Diameter	0.325 inches
Clad Material	Zircaloy-4
Clad I.D.	0.332 inches
Clad O.D.	0.382 inches
Clad Thickness	0.025 inches
Active Fuel Length	150 inches
Full-Length Control Rod	
Number	83
5-Finger	79
4-Finger	4
Clad Material	Inconel-625
Clad Thickness	0.035 inches
Clad O.D.	0.816 inches
Poison	
Material	B_4C / Ag-In-Cd /Inconel
Length	
5-Finger	136" 12.5" 0.6"
4-Finger	135.5" 5.0" 8.6"

TABLE 3.2 (continued)

Full-Length Control Rod (continued)

B_4C pellet	
Diameter	0.737 inches
% T. D. of 2.52 g/cm^3	73
Weight % Boron, Min	77.5

Part Length Control Rod

Number	8 (5-Fingers)
Clad Material	Inconel-625
Clad Thickness	0.035 inches
Clad O.D.	0.816 inches
Poison	
Material	Inconel / WATER / B_4C
Length	75 " 58" 16"
B_4C pellet	
Diameter	0.737 inches
% T. D. of 2.52 g/cm^3	73
Weight % Boron, Min	77.5

Burnable Poison Rod

Absorber Material	Al_2O_3 - B_4C
Pellet Diameter	0.307 inches
Pellet Length	1.0 inches
Pellet Density, Min % T. D.	93
Theoretical Density, Al_2O_3	3.94 g/cm^3
Theoretical Density, B_4C	2.52 g/cm^3
Clad Material	Zircaloy-4
Clad I.D.	0.332 inches
Clad O.D.	0.382 inches
Clad Thickness	0.025 inches
Diametral Gap (Cold)	0.025 inches
Active Length	136.0 inches

Table 3.3

MECHANICAL DESIGN PARAMETERS

ANO-2

Core description	
Power Level	2815 Megawatts - Thermal
Number of Assemblies	177
Number of Control Rods	81
Fuel Assembly Pitch	8.177 inches
Core area	82.25 Square Feet
Core Equivalent Diameter	123 inches
Fuel Assembly Description	
Fuel Rod Array	16 x 16
Fuel Rod Pitch	0.506 inches
Outside Dimension	7.977 inches
Number of Guide Tubes	5
Guide Tube I.D.	0.90 inches
Guide Tube O.D.	0.98 inches
Guide Tube Material	Zircaloy-4
Fuel Rod Description	
Material	UO_2
Stack Height Density	10.061 g/cm^3
Pellet Diameter	0.325 inches
Clad Material	Zircaloy-4
Clad I.D.	0.332 inches
Clad O.D.	0.382 inches
Clad Thickness	0.025 inches
Active Fuel Length	150 inches
Full Length Control Rod	
Number	73 (5-Finger)
Clad Material	Inconel-625
Clad Thickness	0.035 inches
Clad O.D.	0.816 inches
Center Finger	
Poison Material	B_4C / Inconel
Length	135.5" / 12.5"
Outside Fingers	
Poison Material	B_4C / Ag-In-Cd
Length	135.5" / 12.5"

Table 3.3 (continued)

Full Length Control Rod (continued)

B_4C pellet	
Diameter	0.737 inches
% T. D. of 2.52 g/cm^3	73
Weight % Boron, Min	77.5

Part Length Control Rod

Number	8 (5-Fingers)
Clad Material	Inconel-625
Clad Thickness	0.035 inches
Clad O.D.	0.816 inches
Poison	
Material	Inconel / Water / B_4C
Length	75 " 58" 16"
B_4C pellet	
Diameter	0.737 inches
% T. D. of 2.52 g/cm^3	73
Weight % Boron, Min	77.5

Burnable Poison Rod

Absorber Material	Al_2O_3 - B_4C
Pellet Diameter	0.310 inches
Pellet Length	0.50 inches min
Pellet Density, Min % T. D.	85 min
Theoretical Density, Al_2O_3	3.90 g/cm^3
Theoretical Density, B_4C	2.52 g/cm^3
Clad Material	Zircaloy-4
Clad I.D.	0.332 inches
Clad O.D.	0.382 inches
Clad Thickness	0.025 inches
Diametral Gap (Cold)	0.022 inches
Active Length	136.0 inches

Figure 3.1

REACTOR CORE CONTROL ROD PATTERN

SONGS 1

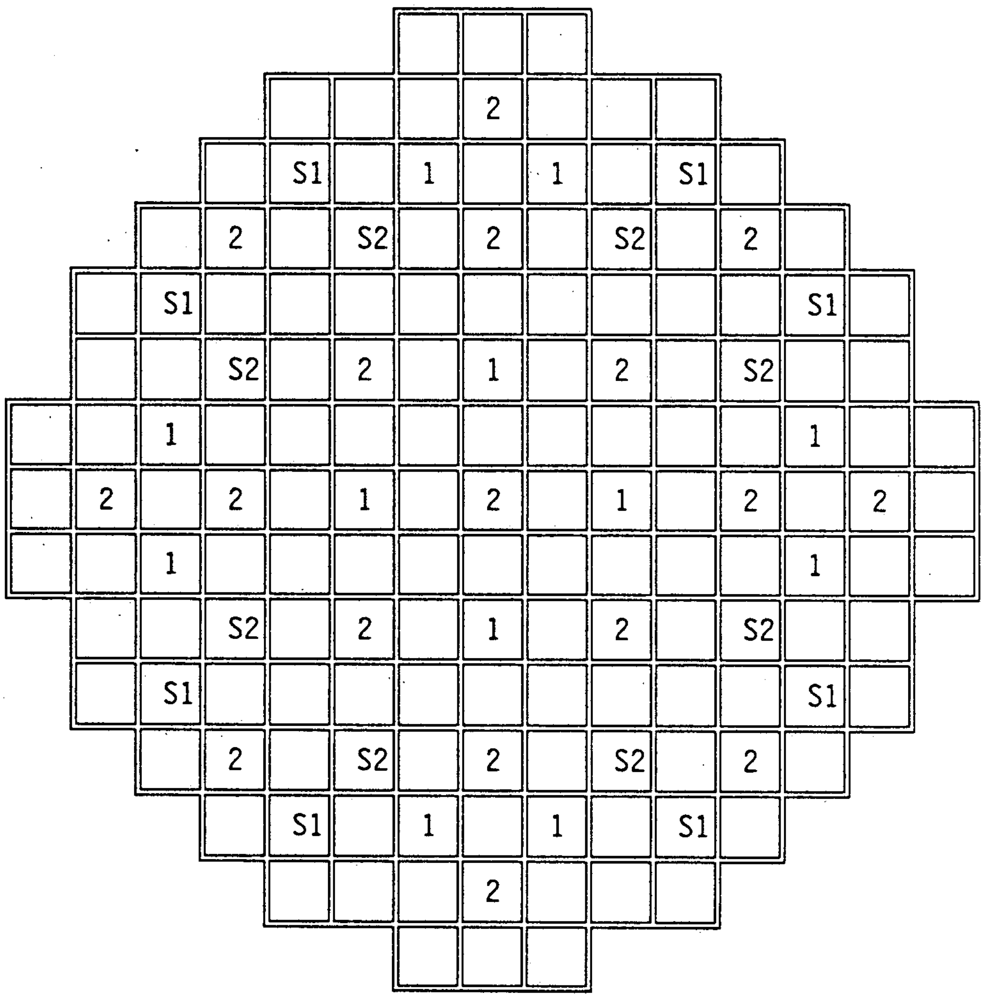

BANK	NUMBER OF RCCA's
1	12
2	17
S1	8
S2	8
-----	------
TOTAL	45

Figure 3.2

TYPICAL FUEL ASSEMBLY

SONGS 1

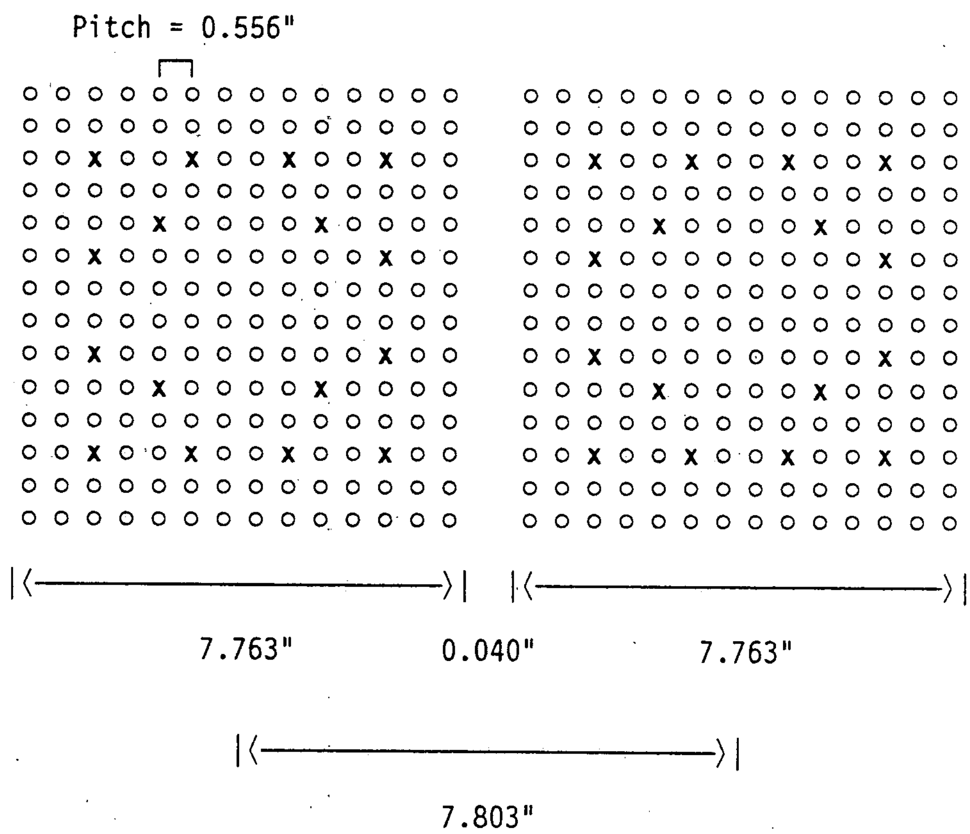

o FUEL ROD LOCATION

x GUIDE TUBE LOCATION

Figure 3.3

REACTOR CORE INSTRUMENTATION LOCATIONS

SONGS 1

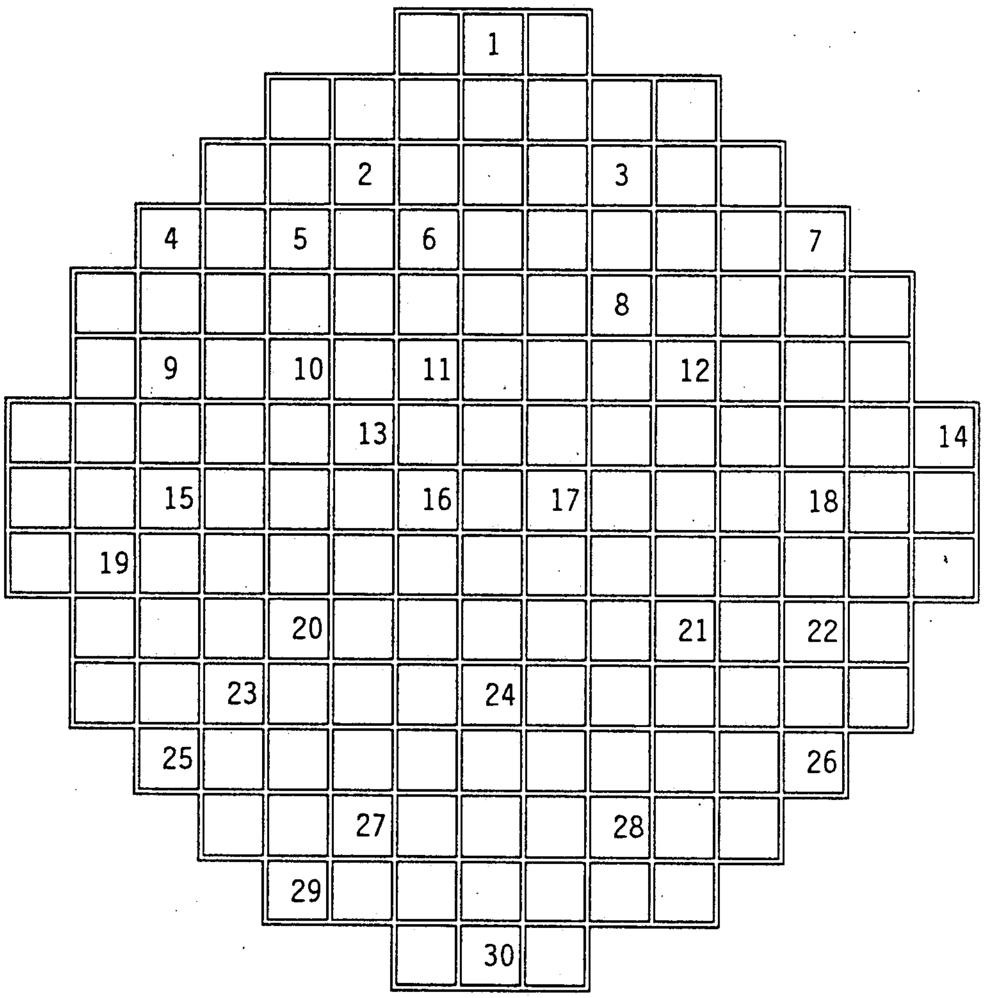

1 - 30 indicate incore instrumentation location

Figure 3.4

REACTOR CORE CONTROL ROD PATTERN

SONGS 2&3

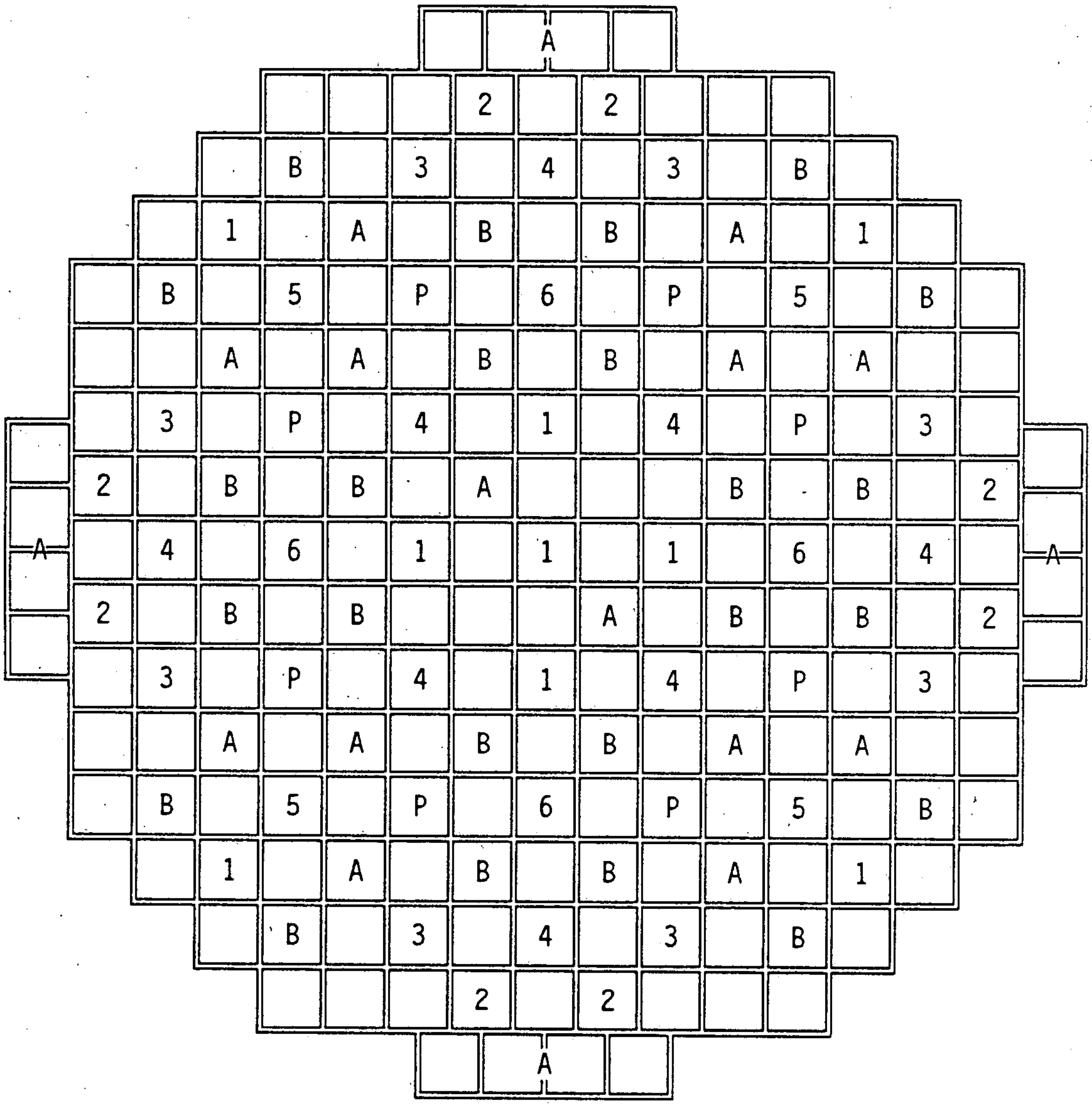

BANK	NUMBER OF CEA's
1	9
2	8
3	8
4	8
5	4
6	4
P	8
A	18
B	24
-----	------
TOTAL	91

Figure 3.5

TYPICAL FUEL ASSEMBLY

SONGS 2&3

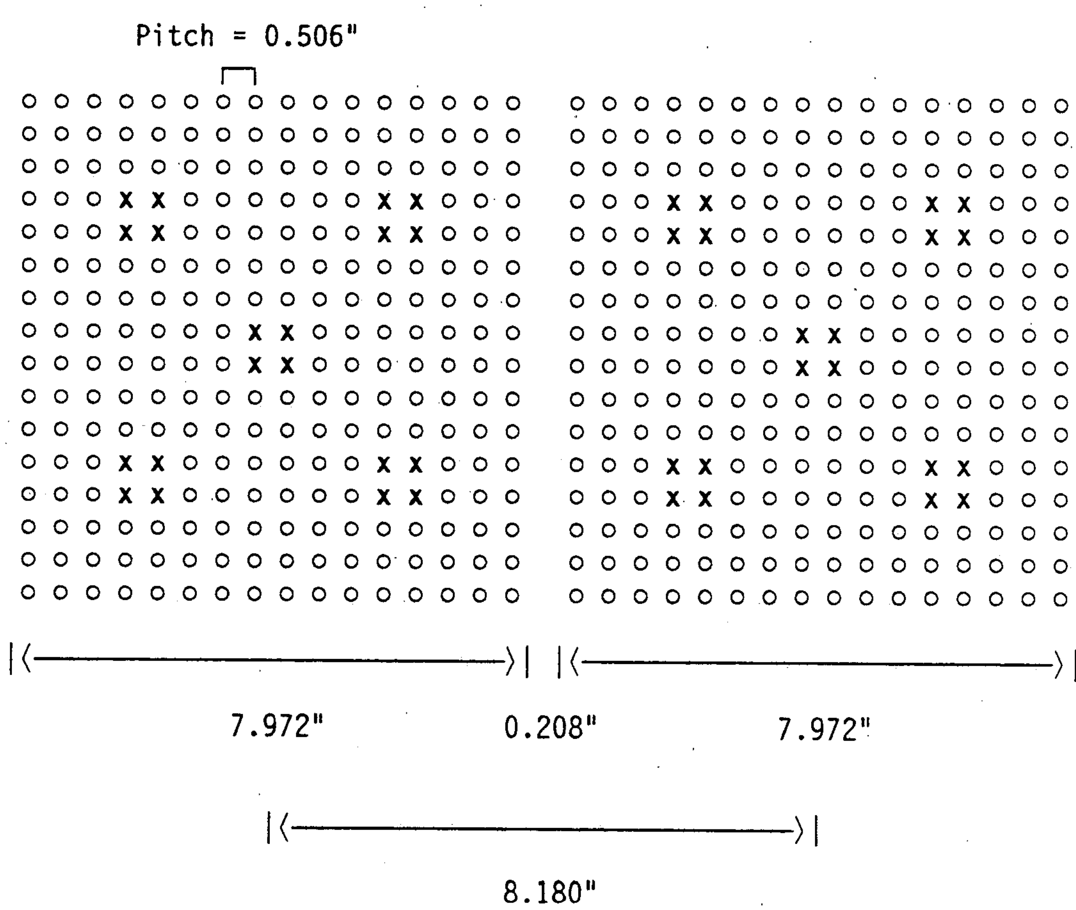

o FUEL ROD LOCATION

x x
x x GUIDE TUBE LOCATION

Figure 3.6

REACTOR CORE INSTRUMENTATION LOCATIONS

SONGS 2&3

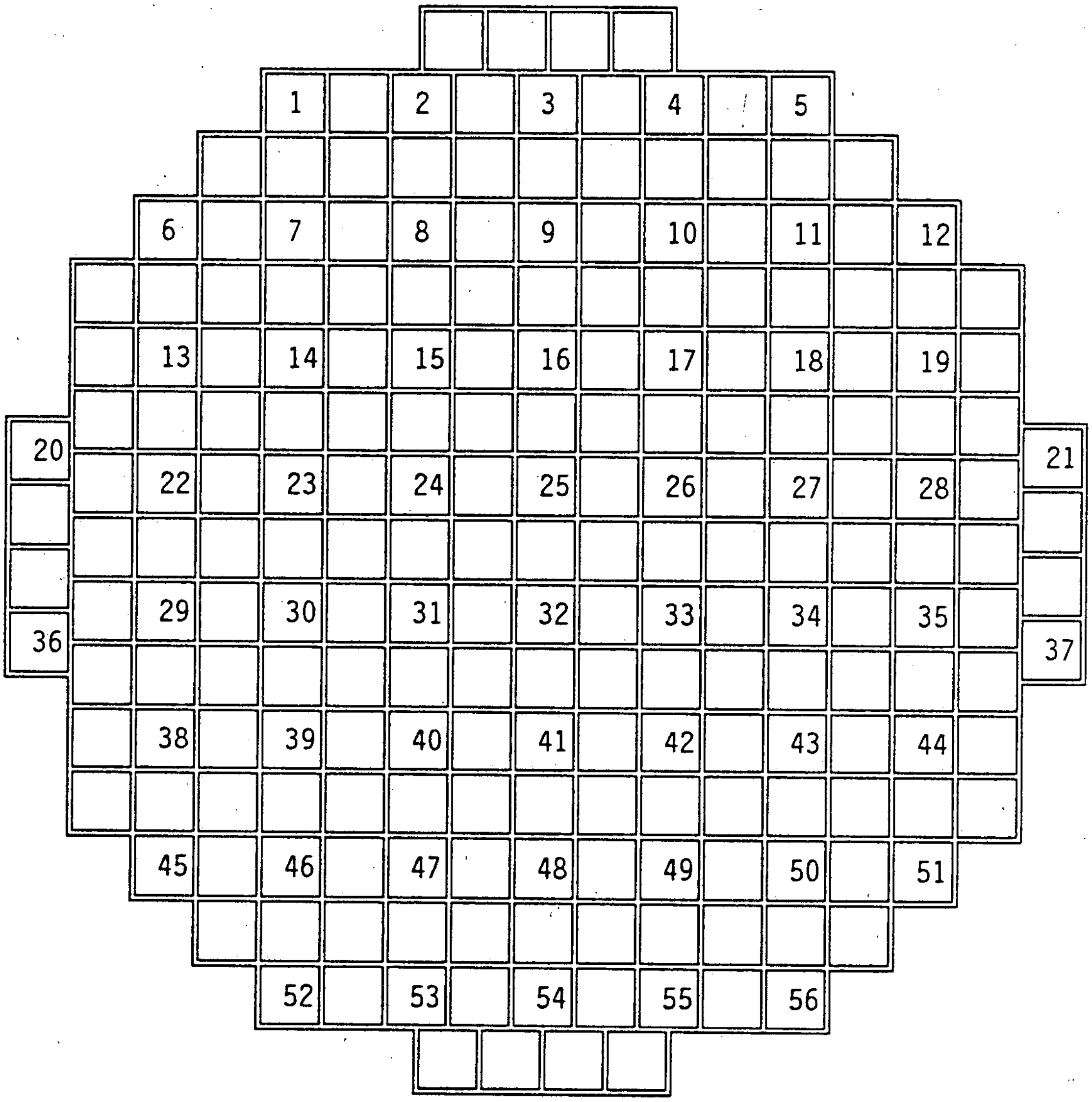

1 - 56 indicates incore instrumentation location

Figure 3.7

REACTOR CORE CONTROL ROD PATTERN - ANO-2

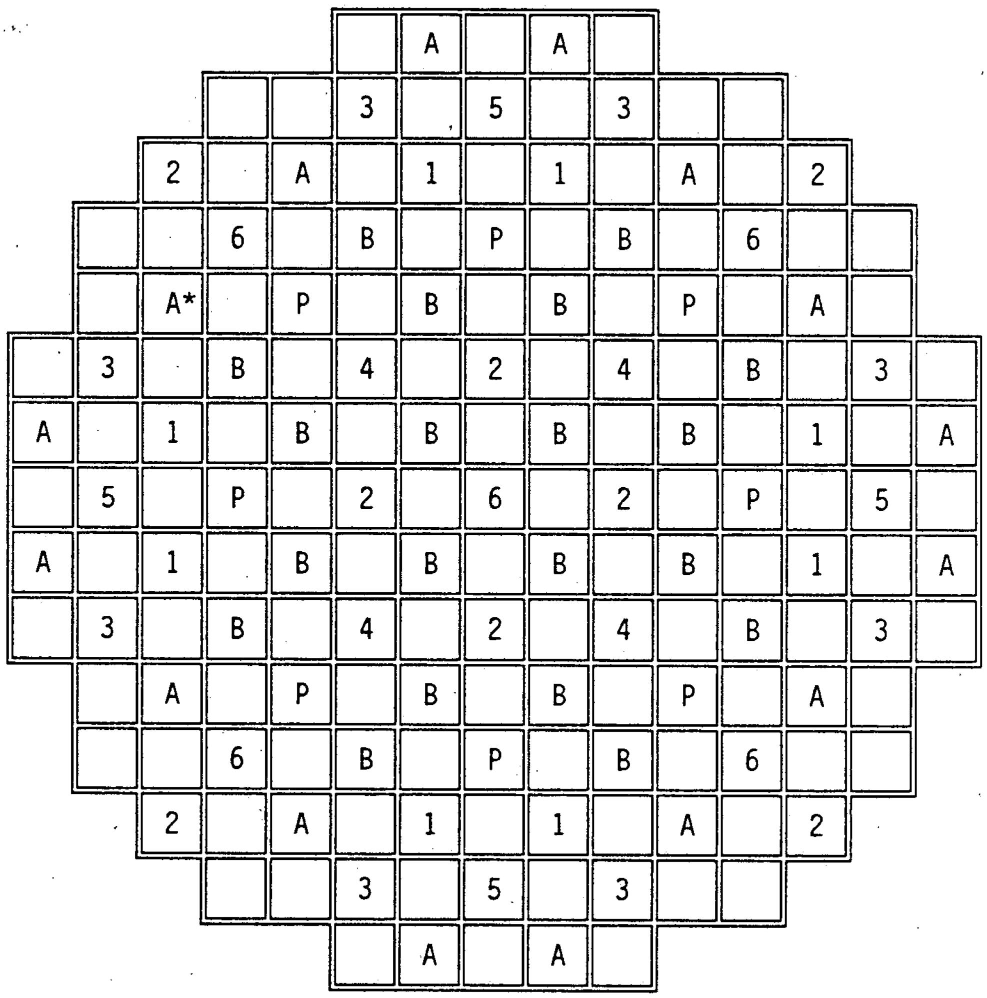

* indicates the location of the worst stuck rod, A-52.

BANK	NUMBER OF RODS
1	8
2	8
3	8
4	4
5	4
6	5
P	8
A	16
B	20
-----	------
TOTAL	81

Figure 3.8

TYPICAL FUEL ASSEMBLY

ANO-2

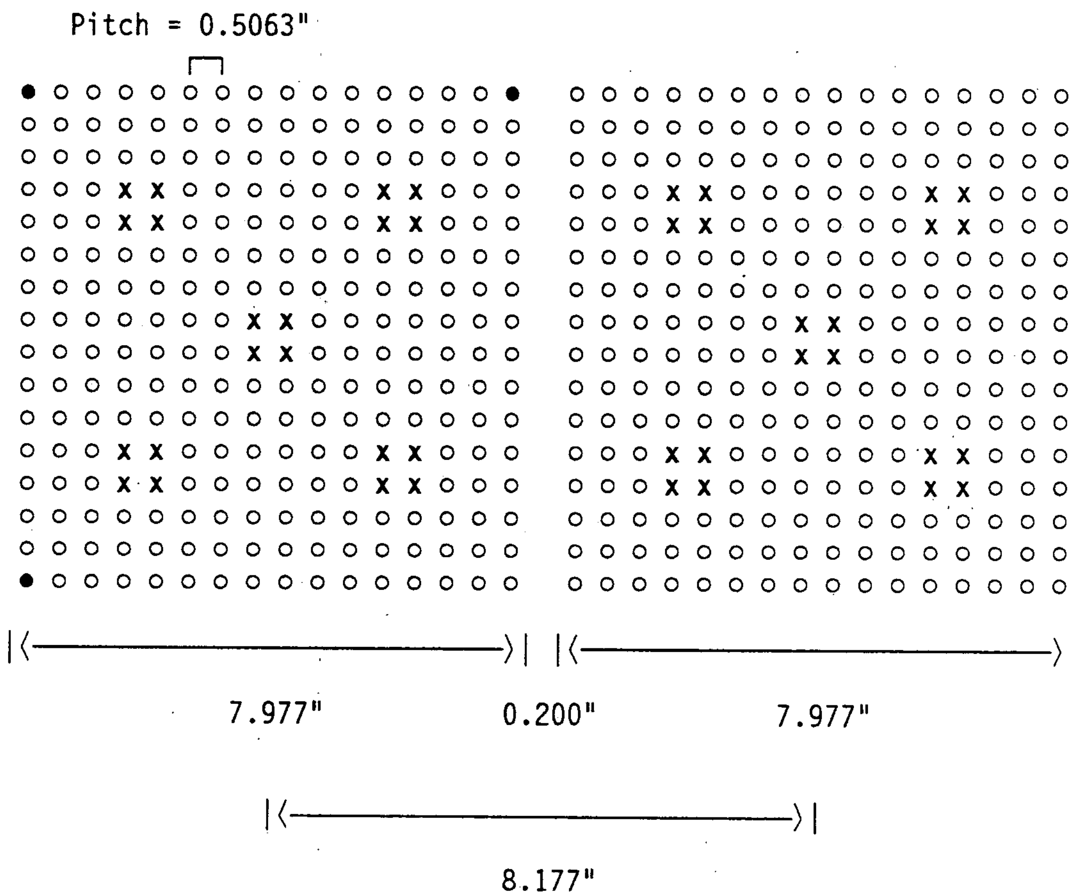

o FUEL ROD LOCATION

x x
x x GUIDE TUBE LOCATION

• TYPICAL ASYMMETRIC BURNABLE ABSORBER LOCATION

FIGURE 3.9

REACTOR CORE INSTRUMENTATION LOCATIONS

ANO-2

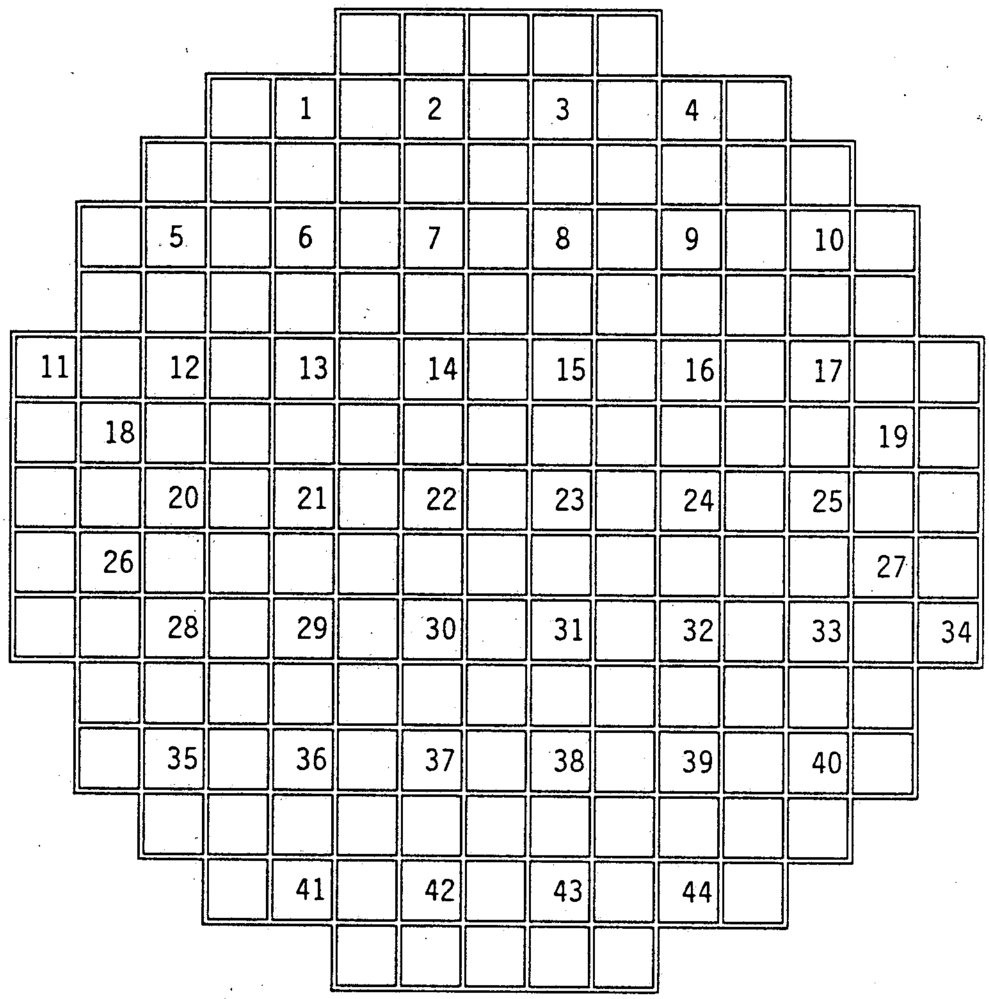

1 - 44 indicate incore instrumentation locations

SECTION 4

BENCHMARK COMPARISONS

4.0 INTRODUCTION

This section compares the calculated parameters and the measured plant data. The measured data are from zero power startup testing and normal operations at San Onofre Nuclear Generating Station (SONGS) Units 1, 2, 3, and Arkansas Nuclear One - Unit 2 (ANO-2). Six cycles at SONGS 1, five cycles from SONGS 2, four cycles from SONGS 3, and one cycle from ANO-2 were analyzed for a total of sixteen cycles including initial and reload cores. For each parameter compared, the sample mean and standard deviation of the observed differences were calculated. Based on the mean, standard deviation, and the sample size, a conservative 95/95 tolerance limit (bias ± reliability factor) was calculated.

Section 4.1 provides the Critical Boron Concentration (CBC) comparisons for Zero Power and Full Power conditions. Differences between calculated and measured data are represented in absolute terms, (Calculated - Measured). The SIMULATE-3 reactivity (1 - 1/Keff) is also calculated for each case.

Section 4.2 presents the Isothermal Temperature Coefficient (ITC) comparison. As in the CBC comparisons, the differences are in absolute terms.

Section 4.3 describes the Power Coefficient (PC) comparison with the differences represented in absolute terms.

Section 4.4 presents the control rod worth comparison. The difference between calculated and measured data is given in relative terms:

Difference = (Calculated - Measured)/Calculated * 100%.

Section 4.5 verifies the ability of SIMULATE-3 to predict the net (N-1) rod worth.

Section 4.6 presents the Inverse Boron Worth (IBW) comparison. The differences are calculated in relative terms.

Section 4.7 compares the SIMULATE-3 assembly (radial and axial) power distributions, axial offset, and incore detector signals with plant measurements. The axial offset differences are quantified in absolute terms, and the assembly peaking factor differences are quantified in relative terms.

4.1 CRITICAL BORON CONCENTRATION

SIMULATE-3 Critical Boron Concentration (CBC) and reactivity predictions were compared to zero-power startup test measurements as well as to full-power operating data. The most reliable measurements are the zero-power startup tests. These measurements are made under well controlled conditions without significant thermal and xenon feedbacks.

The zero-power comparison statistics quantify SIMULATE-3's accuracy in predicting CBC and reactivity for Beginning-of-Cycle (BOC), zero-power conditions without xenon in the core. The full-power operating boron concentration data are from titration of reactor coolant system samples. The measurements are adjusted for control rod insertions and deviations from full power, equilibrium conditions. These full-power comparisons serve as conservative estimates of the SIMULATE-3 uncertainties for at-power equilibrium conditions with thermal feedback.

Sections 4.1.1 and 4.1.2 present the comparisons for zero-power and full-power CBC and reactivity, respectively.

4.1.1 Zero-Power Critical Boron Concentration

Table 4.1 lists the measured and SIMULATE-3 predicted values for BOC, zero-power, xenon free Critical Boron Concentrations (CBC), and SIMULATE-3 calculated reactivities at the measurement conditions for SONGS 1, 2, and 3. Thirty-two measurements from 15 cycles of startup tests are included. Of these measurements, seventeen are unrodded and fifteen are with control rods inserted in the core. Five of the measurements were taken with the reactor critical at low temperatures during initial cycle startups.

The low temperature measurements were taken at 150°F and 320°F for SONGS 1 and 2, respectively. The low temperature cases were included to show temperature dependencies, if any, in the SIMULATE-3 CBC prediction. Comparing the differences between the low temperature and Hot-Zero-Power (>535°F) cases, it is concluded that the SIMULATE-3 CBC predictions are independent of the moderator's temperature.

A three-step statistical analysis was performed on the measured and SIMULATE-3 calculated CBC differences and on the SIMULATE-3 calculated reactivities for the CBCs as measured. First, the sample mean ($\overline{x}$), standard deviation (S), and Root-Mean-Squares (RMS) were calculated for CBC and reactivity differences, respectively. The differences are due to SIMULATE-3 calculational uncertainties, variations in B-10 isotopic concentrations, and measurement (titration) uncertainties. For example boron concentration measurement errors can be as high as 5 ppm. For conservatism, all differences are assumed due only to SIMULATE-3 calculational uncertainties.

Second, the two sample distributions were tested for normality using ANSI standard N15.15-1974 (Reference 15). The normality test is needed because the 95/95 tolerance limit assumes that the population has a normal distribution. The test concludes that both distributions, CBC and reactivity differences, are normal. Finally, the bias, 95/95 reliability factor and tolerance limit are calculated. Table 4.2 lists the results for each distribution using the method as described in Reference 16. The 95/95 tolerance limits for zero-power CBC and reactivity, for all temperatures and rodded conditions, are -7±26 PPM and -0.08±0.26 %Δk/k, respectively.

Table 4.1

Zero Power Critical Boron Comparison

SONGS 1, 2, and 3

(Beginning of Cycle)

UNIT	CYCLE	CASE	CRITICAL PPM MEAS.	CRITICAL PPM SIM-3	S - M (PPM)	REACTIVITY (%ΔK/K)
1	1	150°F, ARO	2250	2268	18	0.157
1	1	150°F, BANK 2 IN	2050	2052	2	0.024
1	1	150°F, BANK1 IN	1898	1892	-6	-0.047
1	1	HZP, ARO	2524	2522	-2	-0.009
1	1	HZP, BANK 2 IN	2197	2187	-10	-0.067
1	1	HZP, BANK 1 IN	1944	1929	-15	-0.108
1	2	HZP, ARO	1609	1595	-14	-0.093
1	3	HZP, ARO	1876	1887	11	0.068
1	4	HZP, ARO	1956	1952	-4	-0.025
1	5	HZP, ARO	1822	1833	11	0.072
1	6	HZP, ARO	1774	1773	-1	-0.004
2	1	320°F, ARO	869	857	-12	-0.171
2	1	320°F, BANKS 6-4 IN	797	783	-14	-0.208
2	1	HZP, ARO	833	824	-9	-0.115
2	1	HZP, BANKS 6-3 IN	629	614	-15	-0.188
2	1	HZP, BANKS 6-1 IN	499	472	-27	-0.342
2	2	HZP, ARO	1198	1174	-24	-0.249
2	2	HZP, BANKS 6-1 IN	883	849	-34	-0.360
2	3	HZP, ARO	1580	1561	-19	-0.171
2	3	HZP, BANK B IN	1382	1370	-12	-0.104
2	4	HZP, ARO	1803	1802	-1	-0.011
2	4	HZP, BANK B IN	1563	1547	-16	-0.127
2	5	HZP, ARO	1620	1640	20	0.164
2	5	HZP, BANKS 6-1 IN	1208	1208	0	0.003

Table 4.1 (continued)

UNIT	CYCLE	CASE	CRITICAL PPM MEAS.	CRITICAL PPM SIM-3	S - M (PPM)	REACTIVITY (%ΔK/K)
3	1	HZP, ARO	823	824	1	-0.001
3	1	HZP, BANKS 6-1 IN	483	472	-11	-0.149
3	2	HZP, ARO	1174	1161	-13	-0.139
3	2	HZP, BANK B IN	968	953	-15	-0.165
3	3	HZP, ARO	1550	1550	0	0.001
3	3	HZP, BANK B IN	1369	1361	-6	-0.067
3	4	HZP, ARO	1822	1831	9	0.071
3	4	HZP, BANKS 6-1 IN	1403	1392	-11	-0.090
				$\bar{x}$	-7	-0.08
				s	12	0.12
				n	32	32

Table 4.2

Statistical Analysis of Zero Power Critical Boron Results

(BOC, No Xenon)

	ΔPPM	%Δk/k
Mean ($\overline{x}$)	-7	-0.08
Standard Deviation (S)	12	0.12
RMS	14	0.14
Normality Test		
Test Value (W)	0.972	0.976
Critical Value*	0.930	0.930
Result	Normal	Normal
Sample Size	32	32
Degree Of Freedom	31	31
$k_{95/95}$	2.197	2.197
$k_{95/95}$ * S	26	0.26
Bias	-7	-0.08
95/95 Tolerance Limit	-7±26	-0.08±0.26

* Level of significance (α) = 0.05

4.1.2 HOT-FULL-POWER CRITICAL BORON CONCENTRATION

Tables 4.3 to 4.10 compare the measured HFP CBCs from core follow calculations for SONGS 2 and 3 Cycles 1-4 to the SIMULATE-3 results. Two low-power CBC measurements, one each from Cycle 1 of SONGS 3 and Cycle 2 of SONGS 2 are also included to demonstrate that there is no significant increase in the differences at power levels less than 100%. There are a total of 112 measurements from eight operating cycles. The reactivity data are plotted against the cycle burnup (GWD/T) in Figure 4.1.

The SIMULATE-3 at-power CBC and reactivity 95/95 tolerance limits were determined using the statistical methods outlined in Section 4.1.1. As summarized in Table 4.11, the 95/95 tolerance limits for all at-power and rodded or unrodded conditions for CBC and reactivity are 2±34 ppm and 0.01±0.35 %$\Delta k/k$, respectively.

Table 4.3

SONGS 2 Cycle 1 HFP Critical Boron Comparison

CYCLE BURNUP GWD/T	EFPD	CRITICAL PPM MEAS.	SIM-3	S - M (PPM)	CRITICAL K-EFF	REACTIVITY (% ΔK/K)
1.934	51.2	476	461	-15	0.99826	-0.174
3.023	80.0	465	441	-24	0.99727	-0.274
4.039	106.9	457	421	-36	0.99600	-0.402
4.978	131.8	432	399	-33	0.99633	-0.368
5.977	158.2	402	380	-22	0.99755	-0.246
7.003	185.4	374	348	-26	0.99712	-0.289
7.987	211.4	342	311	-31	0.99646	-0.355
8.970	237.4	301	274	-27	0.99688	-0.313
9.994	264.5	252	229	-23	0.99733	-0.268
10.944	289.7	204	183	-21	0.99755	-0.246
12.030	318.4	138	125	-13	0.99841	-0.159
12.977	343.5	80	70	-10	0.99876	-0.124

Table 4.4

SONGS 3 Cycle 1 HFP Critical Boron Comparison

CYCLE BURNUP GWD/T	EFPD	CRITICAL PPM MEAS.	SIM-3	S - M (PPM)	CRITICAL K-EFF	REACTIVITY (% ΔK/K)
1.323	35.0	472	457	-15	0.99826	-0.174
2.356	62.4	471	455	-16	0.99820	-0.180
3.345	88.5	455	436	-19	0.99786	-0.214
4.955	131.2	430	410	-20	0.99772	-0.229
6.160	163.1	391	369	-22	0.99756	-0.245
6.935	183.6	377	347	-30	0.99663	-0.338
8.075	213.7	332	314	-18	0.99794	-0.206
9.370	248.0	279	258	-21	0.99757	-0.244
11.590	306.8	163	150	-13	0.99845	-0.155
12.357	327.1	121	107	-14	0.99830	-0.170
13.972	369.8 (55% POWER)	115	94	-21	0.99736	-0.265

Table 4.5

SONGS 2 Cycle 2 HFP Critical Boron Comparison

CYCLE BURNUP GWD/T	EFPD	CRITICAL PPM MEAS.	SIM-3	S - M (PPM)	CRITICAL K-EFF	REACTIVITY (% ΔK/K)
0.800	21.2	741	750	9	1.00091	0.091
1.758	46.5	684	675	-9	0.99909	-0.091
2.258	59.8	654	636	-18	0.99812	-0.188
3.907	103.4	532	501	-31	0.99678	-0.323
5.941	157.3	339	332	-7	0.99927	-0.073
7.054	186.7	260	243	-17	0.99819	-0.181
7.726	204.5	182	187	5	1.00041	0.041
9.241	244.6	56	65	9	1.00107	0.107
9.612	254.4 (80% POWER)	72	77	5	1.00054	0.054

Table 4.6

SONGS 3 Cycle 2 HFP Critical Boron Comparison

CYCLE BURNUP GWD/T	EFPD	CRITICAL PPM MEAS.	SIM-3	S - M (PPM)	CRITICAL K-EFF	REACTIVITY (% ΔK/K)
0.613	16.2	722	750	28	1.00288	0.287
1.133	30.0	690	708	18	1.00182	0.182
2.019	53.4	623	636	13	1.00137	0.137
2.771	73.3	560	575	15	1.00159	0.159
3.929	104.0	471	479	8	1.00092	0.092
4.982	131.9	376	392	16	1.00171	0.171
5.783	153.1	320	326	6	1.00066	0.066
7.041	186.4	203	221	18	1.00197	0.197
7.996	211.7	122	148	26	1.00277	0.276

Table 4.7

SONGS 2 Cycle 3 HFP Critical Boron Comparison

CYCLE BURNUP GWD/T	EFPD	CRITICAL PPM MEAS.	SIM-3	S - M (PPM)	CRITICAL K-EFF	REACTIVITY (% ΔK/K)
1.006	27.1	1045	1060	15	1.00127	0.127
1.987	53.6	977	981	4	1.00035	0.035
2.965	79.9	907	905	-2	0.99986	-0.014
3.907	105.3	834	831	-3	0.99975	-0.025
5.182	139.7	733	731	-2	0.99987	-0.013
6.015	162.1	678	667	-11	0.99900	-0.100
6.957	187.5	593	596	3	1.00024	0.024
8.100	218.3	512	509	-3	0.99973	-0.027
8.965	241.6	441	445	4	1.00031	0.031
10.026	270.2	360	365	5	1.00045	0.045
10.913	294.1	286	299	13	1.00127	0.127
12.078	325.5	205	214	9	1.00084	0.084
13.042	351.5	135	143	8	1.00081	0.081
13.944	375.8	61	77	16	1.00164	0.164

Table 4.8

SONGS 3 Cycle 3 HFP Critical Boron Comparison

CYCLE BURNUP GWD/T	EFPD	CRITICAL PPM MEAS.	SIM-3	S - M (PPM)	CRITICAL K-EFF	REACTIVITY (% ΔK/K)
0.664	17.9	1048	1070	22	1.00190	0.190
0.961	25.9	1026	1044	18	1.00165	0.165
1.997	53.8	960	966	6	1.00055	0.055
3.008	81.1	903	887	-16	0.99865	-0.135
3.860	104.0	840	825	-15	0.99866	-0.134
5.064	136.5	741	728	-13	0.99884	-0.116
6.021	162.3	654	655	1	1.00001	0.001
6.981	188.1	580	581	1	1.00008	0.008
8.100	218.3	492	497	5	1.00049	0.049
8.988	242.2	427	431	4	1.00033	0.033
9.944	268.0	359	360	1	1.00005	0.005
10.908	294.0	281	281	0	1.00135	0.135
12.067	325.2	189	204	15	1.00152	0.152
12.950	349.0	121	140	19	1.00197	0.197
13.986	376.9	42	64	22	1.00228	0.227

Table 4.9

SONGS 2 Cycle 4 HFP Critical Boron Comparison

CYCLE BURNUP GWD/T	EFPD	CRITICAL PPM MEAS.	SIM-3	S - M (PPM)	CRITICAL K-EFF	REACTIVITY (% ΔK/K)
0.709	18.7	1253	1286	33	1.00259	0.258
1.993	52.6	1185	1219	34	1.00274	0.273
2.893	76.3	1154	1174	20	1.00156	0.156
4.080	107.6	1081	1112	31	1.00236	0.235
4.986	131.5	1041	1060	19	1.00149	0.149
5.968	157.4	992	1004	12	1.00100	0.100
6.962	183.6	943	950	7	1.00063	0.063
8.008	211.2	897	890	-7	0.99941	-0.059
8.899	234.7	827	843	16	1.00127	0.127
9.897	261.0	773	786	13	1.00081	0.081
11.091	292.5	705	714	9	1.00072	0.072
12.069	318.3	648	655	7	1.00062	0.062
12.976	342.2	598	599	1	1.00009	0.009
13.616	359.1	554	558	4	1.00035	0.035
14.837	391.3	448	479	31	1.00275	0.274
15.835	417.6	382	408	26	1.00231	0.230
16.680	439.9	324	347	23	1.00205	0.205
17.605	464.3	243	284	41	1.00379	0.378
19.054	502.5	131	172	41	1.00394	0.392
20.028	528.2	65	98	33	1.00323	0.322

Table 4.10

SONGS 3 Cycle 4 HFP Critical Boron Comparison

CYCLE BURNUP GWD/T	EFPD	CRITICAL PPM MEAS.	SIM-3	S - M (PPM)	CRITICAL K-EFF	REACTIVITY (% ΔK/K)
0.482	12.7	1291	1334	43	1.00338	0.337
1.388	36.6	1264	1282	18	1.00143	0.143
2.101	55.4	1248	1232	-16	1.00127	0.127
3.033	80.0	1198	1199	1	1.00010	0.010
3.974	104.8	1153	1147	-6	0.99964	-0.036
4.937	130.2	1118	1096	-22	0.99825	-0.175
6.086	160.5	1032	1031	-1	0.99990	-0.010
6.977	184.0	983	980	-3	0.99977	-0.023
7.955	209.8	938	924	-14	0.99892	-0.108
9.123	240.6	851	859	8	1.00069	0.069
10.105	266.5	803	801	-2	0.99987	-0.013
11.417	301.1	720	731	11	1.00089	0.089
12.312	324.7	666	670	4	1.00029	0.029
13.286	350.4	610	608	-2	0.99986	-0.014
14.041	370.3	557	559	2	1.00013	0.013
15.338	404.5	468	469	1	1.00004	0.004
16.316	430.3	401	398	-3	0.99977	-0.023
17.211	453.9	329	333	4	1.00034	0.034
18.151	478.7	257	264	7	1.00065	0.065
19.168	505.5	173	187	14	1.00135	0.135
20.093	529.9	89	120	31	1.00299	0.298
20.863	550.2	24	55	31	1.00311	0.310

Figure 4.1
SIMULATE-3 Critical Reactivity at HFP vs. Burnup

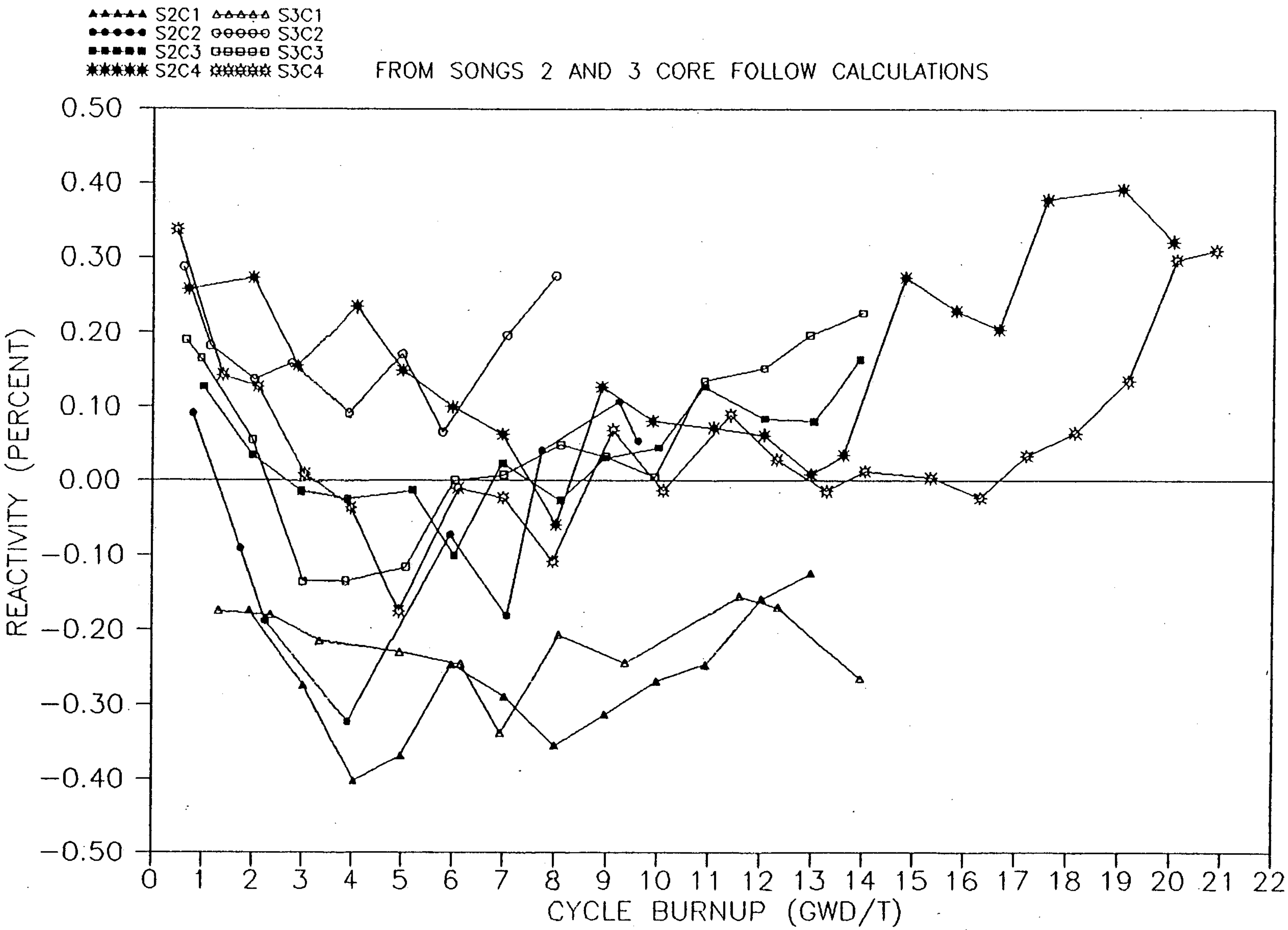

Table 4.11

Statistical Analysis of Hot Full Power

Critical Boron Results

	ΔPPM	%Δk/k
Mean ($\bar{x}$)	+2	0.0121
Standard Deviation (S)	18	0.1810
RMS	18	0.1806
Normality Test		
Test Value (D')	338.1	336.5
Critical Values*	326.8	326.8
	339.8	339.8
Result	Normal	Normal
Sample Size	112	112
Degree of Freedom	111	111
$k_{95/95}$	1.909	1.909
$k_{95/95}$ * S	34	0.35
Bias	2	0.01
95/95 Tolerance Limit	2±34	0.01±0.35

* Level of significance (α) = 0.05

4.2 ISOTHERMAL TEMPERATURE COEFFICIENT

The Isothermal Temperature Coefficient (ITC) is the change in the reactivity due to a 1°F change in the core average moderator and fuel temperature. Tables 4.12 and 4.13 list the comparisons of the calculated ITC's with measurements at SONGS 1, 2, and 3. The temperature, power level, control rod position, and soluble boron concentration are also included. The measurements span a wide range of soluble boron concentrations (145 PPM to 2524 PPM) and temperatures (150°F to 583°F). There are a total of 54 measurements from 14 cycles of operation. The measured and SIMULATE-3 calculated ITC differences have been plotted in Figure 4.2.

A statistical analysis has been performed on the ITC difference, (Calculated - Measured), using the process outlined in Section 4.1.1 to determine the 95/95 tolerance limit for all power, moderator temperature and rodded conditions. As summarized in Table 4.14, the 95/95 tolerance limit (bias ± reliability factor) is $(0.05 \pm 0.24) * 10^{-4}$ $\Delta K/K/°F$.

Table 4.12

Zero-Power ITC comparison

UNIT	CYCLE	(DEG. F)	CONTROL ROD POSITION	BORON (PPM)	ITC (10^{-4} ΔK/K/°F) MEASURED	SIM-3	P - M
1	1	150	ARO	2250	0.340	0.257	-0.083
	1	150	BANK 2 IN	2050	0.240	0.140	-0.100
	1	150	BANK 1 IN	1898	0.160	0.045	-0.115
	1	535	ARO	2524	0.740	0.902	0.162
	1	535	BANK 2 IN	2197	0.230	0.387	0.157
	1	535	BANK 1 IN	1944	-0.170	-0.046	0.124
	2	535	ARO	1609	-0.590	-0.482	0.108
	2	535	BANK 2 IN	1160	-1.357	-1.224	0.133
	3	535	ARO	1876	-0.350	-0.247	0.103
	3	535	BANK 1 IN	1318	-1.190	-1.081	0.109
	4	535	ARO	1956	-0.338	-0.157	0.181
	4	535	BANK 1 IN	1425	-1.204	-0.983	0.221
	6	535	ARO	1774	-0.604	-0.390	0.214
2	1	320	ARO	869	-0.143	-0.093	0.050
	1	320	BANKS 6-4 IN	797	-0.346	-0.325	0.021
	1	545	ARO	833	-0.380	-0.326	0.054
	2	545	ARO	1198	0.075	0.180	0.105
	2	545	BANKS 6-1 IN	883	-0.914	-0.851	0.063
	3	545	ARO	1580	0.050	0.183	0.133
	3	545	BANK B IN	1382	-0.588	-0.545	0.043
	4	545	ARO	1803	0.077	0.212	0.135
	4	545	BANK B IN	1563	-0.364	-0.331	0.033
	5	545	ARO	1620	-0.082	0.013	0.095
	5	545	BANKS 6-1 IN	1208	-0.860	-0.874	-0.014
3	1	545	ARO	823	-0.450	-0.343	0.107
	1	545	BANKS 6-1 IN	484	-1.512	-1.388	0.124
	2	545	ARO	1175	0.052	0.141	0.089
	2	545	BANK B IN	968	-0.570	-0.586	-0.016
	3	545	ARO	1550	0.043	0.143	0.100
	3	545	BANK B IN	1369	-0.613	-0.570	0.043
	4	545	ARO	1822	0.113	0.242	0.129
	4	545	BANKS 6-1 IN	1403	-0.660	-0.612	0.048

Table 4.13

At-Power ITC comparison

UNIT	CYCLE	POWER (%)	BURNUP (GWD/T)	CBC (PPM)	ITC (10^{-4} ΔK/K/°F) MEASURED	SIM-3	P - M
2	1	20	0.103	660	-0.628	-0.632	-0.004
	1	50	0.539	559	-0.824	-0.841	-0.017
	1	80	1.250	512	-0.942	-0.983	-0.041
	1	100	2.050	483	-1.037	-1.156	-0.119
	1	100	9.180	287	-1.647	-1.575	0.072
	2	98	0.208	818	-0.730	-0.760	-0.030
	2	100	1.466	693	-1.250	-1.043	0.207
	2	100	6.650	268	-2.230	-2.037	0.193
	2	100	8.123	145	-2.542	-2.333	0.209
	3	100	0.380	1095	-0.781	-0.761	0.020
	3	100	1.336	1024	-0.923	-0.875	0.048
	3	100	10.202	351	-1.920	-2.152	-0.232
	3	100	12.762	156	-2.300	-2.579	-0.279
	5	100	1.464	1063	-0.983	-1.067	-0.084
3	1	50	0.288	540	-0.826	-0.915	-0.089
	1	100	1.360	471	-1.072	-1.213	-0.141
	1	98	9.067	277	-1.478	-1.562	-0.084
	2	50	0.150	893	-0.559	-0.321	0.238
	2	89	0.378	758	-1.084	-0.862	0.222
	3	100	1.447	991	-0.964	-0.932	0.032
	3	100	9.867	367	-2.220	-2.117	0.103
	4	100	1.520	1255	-0.823	-0.761	0.062

Figure 4.2
Observed ITC Differences vs. Soluble Boron Concentration

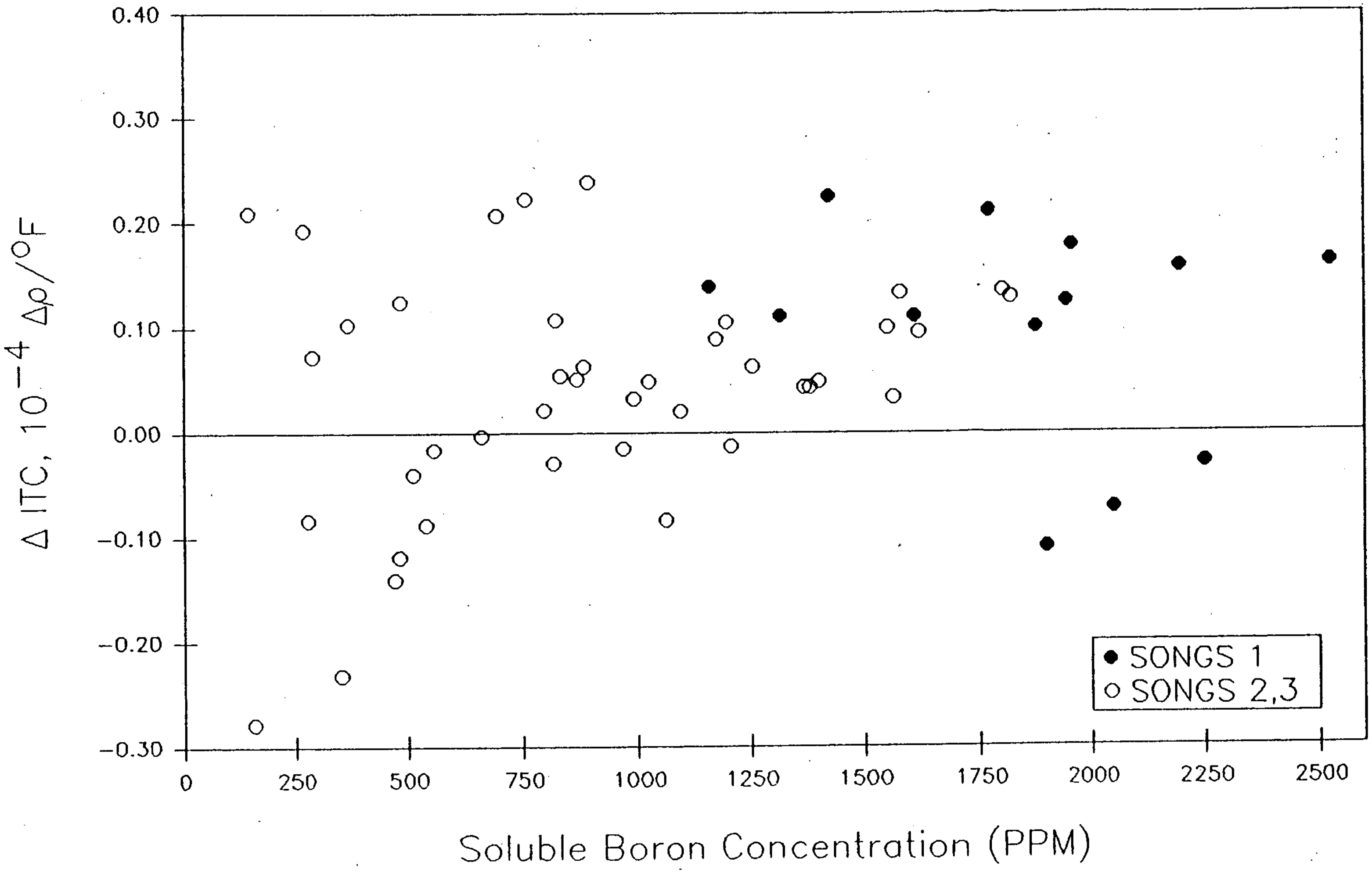

51

Table 4.14

Statistical Analysis of ITC Differences

	ΔITC (10^{-4} ΔK/K/°F)
Mean ($\bar{x}$)	0.053
Standard Deviation (S)	0.115
RMS	0.126
Normality Test	
Test Value (D')	111.9
Critical Values*	113.7, 107.5
Result	Normal
Sample Size	54
Degree Of Freedom	53
$k_{95/95}$	2.046
$k_{95/95}$ * S	0.24
Bias	0.05
95/95 Tolerance Limit	0.05±0.24

* Level of significance (α) = 0.05

4.3 POWER COEFFICIENT

The power coefficient is defined as the change in reactivity due to a change in the core power level. SIMULATE-3 power coefficient predictions were compared with measurements from early cycles of SONGS 2 and 3, summarized in Table 4.15. The differences are given in absolute terms, (Calculated - Measured).

Due to the limited size of the database, a meaningful 95/95 tolerance limit could not be derived. However, all of the differences are within 0.2×10^{-4} $\Delta k/k/\%P$, and the sample mean and standard deviation are 0.03 and 0.09, respectively. Since the differences include both the calculational and the measurement uncertainties, a conservative 95/95 tolerance limit of 0.2×10^{-4} $\Delta k/k/\%P$ can be assumed based on engineering judgment.

Table 4.15

Comparison of Measured and Calculated Power Coefficients

UNIT	CYCLE	POWER %	BURNUP MWD/T	BORON PPM	COEFFICIENT (10^{-4} $\Delta k/k/\%P$) MEASURED	CALCULATED	DIFF.
2	1	50	539	559	-1.104	-1.124	-0.020
2	1	80	1250	512	-0.946	-0.981	-0.035
2	1	100	2050	483	-0.947	-0.879	0.068
2	2	98	208	818	-0.990	-0.911	0.079
2	3	100	380	1095	-1.103	-0.907	0.196
3	1	50	288	540	-1.041	-1.119	-0.078
3	1	100	1360	471	-0.893	-0.893	-0.000
						Mean	0.030
						Standard Deviation	0.092

4.4 CONTROL ROD WORTH

SIMULATE-3's predictions for control rod worth were compared to the zero-power startup measurements from SONGS 1, 2, and 3.

Tables 4.16 through 4.19 list the measured and the calculated control rod worths with the differences (in percent) for beginning-of-cycle, zero power, nominal and off-nominal cases. The differences are plotted in Figure 4.3. Two cases have very small measured rod worths (less than 0.03%ΔK/K). These two cases (Cases 1 and 4 in Table 4.19) were excluded from the statistical analysis to avoid skewing.

A statistical analysis was performed on the control rod worth differences. The analysis determined the bias, standard deviation, and the normality of the difference distribution. The results are summarized in Table 4.20. The bias and standard deviation are 1.18% and 4.89%, respectively.

The uncertainty (S_{OBS}) has two components: the measurement uncertainty (S_M), and the calculational uncertainty (S_C). These two components are related to the observed uncertainty by,

$$S_{OBS}^2 = S_M^2 + S_C^2 \qquad \text{(Eq. 4.4.1)}$$

The measurement uncertainty can be quantified by comparing the measured control rod worths from the initial startup of SONGS 2 and 3. Since these two units are duplicate plants (identical fuel management, enrichments, burnable absorber worth, etc.,) one would expect the measured control rod worths at the beginning of the first cycle to be exactly the same. Therefore, the observed difference in SONGS 2 and 3 measurements can be attributable to the measurement uncertainty. Table 4.21 presents the comparison for a total of seven rod worth measurements. The standard deviation (S_D) of the difference in the measured rod worths, which includes measurement uncertainties from two measurements, is four percent. Therefore, the net measurement uncertainty can be calculated:

$$S_M^2 = 1/2 * S_D^2 = 8.00\% \qquad \text{(Eq. 4.4.2)}$$

Once the measurement uncertainty is quantified, the control rod worth calculational uncertainty can be calculated:

$$S_C = (S_{OBS}^2 - S_M^2)^{1/2} \qquad \text{(Eq. 4.4.3)}$$

$$= ((4.89)^2 - (8.00))^{1/2}$$

$$= 3.99 \ (\%)$$

Finally, the 95/95 reliability factor for the calculational error can be calculated:

$$\text{Reliability Factor} = K_{95/95} * S_C \qquad \text{(Eq. 4.4.5)}$$

$K_{95/95}$ is the critical factor associated with the sample size of 54. From Reference 16, the critical value has been found to be 2.046. Substituting the appropriate values into the above formula, as shown in Table 4.22, the 95/95 tolerance limit (bias ± reliability factor) becomes -1.2±8.2 %.

The tolerance limit will be applied to the SIMULATE-3 calculation of CEA worth at all power and moderator temperature conditions by,

$$\text{Predicted CEA Worth} = (\text{Calculated CEA Worth}) * (1 - \text{Bias} \pm \text{R. F.}) \qquad \text{(Eq. 4.4.6)}$$

Table 4.16

SONGS 1 Control Rod Worth Comparison

Cycle	Case	Reactivity Worth Measured	Reactivity Worth Calculated	Diff. (%)
1	150F BANK 2	1.999	1.918	-4.23
	150F BANK 1	1.484	1.436	-3.34
	HZP, BANK 2	2.504	2.375	-5.43
	HZP, BANK 1	2.001	1.846	-8.40
2	BANK 2	2.103	2.008	-4.73
	SHUTDOWN BANK	3.394	3.156	-7.54
3	BANK 2	2.465	2.369	-4.05
	BANK 1	1.378	1.373	-0.36
4	BANK 2	2.255	2.113	-6.72
	BANK 1	1.554	1.441	-7.84
6	BANK 2	2.123	2.087	1.72

Table 4.17

SONGS 2 Control Rod Worth Comparison

Case List	Reactivity Worth Measured	Reactivity Worth Calculated	Diff. (%)
Cycle 1			
A. CEA Banks Sequentially Inserted :			
1. Bank 6 Worth	0.411	0.395	-4.05
2. Bank 5 Worth	0.383	0.370	-3.51
3. Bank 4 Worth	0.928	0.892	-4.04
4. Bank 3 Worth	1.029	0.976	-5.43
5. Bank 2 Worth	0.662	0.638	-3.76
6. Bank 1 Worth	1.203	1.197	-0.50
7. Bank B Worth (Banks 6-1 & P in)	3.143	3.020	-4.07
B. Other CEA Worth :			
8. Bank P Worth (Other Rods Out)	0.211	0.196	-7.65
9. Bank P Worth (Banks 6-1 In)	0.390	0.353	-10.48
10. Center CEA(2-1) Worth, Other Rods Out	0.085	0.093	8.60
Cycle 2			
A. CEA Banks Sequentially Inserted :			
11. Bank 6 Worth	0.315	0.320	1.56
12. Bank 5 Worth	0.275	0.279	1.43
13. Bank 4 Worth	0.542	0.562	3.56
14. Bank 3 Worth	0.950	0.986	3.65
15. Bank 2 Worth	0.450	0.453	0.66
16. Bank 1 Worth	0.819	0.852	3.87
17. Bank A Worth, Other Rods Out	1.395	1.424	2.04
Cycle 3			
18. Bank B Worth, Other Rods Out	1.608	1.705	5.69
Cycle 4			
19. Bank B Worth, Other Rods Out	1.899	2.052	7.46

Table 4.18

SONGS 3 Control Rod Worth Comparison

Case List	Reactivity Worth Measured	Reactivity Worth Calculated	Diff. (%)
Cycle 1			
A. CEA Banks Sequentially Inserted :			
1. Bank 6 Worth	0.392	0.397	1.26
2. Bank 5 Worth	0.385	0.370	-4.05
3. Bank 4 Worth	0.894	0.892	-0.22
4. Bank 3 Worth	1.054	0.978	-7.77
5. Bank 2 Worth	0.698	0.636	-9.75
6. Bank 1 Worth	1.213	1.198	-1.25
7. Bank P in, Other Rods Out	0.200	0.195	-2.56
8. Center CEA(2-1) Worth, Other Rods Out	0.089	0.089	0.00
Cycle 2			
9. Bank 3 Worth, Other Rods Out	0.686	0.709	3.24
10. Bank B Worth, Other Rods Out	2.183	2.227	1.98
Cycle 3			
11. Bank B Worth, Other Rods Out	1.605	1.695	5.31
12. Bank 1 Worth,	0.416	0.440	5.45
13. Bank 4 Worth,	0.683	0.726	5.92
SONGS - 3 Cycle 4			
14 Bank 6 Worth	0.268	0.284	5.63
15. Bank 5 Worth	0.410	0.430	4.65
16. Bank 4 Worth	0.680	0.706	3.68
17. Bank 3 Worth	0.760	0.783	2.94
18. Bank 2 Worth	0.980	0.995	1.51
19. Bank 1 Worth	0.345	0.325	-6.15

Table 4.19

Control Rod Worths for Off-Nominal Conditions

(SONGS 2 Cycle 1)

Case List	Reactivity Worth Measured	Reactivity Worth Calculated	Diff. (%)
A. Hot Zero Power Dropped Rod Worth			
1. Worst PLCEA (CEA P-30)	0.028	0.024	-16.67
2. Worst SUBGP (CEA P-1)	0.108	0.109	0.92
B. Hot Zero Power Ejected Rod Worth			
3. From ZPDIL (CEA 5-45) (Banks 3 at 47%)	0.257	0.259	0.77
4. From FPDIL (CEA 6-20) (Bank 6 at 71%)	0.014	0.014	0.00
C. Cold Zero Power - Inlet temperature 320 F System Pressure 600 psi			
5. Rod Group 6 Worth	0.230	0.218	-5.51
6. Rod Group 5 Worth	0.270	0.247	-9.31
7. Rod Group 4 Worth	0.616	0.608	-1.32

Figure 4.3
Relative Control Rod Worth Differences vs. the Measured Worth

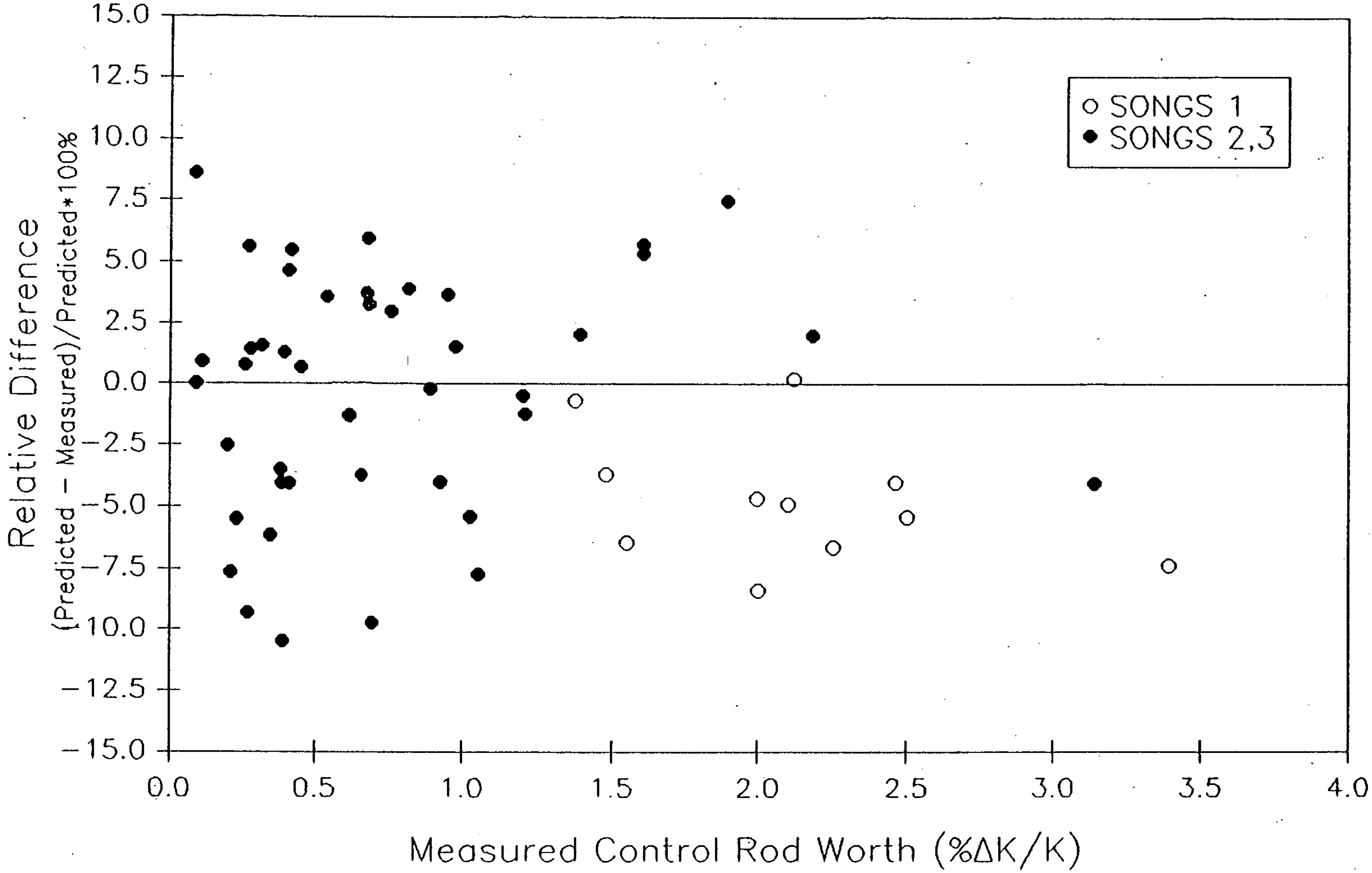

Table 4.20

Statistical Analysis of the Observed Control Rod Worth Differences

	%Worth
Mean	-1.18
Standard Deviation (S)	4.89
RMS	4.99
Normality Test	
Test Value (D')	113.0
Critical Values*	107.5, 113.7
Result	Normal
Sample Size	54
Degree Of Freedom	53
$k_{95/95}$	2.046

* Level of significance (α) = 0.05

Table 4.21

SONGS 2 and 3

Measured Control Rod Worths in Cycle 1

Control Bank	SONGS 2 Boron (PPM)	SONGS 2 Rod Worth (%)	SONGS 3 Boron (PPM)	SONGS 3 Rod Worth (%)	Difference (PERCENT)
6	833	0.411	823	0.392	4.62
5	800	0.383	794	0.385	-0.52
4	770	0.928	766	0.894	3.66
3	700	1.029	701	1.054	-2.43
2	632	0.662	624	0.698	-5.44
1	580	1.203	573	1.213	-0.83
P	833	0.211	823	0.200	5.21
				MEAN (%)	0.61
				RMS (%)	3.75
				S.D. (%)	3.99

Table 4.22

Determination of the Control Rod Worth Tolerance Limit

	%Worth
Observed Mean	-1.18
Observed S	4.89
Observed RMS	4.95
Normality Test	
Test Value (D')	113.0
Critical Values*	107.5, 113.7
Result	Normal
Measurement error	
Observed S_D	3.99
Measurement S_M	2.83
Model S_C	3.99
Sample Size	54
Degree Of Freedom	53
$k_{95/95}$	2.046
$k_{95/95} * S_C$	8.16
Bias	-1.2
95/95 Tolerance Limit (Rounded)	-1.2±8.2

* Level of significance (α) = 0.05

4.5 NET (N-1) ROD WORTH

The net (N-1) rod worth is defined as the reactivity worth of the insertion of all of the control rods except the most reactive rod, which remains stuck out. Due to the intense peaking in the assembly in which the stuck control rod is located, this configuration represents the most severe challenge to any reactor physics method.

SIMULATE-3 capabilities in predicting the net rod worth and the worst stuck rod worth are verified in this section by simulating the measurement performed during the initial startup of Arkansas Nuclear One - Unit 2 (ANO-2). ANO-2 is a Combustion Engineering PWR owned by the Arkansas Power And Light Company. As has been described in Section 3, the basic parameters of this reactor are very similar to those of SONGS 2 and 3. The worst stuck rod was CEA A-52 as identified in Figure 3.7.

Table 4.23 lists the comparison of the SIMULATE-3 calculated All-Rods-In (ARI), Net (N-1), and the worst (most reactive) stuck rod worth with the measurement. The agreement is good, and the observed differences for these cases are all within the 95/95 tolerance limits of -9.4% and +7.0%, as established in the control rod worth comparison in Section 4.4. Therefore, it is concluded that the 95/95 tolerance limit for the control rod worth (Section 4.4) is applicable to the net (N-1) worth also.

Table 4.23

ANO-2 Net (N-1) Rod Worth Comparison

Case	Measured	Calculated	Difference (%)
ARI Worth	12.188	11.587	-5.19
Net (N-1) Worth	10.666	10.177	-4.80
Worst Stuck Rod Worth	1.522	1.410	-7.94

4.6 INVERSE BORON WORTH

This section compares the SIMULATE-3 Inverse Boron Worths (IBW) to the SONGS 1, 2, and 3 measurements. The 95/95 tolerance limit for the IBW using the SIMULATE-3 methodology is also derived.

The IBW is calculated using:

$$IBW = -(CBC_1 - CBC_2) / (\Delta Reactivity) \qquad \text{(Eq. 4.6.1)}$$

where,

CBC_1 is the critical boron concentration for state-point #1,

CBC_2 is the critical boron concentration for state-point #2,

ΔReactivity is the required reactivity change (%$\Delta k/k$) to go from state-point #1 to #2. Normally, this reactivity change is accomplished by control rod insertion/withdrawal.

Table 4.24 compares the calculated IBWs with measurements at BOC, zero-power conditions, for a total of 16 measurements from 14 cycles of operations. The differences are all within 10%. The mean and standard deviation are 2.5% and 5.6%, respectively.

The differences include both the calculational and measurement uncertainties. The measurement uncertainty, which includes boron titration errors and control rod worth measurement errors, could not be quantified due to the insufficient number of duplicate IBW measurements at SONGS 2 and 3. A realistic estimate of the 95/95 tolerance limit associated with the SIMULATE-3 prediction of IBW was not possible. Therefore, an alternative method was used to quantify the reliability factor (RF).

Equation 4.6.1 relates the IBW to the calculated rod worth and CBCs for the two state-points. Assuming that all three variables (CBC_1, CBC_2, and rod worth) are independent estimates, the IBW error can be calculated using:

$$(R.\ F.)_{IBW} = \left((R.\ F.)^2_{CBC1} + (R.\ F.)^2_{CBC2} + (R.\ F.)^2_{CEA} \right)^{1/2} \qquad \text{(Eq. 4.6.2)}$$

Where,

$(R.\ F.)_{CBC}$ is the critical boron concentration reliability factor in percent

$(R.\ F.)_{CEA}$ is the control rod worth reliability factor in percent

Using Table 4.1, a 95/95 reliability factor of 3.1% for the relative (percent) uncertainty in the calculation of the critical boron concentration was derived. In Section 4.4, the 95/95 reliability factor for the control rod worth was found to be 8.2%. Substituting these two values into Eq. 4.6.2, a 95/95 reliability factor of 9.3% was calculated. For conservatism, this reliability factor was rounded to 10%. The conservatism of this 10% reliability factor was corroborated by the fact that all of the IBW differences listed in Table 4.24 were within 10%.

Table 4.24

SONGS 1, 2, and 3 Zero Power IBW Comparison

Unit	Cycle	Tmod (°F)	IBW (PPM/ %Δk/k) Measured	IBW (PPM/ %Δk/k) Calculated	Difference (C-M)/C*100%
1	1	150	101	112	9.8
	1	535	129	141	8.5
	2	535	135	148	8.8
	3	535	152	156	2.6
	4	535	156	158	1.3
	5	535	162	158	-2.5
	6	535	162	158	-2.5
2	1	320	-65	-69	6.0
	1	545	-72	-79	8.6
	2	545	-94	-94	0.1
	3	545	-123	-112	-9.9
	4	545	-126	-124	-1.7
3	1	545	-73	-79	7.0
	2	545	-95	-93	-1.3
	3	545	-113	-112	-1.2
	4	545	-118	-125	5.4
				Mean	2.5
				S	5.6
				RMS	6.0

4.7 ASSEMBLY POWER DISTRIBUTION

The SIMULATE-3 assembly power distribution predictions were verified. The calculated radial and axial power distributions and the calculated rhodium incore detector signals were compared to measurements from Cycles 1 through 4 of SONGS 2 and 3.

SONGS 2 and 3 are equipped with fixed rhodium incore detector systems consisting of 56 strings of detectors. Each string has five detectors of 40 cm in length, centered at axial core heights of 10%, 30%, 50%, 70%, and 90%, respectively. The core power distribution is measured by first taking a snapshot of the detector signals. A snapshot contains signals for all of the detectors at the specific moment. Signals in the snapshot are then corrected for sensitivity depletion and background effects. Finally, a computer program, CECOR (Reference 14), is executed to determine the core power distribution based on the sensitivity and background corrected signals and pre-calculated assembly coupling coefficients and axial boundary conditions.

Section 4.7.1 compares the SIMULATE-3 calculated radial and axial power distributions with CECOR measurements.

Section 4.7.2 details the comparison of the axial offsets for the snapshots used in the axial power distribution comparison in Section 4.7.1. The 95/95 tolerance limit is also derived.

Section 4.7.3 compares the calculated rhodium detector signals with measurements from detector snapshots. Since the detector signals are the true measured quantities, results from these comparisons are also used in the derivation of 95/95 tolerance limits for assembly/nodal peaking factors.

4.7.1 RADIAL AND AXIAL POWER DISTRIBUTIONS

Figures 4.4 to 4.15 compare the SIMULATE-3 axially integrated, quarter core assembly power distributions to CECOR measurements from SONGS 2 Cycles 1 through 4 and SONGS 3 Cycle 3 with burnups close to BOC, MOC, and EOC. These measurements were taken close to Hot-Full-Power and All-Rods-Out conditions. Exact power levels and burnup values are shown in the figures. The CECOR powers shown in these figures are average values from quarter core symmetric locations.

The comparisons demonstrate that the SIMULATE-3 assembly powers agree very well with the CECOR measured powers. The RMS error listed in Table 4.25 for each case is within 0.020 (absolute difference).

Figures 4.16 to 4.27 compare the core average axial power distribution for the corresponding snapshots presented in the assembly power comparison. The 51-node SIMULATE-3 axial powers were derived from the spline-fitting of the 20-node SIMULATE-3 solution. The SIMULATE-3 results agree well with the CECOR measurements. The RMS values of differences, (Calculated - Measured), are well below 0.05 (absolute difference). For those state-points with RMS error greater than 0.02, the two power distributions agree very well except in the top 5% and bottom 5% axial zones of the core. Since the CECOR powers in these regions are inferred using pre-calculated extrapolation distances, one would expect the "measured" CECOR powers to be less accurate. In fact, when these two regions are removed from the comparison, the RMS errors all drop below 0.02. Table 4.25 summarizes the RMS errors for core axial power distributions in the axial region from 5% to 95% core height.

The excellent agreement between SIMULATE-3 and CECOR results demonstrates the ability of the SIMULATE-3 methodology to predict the assembly power distribution accurately. Therefore, the SIMULATE-3 computer program can be used to generate representative power distributions of the reactor core for use in the statistical evaluation of overall uncertainties associated with safety system setpoints as per Reference 17.

Figure 4.4 Axially Integrated Radial Power Density - S2C1F026

Date = 03/08/84
Power Level = 99.5%
Burnup = 7035. MWd/T
Absolute Difference
RMS Error = 0.008
Max Positive Error = 0.016
Box = 55
Max Negative Error = -0.019
Box = 58

CECOR
CECOR - SIMULATE-3

							1 0.596 -0.007	2 0.771 0.005
					3 0.545 -0.009	4 0.759 -0.004	5 0.958 -0.010	6 1.148 0.014	7 1.030 -0.017
				8 0.604 -0.007	9 0.947 -0.002	10 0.982 -0.008	11 0.996 0.007	12 1.125 -0.007	13 1.052 0.006
			14 0.605 -0.006	15 0.789 0.002	16 0.998 -0.008	17 1.002 0.007	18 1.135 -0.002	19 1.069 0.004	20 1.170 -0.003
	21 0.544 -0.010	22 0.948 -0.001	23 1.000 -0.005	24 1.000 0.007	25 1.138 -0.002	26 1.078 0.009	27 1.189 -0.005	28 1.073 -0.019
	29 0.759 -0.004	30 0.983 -0.007	31 1.003 0.008	32 1.141 0.001	33 1.081 0.011	34 1.199 0.001	35 1.107 0.007	36 1.215 0.000
45 0.596 -0.007	37 0.960 -0.008	38 0.997 0.008	39 1.136 -0.002	40 1.078 0.009	41 1.196 -0.002	42 1.111 0.009	43 1.221 -0.001	44 1.123 0.011
54 0.771 0.005	46 1.149 0.015	47 1.126 -0.006	48 1.069 0.005	49 1.189 -0.005	50 1.106 0.006	51 1.220 -0.002	52 1.123 0.008	53 1.227 -0.004
	55 1.063 0.016	56 1.056 0.010	57 1.172 -0.007	58 1.073 -0.019	59 1.207 -0.009	60 1.120 0.007	61 1.232 0.001	62 1.127 0.008

Figure 4.5 Axially Integrated Radial Power Density - S2C1F038

Date = 06/13/84
Power Level = 99.8%
Burnup = 10687. MWd/T
Absolute Difference
RMS Error = 0.008
Max Positive Error = 0.022
Box = 55
Max Negative Error = -0.014
Box = 3

Box	CECOR	CECOR - SIMULATE-3
1	0.587	-0.009
2	0.751	-0.001
3	0.548	-0.014
4	0.757	-0.008
5	0.961	-0.009
6	1.151	0.017
7	1.063	-0.009
8	0.608	-0.013
9	0.973	-0.001
10	1.022	-0.005
11	0.994	0.004
12	1.155	0.001
13	1.053	0.008
14	0.610	-0.010
15	0.803	-0.002
16	1.047	-0.005
17	1.011	0.003
18	1.158	0.000
19	1.061	0.005
20	1.187	0.000
21	0.549	-0.013
22	0.976	0.002
23	1.050	-0.002
24	1.012	0.004
25	1.162	0.000
26	1.063	0.005
27	1.194	0.003
28	1.078	0.010
29	0.759	-0.006
30	1.025	-0.002
31	1.015	0.007
32	1.166	0.004
33	1.063	0.005
34	1.189	-0.001
35	1.069	0.001
36	1.196	0.001
37	0.965	-0.005
38	0.998	0.008
39	1.166	0.008
40	1.064	0.006
41	1.186	-0.003
42	1.066	-0.001
43	1.187	-0.005
44	1.067	0.001
45	0.588	-0.009
46	1.153	0.019
47	1.163	0.009
48	1.064	0.008
49	1.194	0.003
50	1.069	0.001
51	1.185	-0.007
52	1.061	-0.003
53	1.178	-0.012
54	0.751	-0.001
55	1.094	0.022
56	1.056	0.011
57	1.193	0.006
58	1.076	0.008
59	1.193	-0.002
60	1.064	-0.002
61	1.185	-0.005
62	1.059	-0.004

Figure 4.6 Axially Integrated Radial Power Density - S2C2F051

Date = 08/08/85
Power Level = 99.9%
Burnup = 3701. MWd/T
Absolute Difference
RMS Error = 0.011
Max Positive Error = 0.030
Box = 58
Max Negative Error = -0.028
Box = 24

Box	CECOR	CECOR - SIMULATE-3
1	0.689	-0.007
2	0.862	-0.006
3	0.724	-0.010
4	0.964	-0.001
5	1.115	0.009
6	0.880	0.021
7	0.967	0.007
8	0.741	-0.014
9	1.136	-0.007
10	0.917	0.008
11	1.080	0.001
12	1.030	0.000
13	0.931	0.015
14	0.746	-0.007
15	0.862	-0.010
16	0.850	-0.008
17	0.915	-0.006
18	1.248	-0.001
19	1.073	0.011
20	1.279	0.012
21	0.728	-0.004
22	1.143	0.002
23	0.854	-0.002
24	0.992	-0.028
25	0.958	-0.015
26	1.032	0.002
27	1.202	0.006
28	1.063	0.017
29	0.966	0.001
30	0.920	0.012
31	0.920	-0.001
32	0.961	-0.012
33	1.148	-0.015
34	1.180	0.000
35	1.130	-0.001
36	1.017	0.012
37	1.112	0.007
38	1.082	0.003
39	1.255	0.006
40	1.035	0.004
41	1.180	-0.001
42	1.119	-0.006
43	0.981	0.003
44	1.239	0.007
45	0.690	-0.006
46	0.879	0.020
47	1.028	-0.002
48	1.074	0.012
49	1.203	0.007
50	1.129	-0.003
51	0.975	-0.002
52	1.017	-0.022
53	0.924	0.008
54	0.861	-0.007
55	0.962	0.003
56	0.933	0.017
57	1.292	0.025
58	1.075	0.030
59	1.014	0.009
60	1.222	-0.010
61	0.912	-0.004
62	0.784	-0.013

Figure 4.7 Axially Integrated Radial Power Density - S2C2F055

Date = 09/11/85
Power Level = 100.1%
Burnup = 4970. MWd/T
Absolute Difference
RMS Error = 0.010
Max Positive Error = 0.022
Box = 6
Max Negative Error = -0.026
Box = 24

Box	CECOR	CECOR - SIMULATE-3
1	0.695	-0.006
2	0.870	-0.002
3	0.724	-0.012
4	0.960	-0.002
5	1.110	0.008
6	0.889	0.022
7	0.976	0.011
8	0.748	-0.015
9	1.135	-0.006
10	0.920	0.008
11	1.078	0.002
12	1.033	0.001
13	0.937	0.016
14	0.752	-0.009
15	0.874	-0.009
16	0.862	-0.007
17	0.924	-0.004
18	1.239	-0.001
19	1.070	0.011
20	1.266	0.007
21	0.728	-0.007
22	1.141	0.002
23	0.867	0.000
24	1.002	-0.026
25	0.966	-0.012
26	1.030	0.003
27	1.191	0.003
28	1.058	0.006
29	0.962	0.000
30	0.924	0.012
31	0.927	-0.001
32	0.967	-0.010
33	1.142	-0.012
34	1.170	0.002
35	1.120	-0.003
36	1.013	0.010
37	1.108	0.007
38	1.080	0.003
39	1.246	0.006
40	1.032	0.005
41	1.168	-0.002
42	1.112	-0.006
43	0.979	0.002
44	1.228	0.006
45	0.696	-0.005
46	0.888	0.022
47	1.031	-0.001
48	1.071	0.012
49	1.191	0.003
50	1.119	-0.005
51	0.975	-0.001
52	1.018	-0.022
53	0.929	0.008
54	0.868	-0.004
55	0.970	0.005
56	0.939	0.018
57	1.278	0.020
58	1.069	0.017
59	1.010	0.007
60	1.213	-0.009
61	0.917	-0.004
62	0.795	-0.012

Figure 4.8 Axially Integrated Radial Power Density - S2C3F005

Date = 08/22/86
Power Level = 100.2%
Burnup = 2224. MWd/T
Absolute Difference
RMS Error = 0.012
Max Positive Error = 0.024
Box = 55
Max Negative Error = -0.024
Box = 17

CECOR
CECOR - SIMULATE-3

						1 0.758 -0.007	2 0.958 -0.014	
				3 0.688 -0.011	4 0.928 -0.010	5 1.142 0.018	6 1.098 0.013	7 0.988 -0.003
			8 0.812 -0.003	9 1.036 0.014	10 0.831 0.002	11 1.102 0.008	12 0.940 0.002	13 1.223 -0.022
		14 0.817 0.003	15 1.139 0.013	16 1.158 0.010	17 1.112 -0.024	18 0.888 -0.010	19 1.192 -0.015	20 0.998 -0.004
	21 0.690 -0.009	22 1.039 0.018	23 1.163 0.017	24 0.878 -0.007	25 0.940 -0.008	26 1.208 -0.012	27 0.893 -0.001	28 1.123 -0.015
	29 0.927 -0.010	30 0.830 0.003	31 1.114 -0.019	32 0.940 -0.007	33 0.908 -0.010	34 1.180 0.008	35 1.142 0.019	36 0.925 0.019
45 0.759 -0.006	37 1.135 0.012	38 1.101 0.008	39 0.892 -0.005	40 1.206 -0.012	41 1.173 0.003	42 0.911 0.000	43 1.150 0.008	44 1.198 0.024
54 0.957 -0.014	46 1.097 0.013	47 0.940 0.002	48 1.191 -0.015	49 0.890 -0.002	50 1.135 0.014	51 1.143 0.003	52 0.801 0.000	53 0.756 0.021
	55 1.016 0.024	56 1.244 -0.001	57 1.012 0.010	58 1.127 -0.011	59 0.906 0.000	60 1.167 -0.007	61 0.721 -0.014	62 0.602 0.004

Figure 4.9 Axially Integrated Radial Power Density - S2C3F027

Date = 02/25/87
Power Level = 99.1%
Burnup = 8746. MWd/T
Absolute Difference
RMS Error = 0.013
Max Positive Error = 0.035
Box = 44
Max Negative Error = -0.023
Box = 3

CECOR
CECOR - SIMULATE-3

							1 0.703 -0.019	2 0.867 -0.022
				3 0.671 -0.023	4 0.890 -0.017	5 1.075 0.001	6 1.018 0.003	7 0.921 -0.014
			8 0.791 -0.017	9 1.004 0.006	10 0.844 0.003	11 1.078 0.005	12 0.934 0.002	13 1.224 -0.019
		14 0.796 -0.012	15 1.125 0.004	16 1.141 0.003	17 1.214 -0.014	18 0.933 -0.004	19 1.248 -0.007	20 1.042 0.001
	21 0.674 -0.020	22 1.008 0.011	23 1.146 0.009	24 0.909 -0.003	25 0.977 -0.003	26 1.256 -0.001	27 0.947 0.008	28 1.257 -0.009
	29 0.889 -0.017	30 0.845 0.004	31 1.217 -0.009	32 0.978 -0.001	33 0.924 -0.001	34 1.157 0.015	35 1.134 0.021	36 0.963 0.029
45 0.703 -0.019	37 1.069 -0.005	38 1.077 0.004	39 0.936 0.001	40 1.255 -0.001	41 1.152 0.011	42 0.907 0.010	43 1.131 0.017	44 1.224 0.035
54 0.867 -0.022	46 1.017 0.003	47 0.934 0.001	48 1.249 -0.006	49 0.946 0.007	50 1.130 0.019	51 1.126 0.014	52 0.830 0.009	53 0.806 0.033
	55 0.948 0.013	56 1.242 -0.001	57 1.056 0.015	58 1.262 -0.004	59 0.943 0.009	60 1.195 0.006	61 0.770 -0.003	62 0.673 0.017

Figure 4.10 Axially Integrated Radial Power Density - S2C3F048

Date = 07/22/87
Power Level = 99.8%
Burnup = 13943. MWd/T
Absolute Difference
RMS Error = 0.013
Max Positive Error = 0.039
Box = 44
Max Negative Error = -0.026
Box = 3

CECOR
CECOR - SIMULATE-3

						1 0.691 -0.024	2 0.842 -0.020	
				3 0.673 -0.026	4 0.880 -0.016	5 1.053 -0.004	6 0.991 0.002	7 0.905 -0.012
			8 0.787 -0.024	9 0.992 0.005	10 0.858 0.004	11 1.066 0.004	12 0.936 0.002	13 1.228 -0.010
		14 0.794 -0.018	15 1.126 0.006	16 1.131 0.003	17 1.266 0.004	18 0.954 -0.001	19 1.270 0.004	20 1.052 0.000
	21 0.675 -0.023	22 0.996 0.009	23 1.136 0.009	24 0.919 -0.006	25 0.987 -0.005	26 1.268 0.007	27 0.963 0.006	28 1.314 0.012
	29 0.880 -0.017	30 0.858 0.005	31 1.269 0.009	32 0.987 -0.004	33 0.919 -0.006	34 1.127 0.008	35 1.111 0.014	36 0.971 0.027
45 0.691 -0.024	37 1.049 -0.009	38 1.066 0.004	39 0.956 0.002	40 1.267 0.007	41 1.122 0.004	42 0.896 0.003	43 1.109 0.011	44 1.235 0.039
54 0.842 -0.020	46 0.990 0.002	47 0.935 0.001	48 1.271 0.005	49 0.963 0.007	50 1.108 0.012	51 1.105 0.008	52 0.847 0.007	53 0.840 0.034
	55 0.927 0.009	56 1.247 0.009	57 1.069 0.017	58 1.316 0.014	59 0.951 0.006	60 1.204 0.008	61 0.800 -0.006	62 0.721 0.017

Figure 4.11 Axially Integrated Radial Power Density - S2C4F007

Date = 2/17/88
Power Level = 99.9%
Burnup = 2214. MWd/T
Absolute Difference
RMS Error = 0.019
Max Positive Error = 0.032
Box = 7
Max Negative Error = -0.054
Box = 60

CECOR
CECOR - SIMULATE-3

						1 0.361 0.001	2 0.683 0.002	
				3 0.375 0.006	4 0.825 0.011	5 0.950 0.008	6 1.030 0.010	7 0.891 0.032
			8 0.452 0.003	9 1.005 0.013	10 1.120 0.028	11 1.270 0.020	12 1.220 0.027	13 1.274 0.011
		14 0.456 0.006	15 1.038 0.010	16 1.157 0.010	17 1.294 0.001	18 1.221 0.014	19 1.320 0.000	20 1.071 -0.005
	21 0.376 0.007	22 1.011 0.019	23 1.169 0.022	24 1.259 -0.013	25 1.042 -0.016	26 1.262 -0.021	27 1.120 -0.004	28 1.206 -0.014
	29 0.827 0.012	30 1.121 0.029	31 1.299 0.006	32 1.048 -0.010	33 1.177 -0.035	34 0.974 -0.011	35 1.159 -0.033	36 0.754 0.024
45 0.362 0.001	37 0.953 0.010	38 1.270 0.019	39 1.219 0.012	40 1.264 -0.019	41 0.977 -0.008	42 1.144 -0.022	43 1.032 -0.013	44 1.096 -0.024
54 0.684 0.003	46 1.031 0.011	47 1.219 0.026	48 1.320 0.000	49 1.120 -0.004	50 1.159 -0.034	51 1.027 -0.018	52 0.864 -0.034	53 0.824 -0.010
	55 0.873 0.015	56 1.264 0.001	57 1.081 0.005	58 1.188 -0.032	59 0.713 -0.017	60 1.066 -0.054	61 0.793 -0.042	62 0.593 -0.027

Figure 4.12 Axially Integrated Radial Power Density - S2C4F042

Date = 10/31/88
Power Level = 99.1%
Burnup = 10983. MWd/T
Absolute Difference
RMS Error = 0.010
Max Positive Error = 0.020
Box = 18
Max Negative Error = -0.024
Box = 61

CECOR
CECOR - SIMULATE-3

							1 0.390 -0.008	2 0.701 -0.002
				3 0.353 -0.007	4 0.775 -0.003	5 0.991 -0.002	6 1.090 0.006	7 0.891 0.016
			8 0.422 -0.012	9 0.921 -0.003	10 1.027 0.014	11 1.285 0.019	12 1.181 0.019	13 1.306 0.008
		14 0.426 -0.008	15 0.943 -0.006	16 1.042 -0.002	17 1.275 0.002	18 1.174 0.020	19 1.354 0.010	20 1.069 0.000
	21 0.354 -0.006	22 0.925 0.001	23 1.052 0.008	24 1.242 -0.013	25 1.027 -0.009	26 1.312 -0.004	27 1.123 0.002	28 1.281 -0.006
	29 0.775 -0.002	30 1.024 0.011	31 1.276 0.003	32 1.031 -0.005	33 1.245 -0.022	34 1.004 0.000	35 1.255 -0.009	36 0.810 0.018
45 0.388 -0.010	37 0.996 0.003	38 1.282 0.016	39 1.166 0.011	40 1.310 -0.006	41 1.004 0.000	42 1.227 -0.003	43 1.047 0.004	44 1.175 -0.003
54 0.700 -0.002	46 1.089 0.005	47 1.177 0.016	48 1.350 0.006	49 1.122 0.001	50 1.253 -0.011	51 1.040 -0.004	52 0.870 -0.019	53 0.836 0.001
	55 0.887 0.011	56 1.302 0.004	57 1.075 0.006	58 1.275 -0.012	59 0.794 0.003	60 1.156 -0.023	61 0.810 -0.024	62 0.626 -0.011

Figure 4.13 Axially Integrated Radial Power Density - S3C3F011

Date = 06/17/87
Power Level = 100.2%
Burnup = 3480. MWd/T
Absolute Difference
RMS Error = 0.011
Max Positive Error = 0.022
Box = 55
Max Negative Error = -0.032
Box = 62

Box	CECOR	CECOR - SIMULATE-3
1	0.750	-0.008
2	0.940	-0.015
3	0.693	-0.007
4	0.919	-0.013
5	1.121	0.007
6	1.082	0.013
7	0.978	-0.003
8	0.823	0.008
9	1.035	0.018
10	0.828	0.002
11	1.096	0.008
12	0.941	0.005
13	1.231	-0.016
14	0.814	0.001
15	1.141	0.014
16	1.160	0.016
17	1.137	-0.018
18	0.903	-0.001
19	1.208	-0.010
20	1.019	0.006
21	0.685	-0.014
22	1.028	0.012
23	1.153	0.011
24	0.889	0.003
25	0.956	0.001
26	1.221	-0.007
27	0.906	0.003
28	1.149	-0.021
29	0.918	-0.014
30	0.828	0.002
31	1.132	-0.020
32	0.954	0.001
33	0.914	-0.002
34	1.171	0.007
35	1.136	0.016
36	0.918	0.009
37	1.126	0.012
38	1.094	0.007
39	0.900	-0.003
40	1.216	-0.010
41	1.167	0.005
42	0.907	0.003
43	1.137	0.002
44	1.188	0.009
45	0.753	-0.005
46	1.082	0.013
47	0.938	0.002
48	1.204	-0.014
49	0.899	-0.003
50	1.130	0.012
51	1.135	0.002
52	0.800	-0.007
53	0.750	0.002
54	0.941	-0.014
55	1.003	0.022
56	1.242	-0.005
57	1.021	0.008
58	1.153	-0.017
59	0.913	0.004
60	1.169	-0.010
61	0.726	-0.022
62	0.610	-0.032

Figure 4.14 Axially Integrated Radial Power Density - S3C3F026

Date = 11/04/87
Power Level = 99.8%
Burnup = 8395. MWd/T
Absolute Difference
RMS Error = 0.011
Max Positive Error = 0.020
Box = 44
Max Negative Error = -0.022
Box = 2

Box	CECOR	CECOR - SIMULATE-3
1	0.705	-0.019
2	0.870	-0.022
3	0.678	-0.017
4	0.888	-0.020
5	1.069	-0.008
6	1.020	0.002
7	0.925	-0.014
8	0.805	-0.005
9	1.011	0.012
10	0.837	0.001
11	1.076	0.003
12	0.936	0.004
13	1.228	-0.017
14	0.799	-0.010
15	1.131	0.009
16	1.150	0.012
17	1.214	-0.009
18	0.936	0.002
19	1.250	-0.004
20	1.049	0.008
21	0.677	-0.018
22	1.007	0.009
23	1.143	0.007
24	0.912	0.005
25	0.984	0.004
26	1.258	0.002
27	0.946	0.010
28	1.250	-0.011
29	0.890	-0.018
30	0.838	0.002
31	1.210	-0.012
32	0.982	0.004
33	0.926	0.003
34	1.155	0.012
35	1.131	0.018
36	0.947	0.016
37	1.074	-0.003
38	1.076	0.005
39	0.934	0.001
40	1.254	0.000
41	1.153	0.011
42	0.904	0.009
43	1.125	0.009
44	1.210	0.020
45	0.708	-0.017
46	1.021	0.004
47	0.934	0.002
48	1.247	-0.006
49	0.941	0.006
50	1.128	0.017
51	1.125	0.011
52	0.823	0.001
53	0.789	0.011
54	0.871	-0.021
55	0.951	0.012
56	1.242	-0.003
57	1.054	0.013
58	1.255	-0.005
59	0.942	0.011
60	1.192	0.002
61	0.764	-0.014
62	0.664	-0.021

Figure 4.15 Axially Integrated Radial Power Density - S3C3F044

Date = 03/23/88
Power Level = 99.8%
Burnup = 12974. MWd/T
Absolute Difference
RMS Error = 0.012
Max Positive Error = 0.027
Box = 44
Max Negative Error = -0.025
Box = 1

Box	CECOR	CECOR - SIMULATE-3
1	0.689	-0.025
2	0.841	-0.024
3	0.674	-0.022
4	0.875	-0.021
5	1.045	-0.014
6	0.991	0.000
7	0.905	-0.015
8	0.798	-0.012
9	0.997	0.009
10	0.847	-0.001
11	1.065	0.002
12	0.937	0.004
13	1.231	-0.010
14	0.792	-0.018
15	1.129	0.009
16	1.139	0.009
17	1.264	0.004
18	0.956	0.004
19	1.273	0.005
20	1.063	0.009
21	0.674	-0.022
22	0.994	0.006
23	1.133	0.004
24	0.922	0.004
25	0.995	0.004
26	1.273	0.009
27	0.966	0.012
28	1.309	0.007
29	0.877	-0.019
30	0.849	0.002
31	1.261	0.002
32	0.992	0.002
33	0.924	0.000
34	1.131	0.008
35	1.115	0.014
36	0.961	0.019
37	1.049	-0.010
38	1.065	0.002
39	0.955	0.003
40	1.269	0.007
41	1.130	0.008
42	0.897	0.007
43	1.109	0.009
44	1.223	0.027
45	0.690	-0.024
46	0.991	0.000
47	0.934	0.001
48	1.271	0.003
49	0.961	0.007
50	1.113	0.015
51	1.110	0.011
52	0.840	0.003
53	0.822	0.020
54	0.841	-0.024
55	0.928	0.008
56	1.245	0.003
57	1.069	0.016
58	1.314	0.012
59	0.952	0.011
60	1.203	0.007
61	0.793	-0.009
62	0.708	-0.014

Figure 4.16 Core Average Axial Power Distribution - S2C1F026

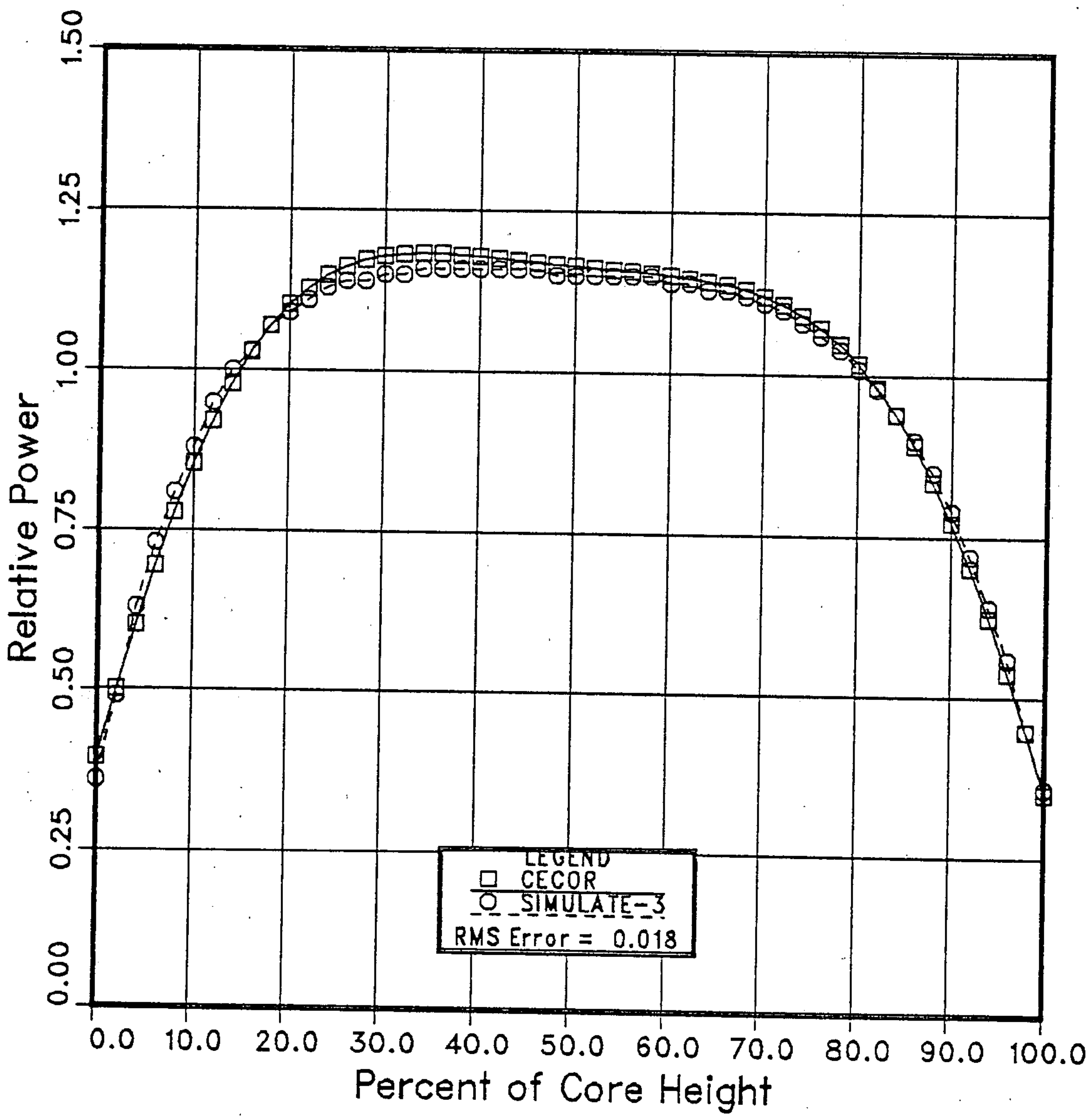

Figure 4.17 Core Average Axial Power Distribution - S2C1F038

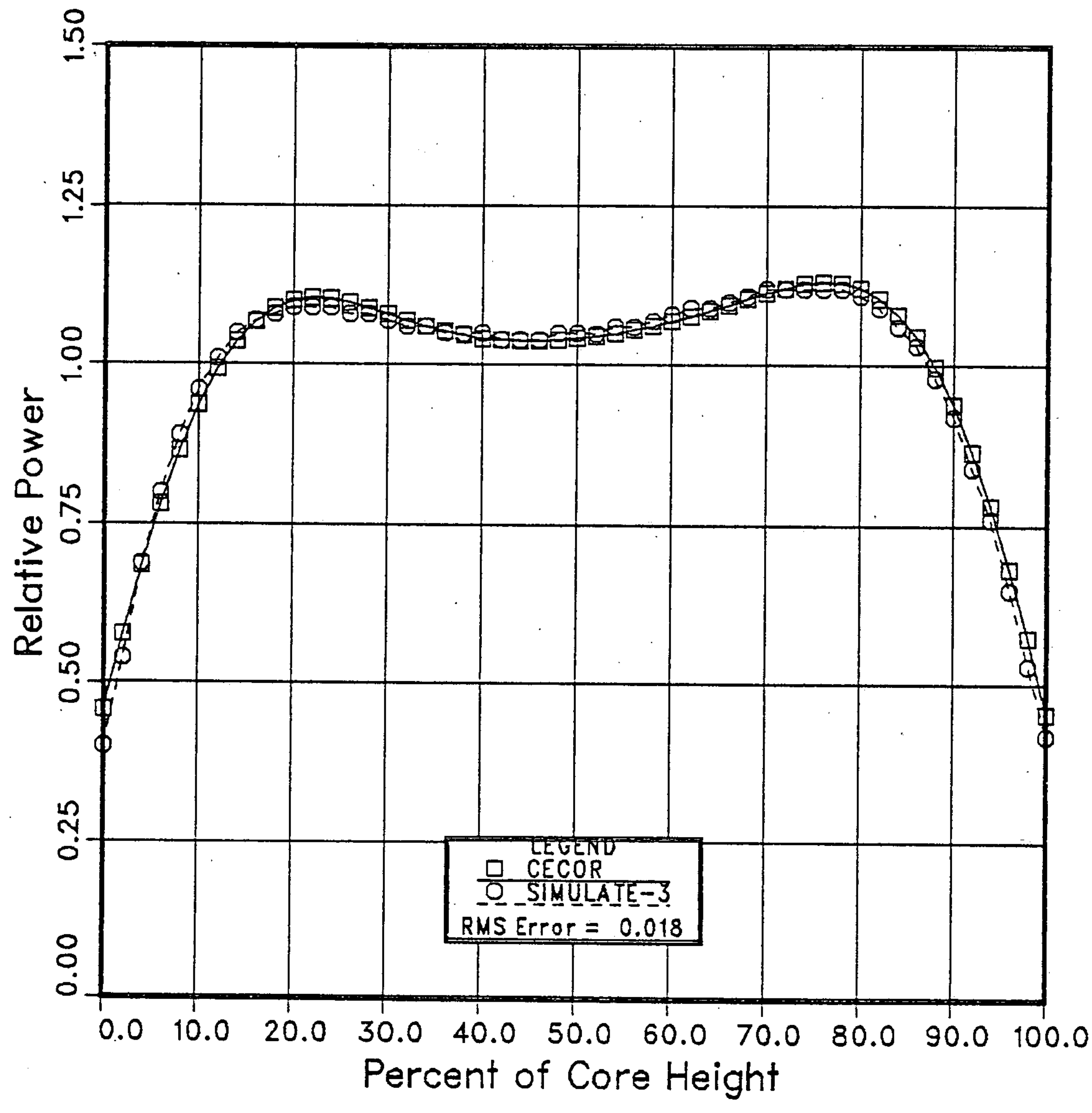

Figure 4.18 Core Average Axial Power Distribution - S2C2F051

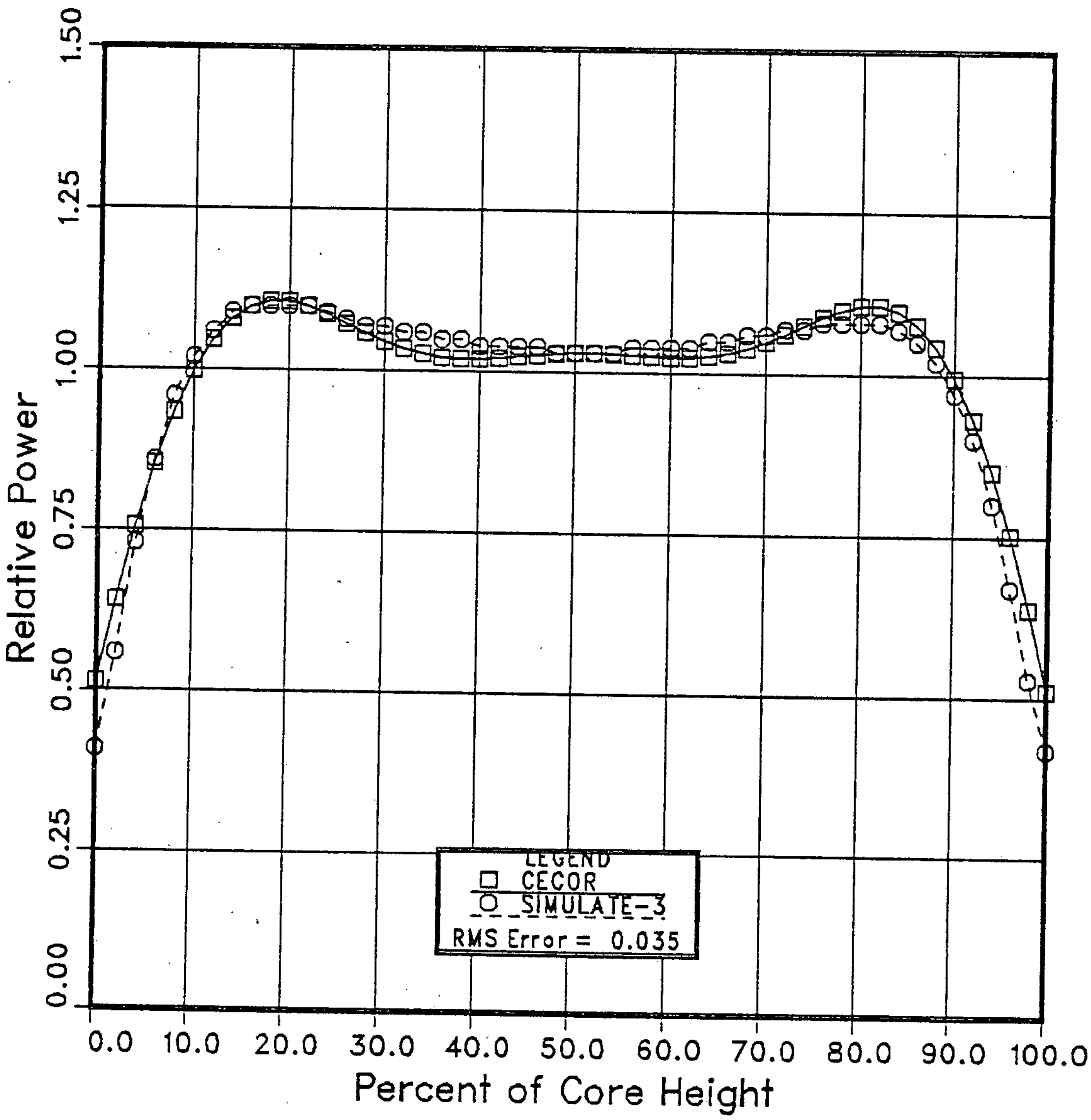

Figure 4.19 Core Average Axial Power Distribution - S2C2F055

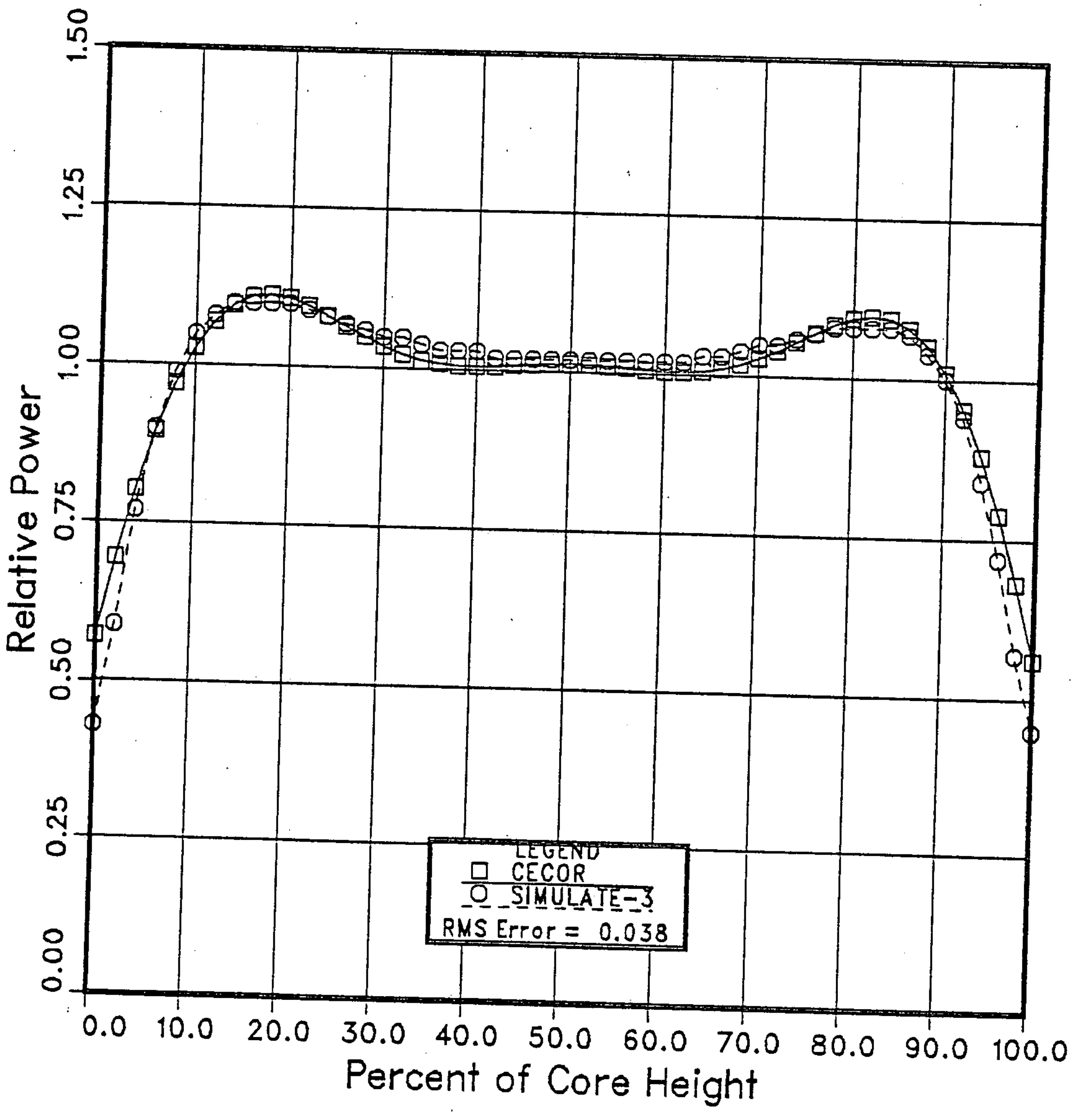

Figure 4.20 Core Average Axial Power Distribution - S2C3F005

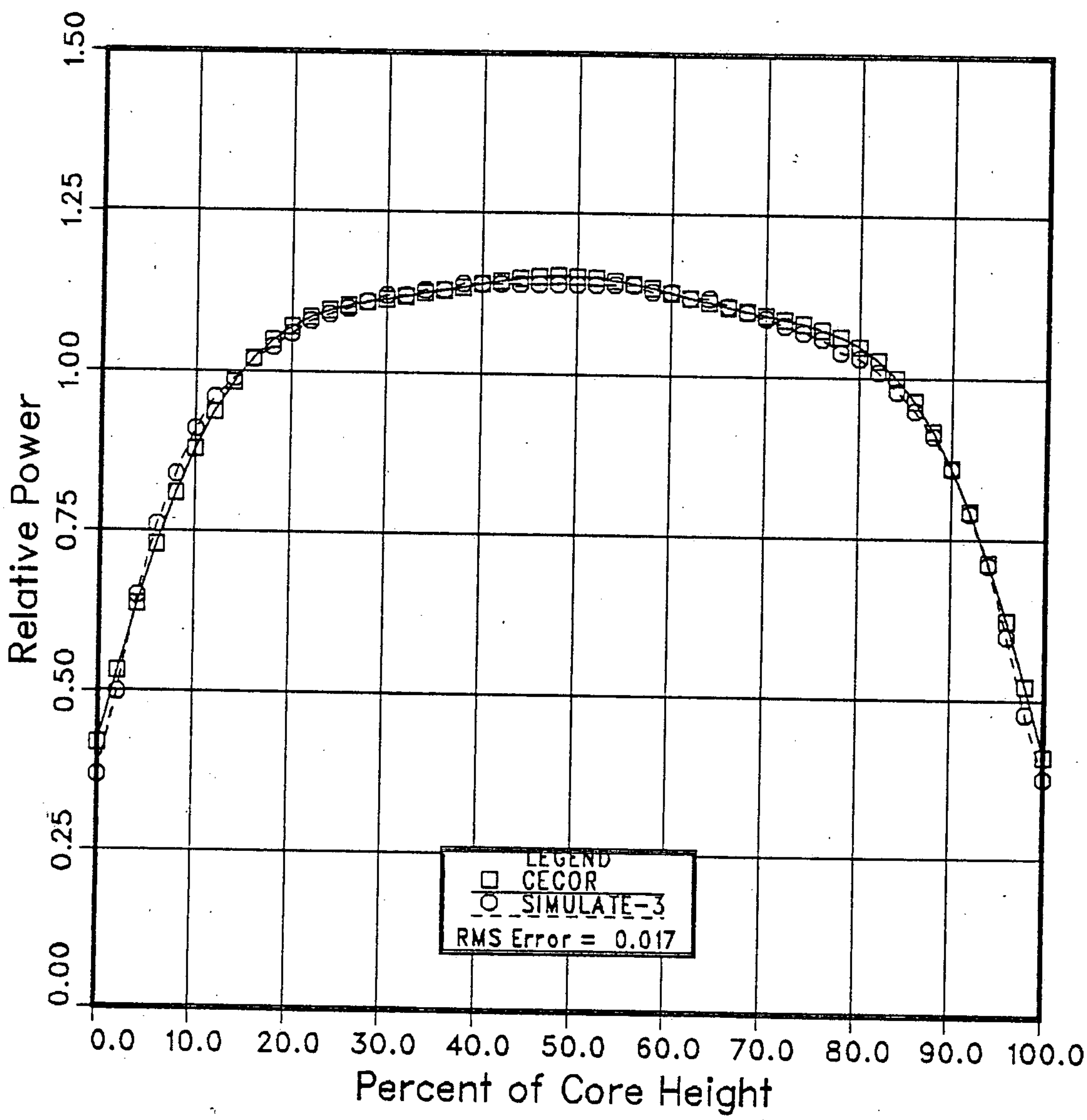

Figure 4.21 Core Average Axial Power Distribution - S2C3F027

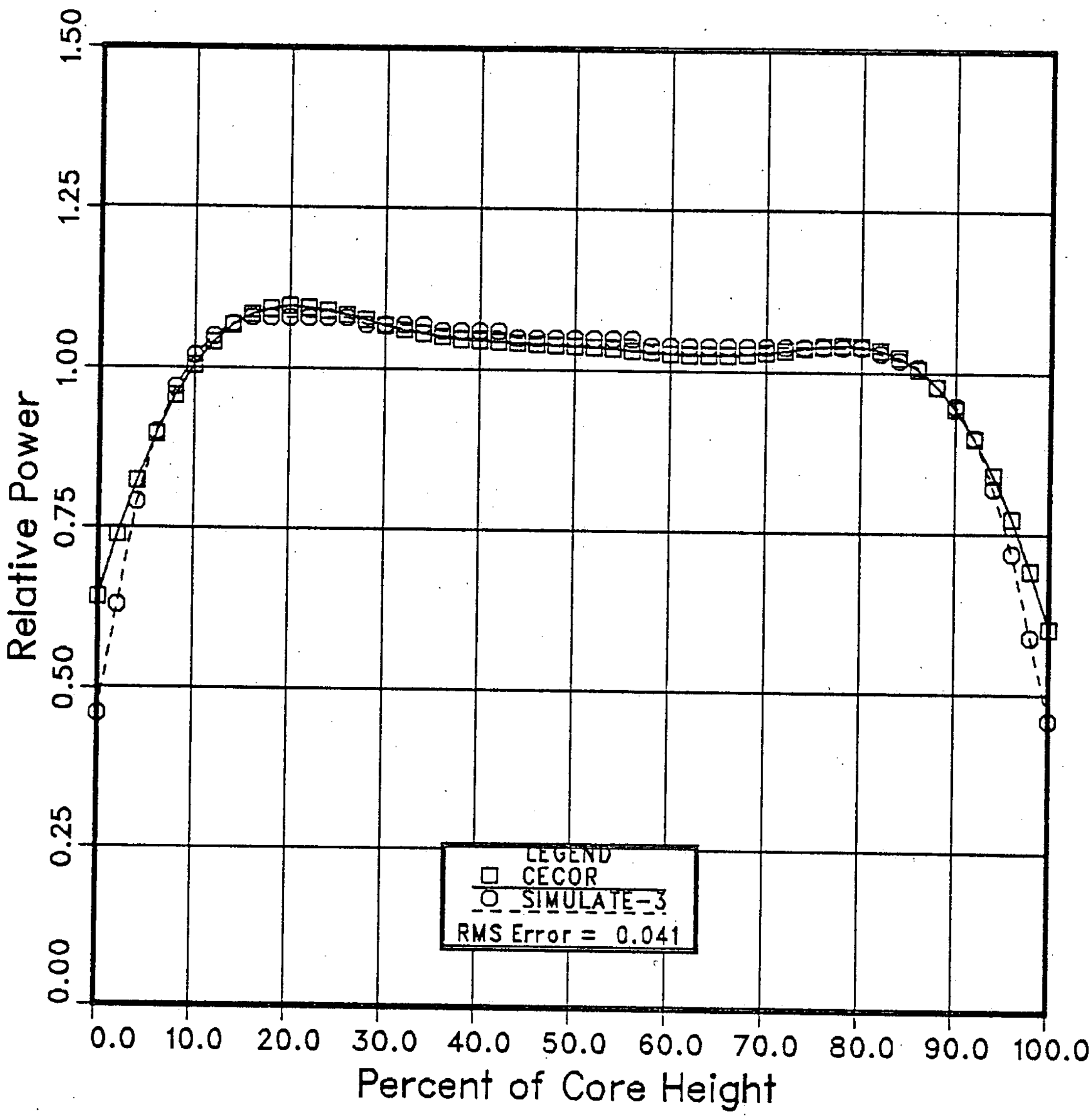

Figure 4.22 Core Average Axial Power Distribution - S2C3F048

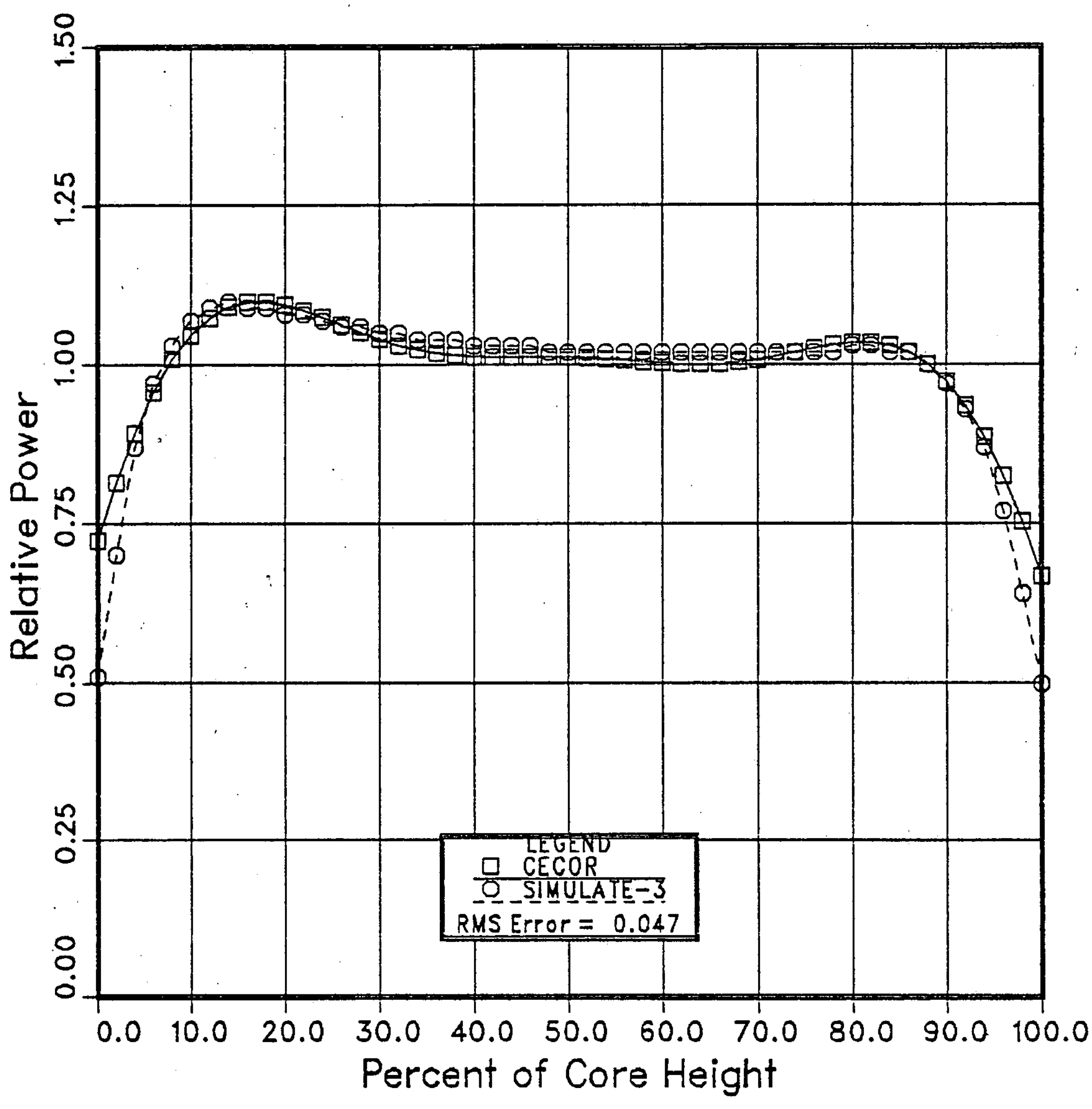

Figure 4.23 Core Average Axial Power Distribution - S2C4F007

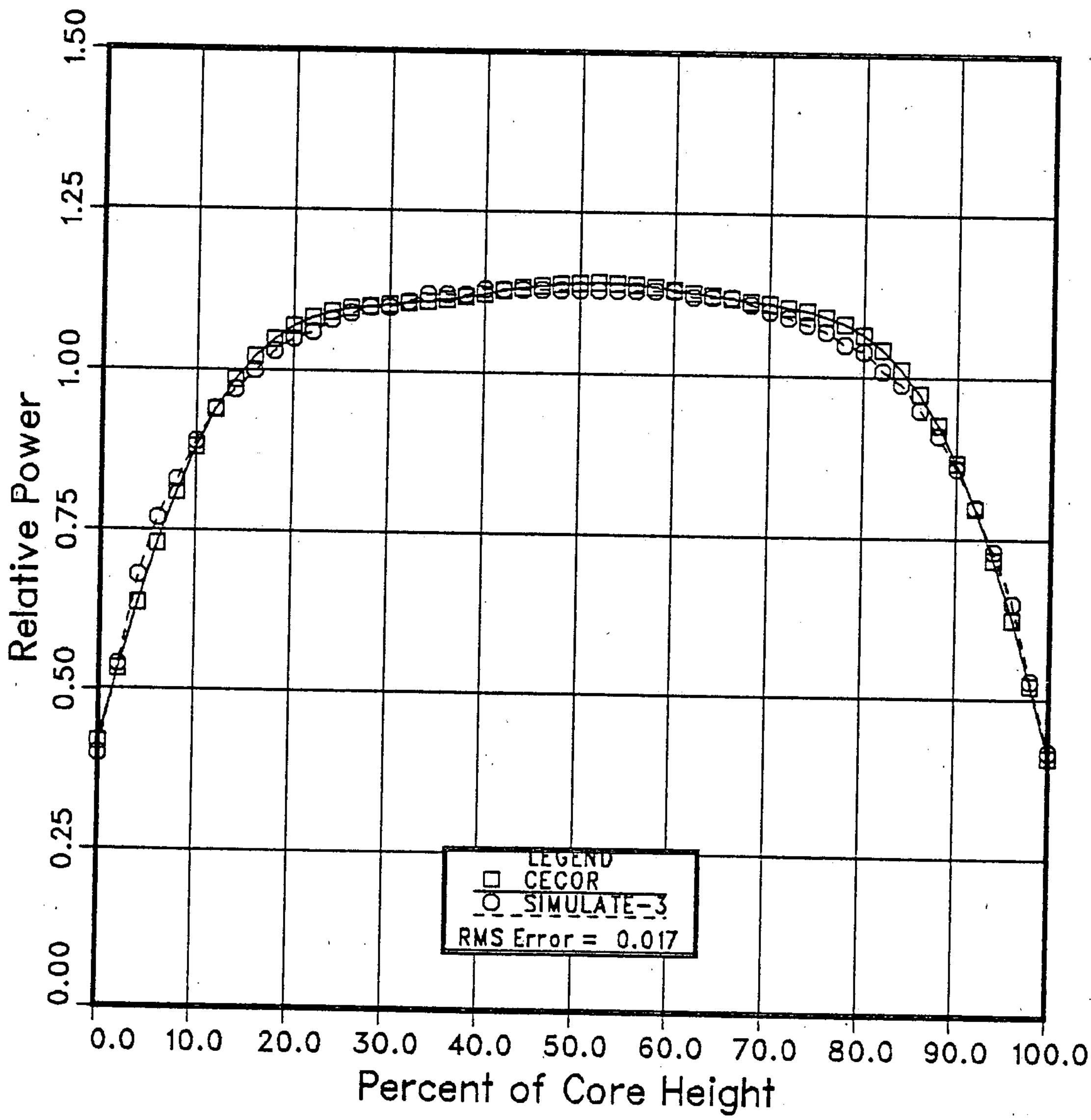

Figure 4.24 Core Average Axial Power Distribution - S2C4F042

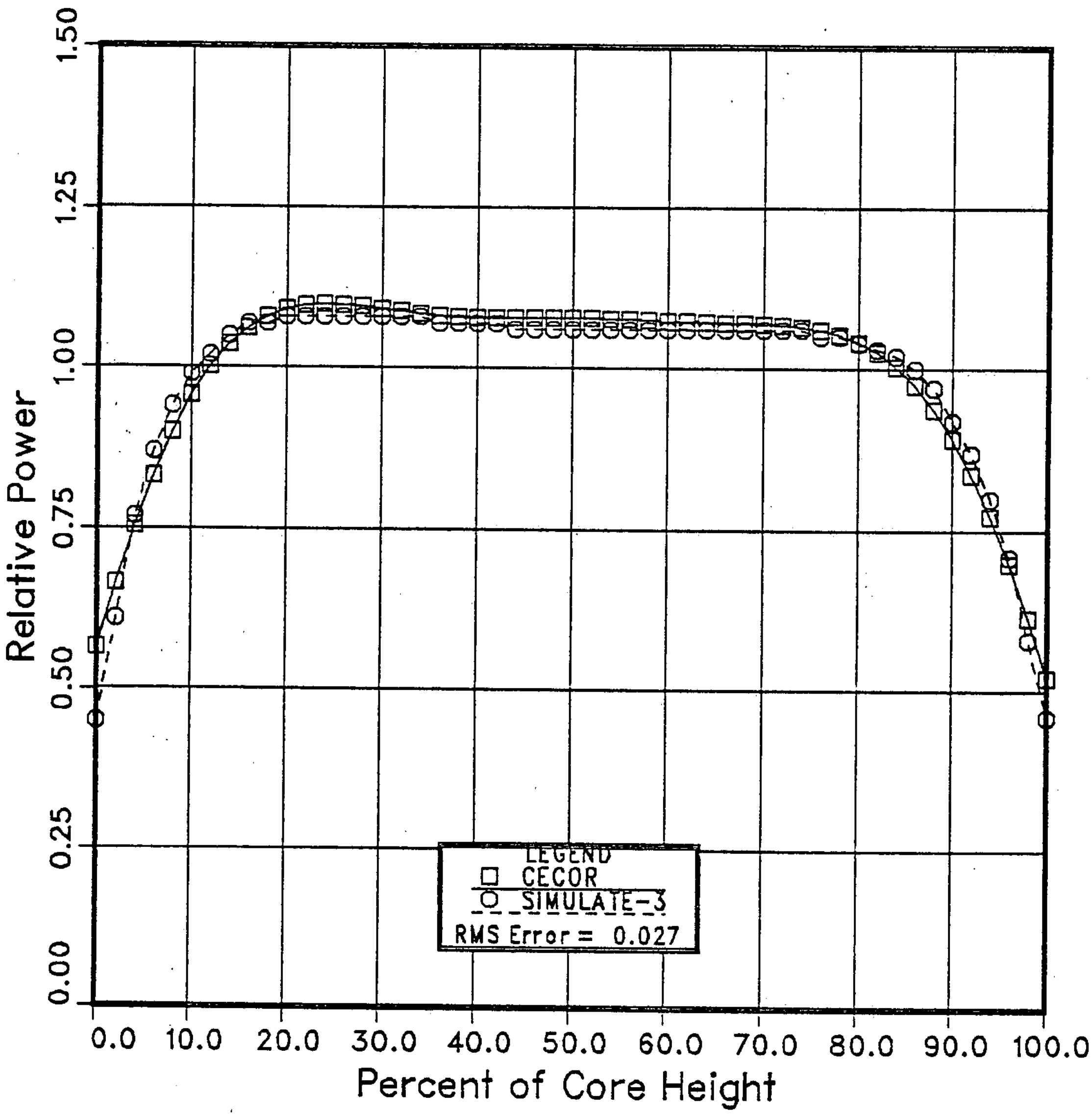

Figure 4.25 Core Average Axial Power Distribution - S3C3F011

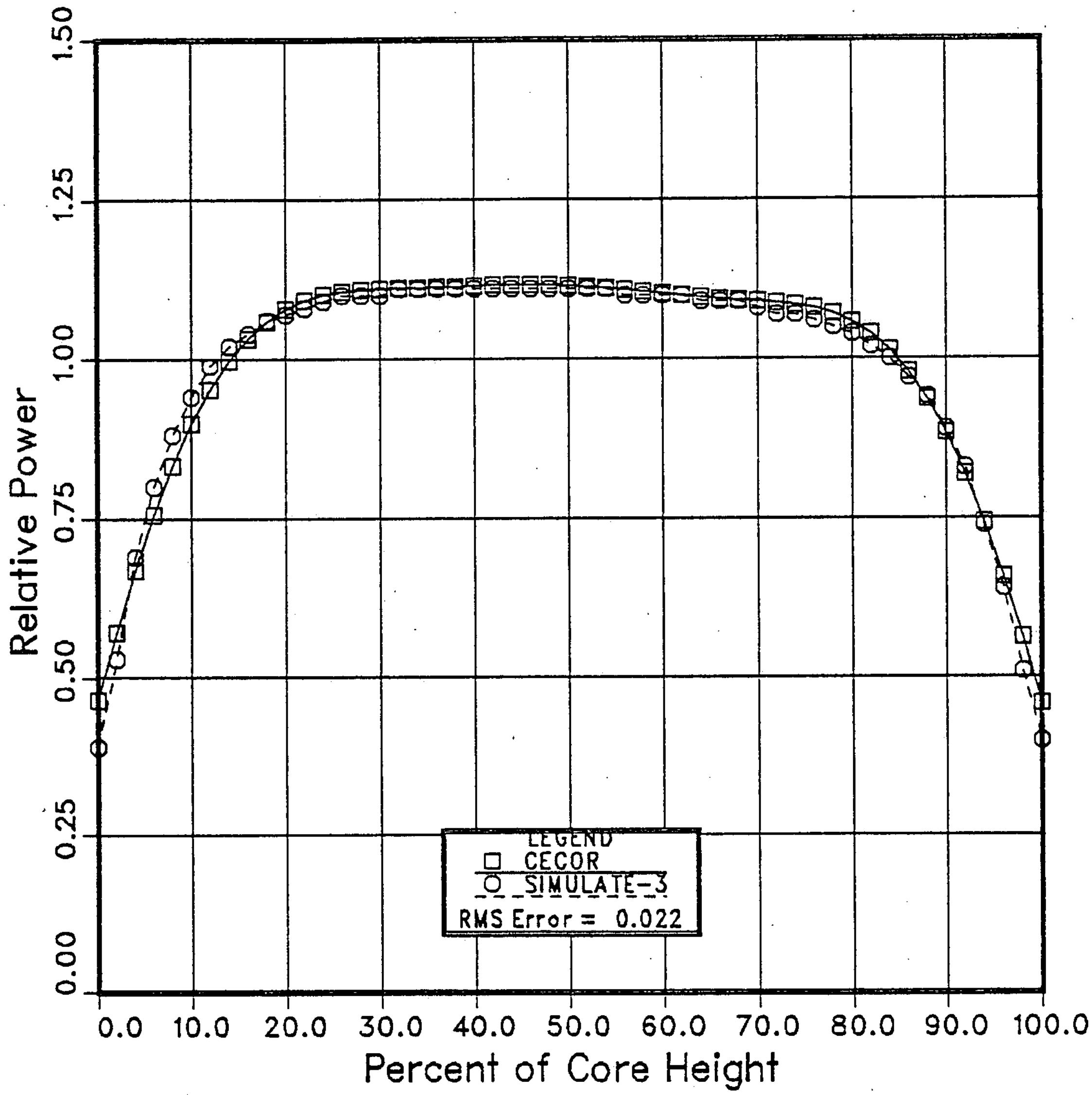

Figure 4.26 Core Average Axial Power Distribution - S3C3F026

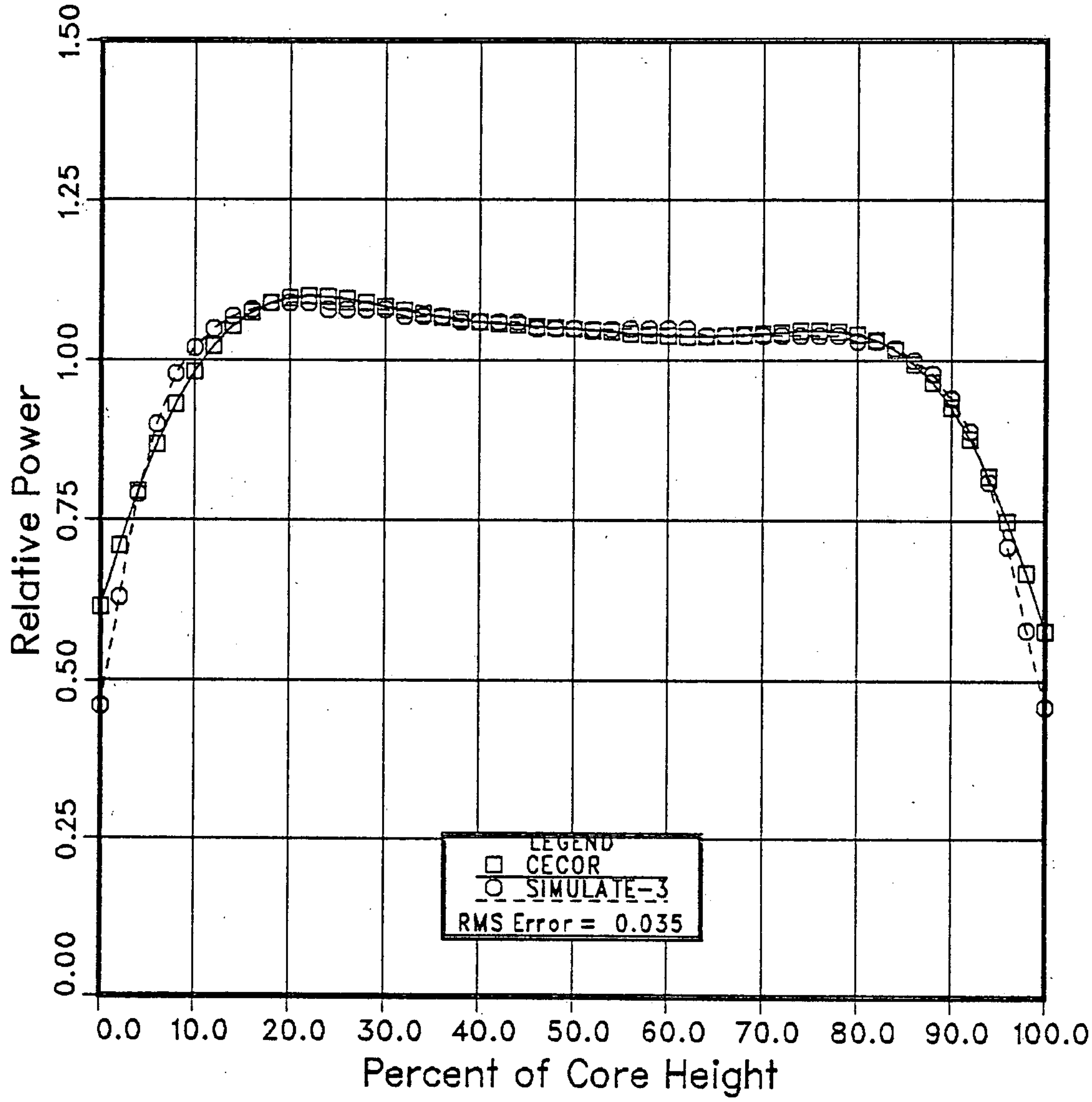

Figure 4.27 Core Average Axial Power Distribution - S3C3F044

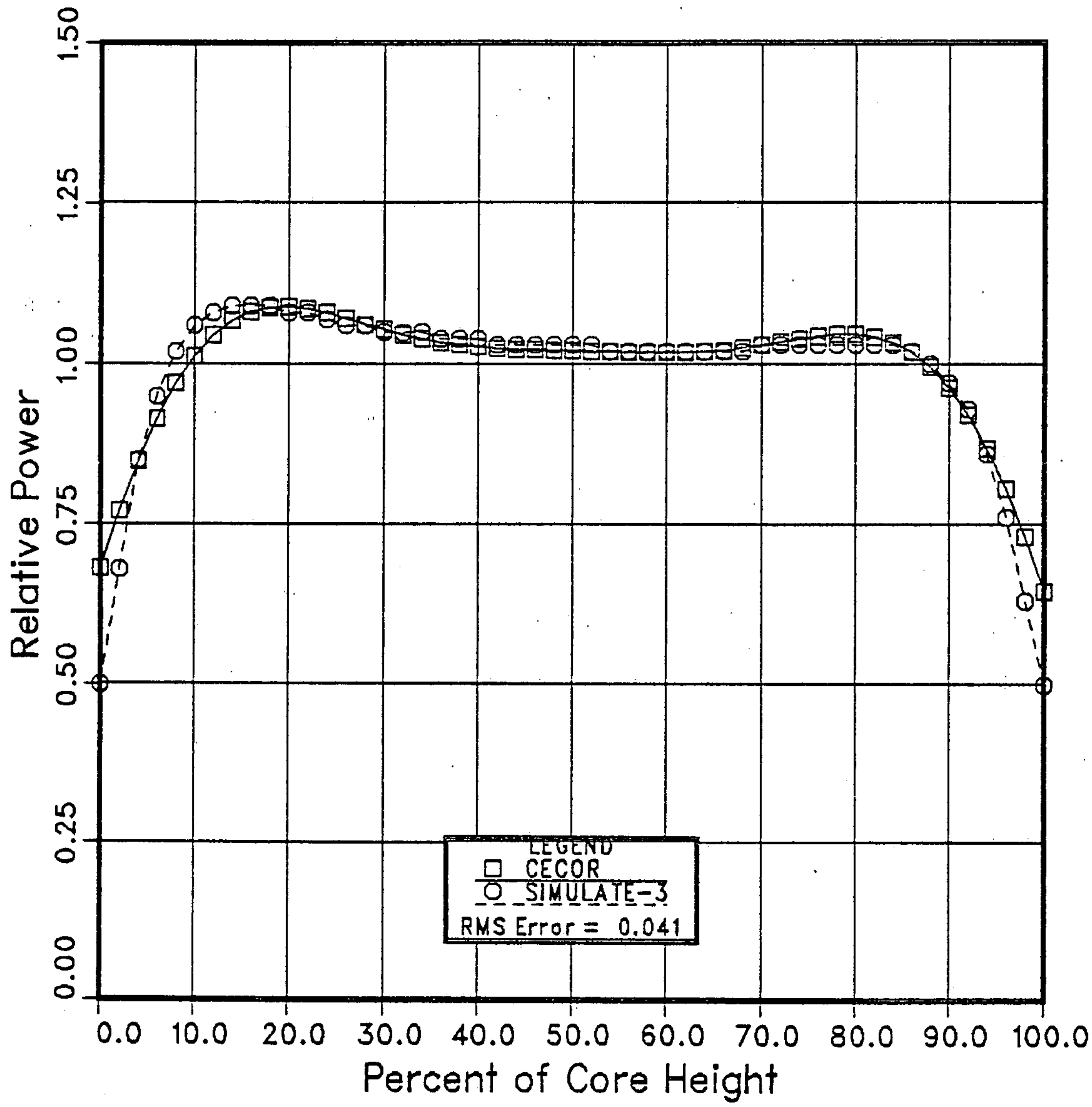

Table 4.25

Radial and Axial Power Distribution RMS Errors

SNAPSHOT ID	RADIAL RMS ERROR	AXIAL RMS ERROR
S2C1F026	0.008	0.0177
S2C1F038	0.008	0.0127
S2C2F051	0.011	0.0195
S2C2F055	0.010	0.0157
S2C3F005	0.012	0.0126
S2C3F027	0.013	0.0108
S2C3F048	0.013	0.0133
S2C4F007	0.019	0.0154
S2C4F042	0.010	0.0182
S3C3F011	0.011	0.0160
S3C3F026	0.011	0.0135
S3C3F044	0.012	0.0151

4.7.2 AXIAL OFFSET

Table 4.26 compares the axial offset, as defined in Eq. 4.7.1, for the axial power distributions shown in Figures 4.16 through 4.27. Altogether, 12 measurements from five cycles of operation were compared.

$$\text{Axial Offset} = (P_T - P_B) / (P_T + P_B) \qquad \text{(Eq. 4.7.1)}$$

P_T = Power in the top half of the core, and

P_B = Power in the bottom half of the core.

As summarized in Table 4.26, the mean and the standard deviation for the differences, (Calculated - Measured), are -0.003 and 0.005, respectively. The maximum difference is -0.011.

The 95/95 reliability factor for the calculation of the axial offset is determined using:

$$\begin{aligned}\text{Reliability Factor} &= K_{95/95} * (\text{Standard Deviation}) \\ &= K_{95/95} * 0.005 \qquad \text{(Eq. 4.7.2)}\end{aligned}$$

From Reference 16, the critical factor, $K_{95/95}$, for the sample size of 12 is 2.736. Using this value, the 95/95 reliability factor becomes 0.014.

The mean and the reliability factor are applied to the SIMULATE-3 calculation of the axial offset using:

$$\begin{aligned}\text{Predicted Axial Offset} &= (\text{Calculated Axial Offset}) * \\ &\quad (1 - \text{Bias} \pm \text{Reliability Factor}) \\ &\qquad \text{(Eq. 4.7.3)}\end{aligned}$$

Table 4.26

Axial Offset Comparison

Snapshot	Axial Offset Measured	Axial Offset Calculated	Difference
S2C1F026	-0.028	-0.025	0.003
S2C1F038	0.008	0.005	-0.003
S2C2F051	0.001	-0.010	-0.011
S2C2F055	-0.004	-0.009	-0.005
S2C3F005	-0.008	-0.013	-0.005
S2C3F027	-0.020	-0.018	0.002
S2C3F048	-0.021	-0.024	-0.003
S2C4F007	-0.001	-0.004	-0.004
S2C4F042	-0.022	-0.013	0.008
S3C3F011	-0.007	-0.014	-0.007
S3C3F026	-0.020	-0.021	-0.001
S3C3F044	-0.015	-0.021	-0.007
		Mean	-0.003
		S	0.005

4.7.3 INCORE DETECTOR SIGNAL COMPARISON

This section compares the SIMULATE-3 predicted rhodium detector reaction rates with the measured rhodium detector signals for SONGS 2 and 3. Also, the 95/95 tolerance limits were derived for the following assembly peaking factors: F^S_{XY} - planar peak power, F^S_Q - overall peak power, and F^S_R - radial power sharing ($F^S_{\Delta H}$).

Seventy-two incore detector snapshots taken close to All-Rods-Out and Hot-Full-Power conditions from Cycles 1 through 4 of SONGS 2 and 3 were used. Tables 4.27 and 4.28 summarize the conditions of these snapshots.

The detector comparison was performed in the following manner:

1. Corrected each measured detector signal for self-shielding effects based on the fraction of rhodium atoms remaining.

2. Determined Overall peak power (F^S_Q):

   At each instrumented location the difference between the SIMULATE-3 calculated signal and the corrected detector signal was found (Calculated - Measured).

3. Determined Assembly power sharing (F^S_R, $F^S_{\Delta H}$):

   At each instrumented assembly all five levels of the predicted and measured signals were summed up separately, and the difference was found.

4. Determined Planar peak power (F^S_{XY}):

   For each level, the predicted and measured signals were normalized, and the difference at each detector location was calculated.

5. Calculated the mean ($\bar{x}$) and the standard deviation (S_{obs}) for the differences in 2, 3, and 4.

6. The detector measurement uncertainty at any axial level was reflected in the variations in the detector signals from symmetric core locations. The measurement uncertainty was estimated using:

$$S^2_{meas}(\ell) = (1./(N_\ell - 1))* (\sum_g \sum_k((RR_m(k,g,\ell)-\overline{RR}_m(g,\ell))/\overline{RR}_m(g,\ell))^2 \qquad \text{(Eq. 4.7.1)}$$

Where,

ℓ = axial detector level index from 1 to 5

g = symmetric detector group index from Table 4.29

k = detector location index within each symmetric group

N_ℓ = total number of comparisons in level ℓ.

$RR_m(k,g,\ell)$ = measured individual detector signal

$\overline{RR}_m(g,\ell)$ = average signal at level ℓ in group g

7. Similar to the level-by-level measurement uncertainties, the detector channel (sum of five levels) measurement uncertainty was determined using:

$$S^2_{meas} = (1./(N - 1))*(\sum_g \sum_k((RR_m(k,g)-\overline{RR}_m(g))/\overline{RR}_m(g))^2 \qquad \text{(Eq. 4.7.2)}$$

Where,

N = total number of detector channels

$RR_m(k,g)$ = measured signal in channel k, group g

$\overline{RR}_m(g)$ = average signal in group g

8. Calculated the model uncertainties for planar peak power, overall peak power, and assembly power sharing by subtracting the measurement uncertainties from the variances of the observed differences using:

$$S^2_{model} = S^2_{obs} - S^2_{meas} \qquad \text{(Eq. 4.7.3)}$$

Using the above procedure, the standard deviations for the snapshots listed in Tables 4.27 and 4.28 were calculated. Tables 4.30 and 4.31 summarize the results, including the assembly power peaking factors. Bartlett's test (Reference 18) was used to determine the poolability of standard deviations from all the snapshots for each reactor unit. Passing the poolability test snapshots for each reactor unit. Passing the poolability test would allow for the pooling of the comparisons from all of the snapshots into one large sample to take advantage of the combined sample size and the reduced 95/95 (probability/confidence) k-value.

Table 4.3.2 summarizes the parameters used to determine whether the snapshot data could be combined into a single statistical sample. When compared with the critical values from a χ^2 distribution, the individual snapshot results cannot be pooled. For conservatism then, the maximum standard deviations were used. Table 4.33 lists the maximum standard deviations for both reactor units.

For the purpose of calculating the relative (%) uncertainties associated with SIMULATE-3 predictions of peak assembly/nodal powers, the standard deviations can be converted from power fraction (absolute) units to a percentage basis by dividing by the minimum peak assembly power for each reactor unit. Table 4.34 summarizes the maximum standard deviations S^s_{FXY}, S^s_{FQ}, and S^s_{FR} in percent.

The 95/95 tolerance limits for assembly peaking factors (F^S_{XY}, F^S_Q, and F^S_R) were calculated by multiplying the standard deviations listed in Table 4.34 with the k-value corresponding to the size of each sample. Table 4.35 summarizes the 95/95 tolerance limits for the assembly peaking factors. The 95/95 tolerance limits for F^S_{XY}, F^S_Q, and F^S_R are 4.80%, 4.17%, and 3.34%, respectively for all power levels and rodded conditions.

Table 4.27

SONGS 2 Snapshot Information

CYCLE	SNAPSHOT ID	DATE	TIME	BURNUP GWD/T	POWER (%)	BANK 6 POSITION
1	S2C1F011	08/30/83	10:54:24	3.017	99.8	150.0
1	S2C1F014	09/20/83	11:04:11	3.747	99.7	150.0
1	S2C1F026	03/08/84	05:02:00	7.289	99.5	150.0
1	S2C1F034	05/17/84	14:01:53	9.689	99.9	150.0
1	S2C1F037	06/08/84	15:10:43	10.523	99.4	150.0
1	S2C1F038	06/13/84	15:09:48	10.687	99.8	150.0
1	S2C1F039	08/01/84	10:14:13	11.088	100.4	142.5
2	S2C2F046	06/24/85	18:29:32	2.092	99.8	144.0
2	S2C2F051	08/08/85	14:28:57	3.701	99.9	142.5
2	S2C2F053	08/28/85	09:52:12	4.433	99.5	124.5
2	S2C2F055	09/11/85	16:41:14	4.972	100.0	150.0
2	S2C2F064	12/14/85	08:51:59	7.019	99.5	145.5
2	S2C2F067	01/02/86	14:36:28	7.690	100.2	145.5
2	S2C2F069	01/23/86	09:30:18	8.402	99.6	150.0
2	S2C2F077	03/12/86	13:02:45	10.009	70.2	142.5
3	S2C3F005	08/22/86	09:36:13	2.240	100.0	142.5
3	S2C3F012	09/10/86	10:38:35	2.898	100.0	147.0
3	S2C3F021	12/17/86	02:44:28	6.263	98.8	150.0
3	S2C3F027	02/18/87	08:43:24	8.746	99.1	150.0
3	S2C3F034	02/25/87	08:43:24	10.653	100.0	150.0
3	S2C3F035	04/22/87	08:26:46	10.911	99.7	150.0
3	S2C3F040	04/29/87	08:37:35	12.227	99.7	142.5
3	S2C3F041	06/03/87	10:28:45	12.445	100.0	150.0
3	S2C3F042	06/10/87	07:17:22	12.704	100.0	150.0
3	S2C3F047	06/17/87	07:20:24	13.684	99.9	150.0
3	S2C3F048	07/15/87	07:54:08	13.943	99.8	150.0
4	S2C4F001	07/29/87	09:37:12	0.471	99.2	150.0
4	S2C4F005	12/31/87	10:11:57	1.691	99.8	150.0
4	S2C4F007	2/ 3/88	10: 6: 5	2.214	99.9	150.0
4	S2C4F008	2/17/88	6:13: 7	2.480	99.6	150.0
4	S2C4F010	2/29/88	14:22:51	2.746	100.0	150.0
4	S2C4F012	3/ 2/88	10:33:16	3.273	99.4	150.0
4	S2C4F016	4/27/88	8:36:27	4.347	99.8	150.0
4	S2C4F020	5/18/88	11: 3:34	5.130	99.8	150.0
4	S2C4F024	6/15/88	8:43:42	6.191	99.5	150.0
4	S2C4F025	6/22/88	5: 0:23	6.454	99.8	150.0
4	S2C4F030	7/27/88	7:49:54	7.754	99.9	150.0
4	S2C4F032	8/10/88	8:42:55	8.273	99.3	150.0
4	S2C4F039	9/28/88	11:36:52	10.009	99.7	150.0
4	S2C4F043	10/26/88	7: 4:13	10.983	99.1	150.0

Table 4.28

SONGS 3 Snapshot Information

CYCLE	SNAPSHOT ID	DATE	TIME	BURNUP GWD/T	POWER (%)	BANK 6 POSITION
1	S3C1F013	05/31/84	10:01:17	4.051	99.8	145.5
1	S3C1F039	05/02/85	18:15:47	10.736	99.4	148.5
2	S3C2F019	05/07/86	12:52:37	2.779	99.5	145.5
2	S3C2F020	05/14/86	09:37:58	3.035	99.9	145.5
2	S3C2F022	05/27/86	13:54:17	3.531	99.6	148.5
2	S3C2F023	06/04/86	10:43:12	3.829	96.8	144.0
2	S3C2F027	07/09/86	10:46:46	5.122	85.1	148.5
2	S3C2F028	07/16/86	09:36:08	5.305	100.0	148.5
2	S3C2F032	08/20/86	10:34:18	6.433	99.7	150.0
2	S3C2F039	11/05/86	10:25:17	8.167	83.6	150.0
2	S3C2F040	11/12/86	09:23:21	8.411	83.2	145.5
2	S3C2F043	12/03/86	08:49:41	9.029	84.3	148.5
2	S3C2F044	12/11/86	09:17:27	9.319	83.6	148.5
2	S3C2F046	12/31/86	08:49:49	9.913	66.4	144.0
3	S3C3F007	05/06/87	09:04:16	1.963	99.8	150.0
3	S3C3F010	06/03/87	15:05:13	2.981	99.8	150.0
3	S3C3F011	06/17/87	07:25:59	3.481	100.2	148.5
3	S3C3F017	08/26/87	08:44:32	5.801	99.9	148.5
3	S3C3F021	09/23/87	07:46:15	6.911	99.5	150.0
3	S3C3F023	10/07/87	08:40:11	7.884	99.4	150.0
3	S3C3F026	11/04/87	07:36:17	8.398	99.8	150.0
3	S3C3F030	12/02/87	07:34:13	9.431	100.0	150.0
3	S3C3F032	12/23/87	08:27:08	10.373	99.7	150.0
3	S3C3F034	01/06/88	08:38:42	10.891	99.8	150.0
3	S3C3F035	01/13/88	13:35:31	11.527	95.3	148.5
3	S3C3F039	02/17/88	06:29:10	12.043	99.8	148.5
3	S3C3F041	03/02/88	09:52:15	12.455	99.6	148.5
3	S3C3F043	03/16/88	07:36:58	12.963	99.9	150.0
3	S3C3F046	04/06/88	09:09:44	13.497	99.7	150.0
4	S3C4F005	9/21/88	13: 2:43	1.035	99.7	150.0
4	S3C4F006	9/28/88	13:35: 6	1.299	99.6	150.0
4	S3C4F007	10/ 5/88	9:10:31	1.564	99.9	150.0

Table 4.29

SONGS 2&3 Symmetric Detector Groups

Group	Detector Number*			
1	1,	5,	52,	56
2	2,	4,	53,	55
3	3,	54		
4	6,	12,	45,	51
5	7,	11,	46,	50
6	8,	10,	47,	49
7	9,	48		
8	13,	19,	38,	44
9	14,	18,	39,	43
10	15,	17,	40,	42
11	16,	41		
12	20,	21,	36,	37
13	22,	28,	29,	35
14	23,	27,	30,	34
15	24,	26,	31,	33
16	25,	32		

* Detector locations are shown in Figure 3.6

Table 4.30

SONGS 2 Incore Detector Statistics

SNAPSHOT	BURNUP GWD/T	TOTAL S	TOTAL DF	SHARING S	SHARING DF	LEVEL - 5 S	LEVEL - 5 DF	LEVEL - 4 S	LEVEL - 4 DF	LEVEL - 3 S	LEVEL - 3 DF	LEVEL - 2 S	LEVEL - 2 DF	LEVEL - 1 S	LEVEL - 1 DF	RADIAL PEAKING
S2C1F011	3.017	0.0195	273	0.0039	50	0.0121	55	0.0069	54	0.0042	55	0.0028	55	0.0157	50	1.240
S2C1F014	3.747	0.0219	275	0.0036	52	0.0123	55	0.0070	54	0.0032	55	0.0039	55	0.0157	52	1.235
S2C1F026	7.289	0.0213	273	0.0055	53	0.0169	54	0.0089	53	0.0086	54	0.0107	54	0.0116	54	1.231
S2C1F034	9.689	0.0154	268	0.0060	52	0.0119	53	0.0063	52	0.0089	53	0.0095	53	0.0133	53	1.204
S2C1F037	10.523	0.0150	268	0.0062	52	0.0122	53	0.0068	52	0.0097	53	0.0090	53	0.0136	53	1.196
S2C1F038	10.687	0.0159	268	0.0067	52	0.0129	53	0.0077	52	0.0097	53	0.0094	53	0.0133	53	1.195
S2C1F039	11.088	0.0219	266	0.0048	48	0.0155	53	0.0061	52	0.0072	54	0.0060	53	0.0098	50	1.187
S2C2F046	2.092	0.0234	259	0.0152	47	0.0143	51	0.0145	51	0.0130	52	0.0181	51	0.0248	50	1.284
S2C2F051	3.701	0.0180	256	0.0086	47	0.0132	51	0.0091	52	0.0085	51	0.0103	50	0.0171	48	1.267
S2C2F053	4.433	0.0229	256	0.0079	47	0.0138	51	0.0090	52	0.0087	51	0.0096	50	0.0159	48	1.261
S2C2F055	4.972	0.0129	254	0.0076	46	0.0108	51	0.0091	52	0.0066	50	0.0098	50	0.0144	47	1.258
S2C2F064	7.019	0.0182	266	0.0087	47	0.0158	52	0.0100	52	0.0089	52	0.0117	54	0.0115	52	1.237
S2C2F067	7.690	0.0189	265	0.0090	46	0.0123	51	0.0113	52	0.0102	52	0.0134	54	0.0127	52	1.231
S2C2F069	8.402	0.0195	264	0.0095	45	0.0123	50	0.0122	52	0.0109	52	0.0138	54	0.0127	52	1.227
S2C2F077	10.009	0.0191	266	0.0130	47	0.0166	52	0.0131	52	0.0133	52	0.0173	54	0.0137	52	1.210
S2C3F005	2.240	0.0154	263	0.0083	44	0.0101	52	0.0086	52	0.0054	52	0.0099	54	0.0193	49	1.245
S2C3F012	2.898	0.0141	263	0.0078	44	0.0090	52	0.0077	51	0.0052	52	0.0086	54	0.0182	50	1.244
S2C3F021	6.263	0.0170	264	0.0073	45	0.0079	52	0.0101	52	0.0091	52	0.0111	54	0.0127	50	1.245
S2C3F027	8.746	0.0139	265	0.0098	46	0.0122	52	0.0133	52	0.0115	52	0.0134	54	0.0130	51	1.266
S2C3F034	10.653	0.0141	265	0.0105	46	0.0103	52	0.0138	52	0.0122	52	0.0149	54	0.0145	51	1.288
S2C3F035	10.911	0.0144	265	0.0109	46	0.0112	52	0.0141	52	0.0123	52	0.0154	54	0.0146	51	1.291
S2C3F040	12.227	0.0204	265	0.0122	46	0.0166	52	0.0154	52	0.0128	52	0.0161	54	0.0156	51	1.283
S2C3F041	12.445	0.0159	265	0.0120	46	0.0120	52	0.0153	52	0.0132	52	0.0167	54	0.0157	51	1.300
S2C3F042	12.704	0.0169	265	0.0120	46	0.0131	52	0.0151	52	0.0128	52	0.0166	54	0.0155	51	1.301
S2C3F047	13.684	0.0216	265	0.0129	46	0.0139	52	0.0158	52	0.0137	52	0.0175	54	0.0162	51	1.302
S2C3F048	13.943	0.0179	265	0.0130	46	0.0138	52	0.0159	52	0.0140	52	0.0179	54	0.0163	51	1.302
S2C4F001	0.471	0.0210	257	0.0175	42	0.0194	49	0.0176	52	0.0160	52	0.0182	52	0.0229	48	1.309
S2C4F005	1.691	0.0195	255	0.0166	40	0.0196	49	0.0181	52	0.0127	50	0.0190	52	0.0239	48	1.318
S2C4F007	2.214	0.0200	256	0.0185	41	0.0183	49	0.0182	52	0.0158	51	0.0196	52	0.0231	48	1.320
S2C4F008	2.480	0.0208	256	0.0188	41	0.0184	49	0.0179	52	0.0165	51	0.0197	52	0.0238	48	1.321
S2C4F010	2.746	0.0198	255	0.0166	40	0.0178	49	0.0178	52	0.0132	50	0.0194	52	0.0235	48	1.322
S2C4F012	3.273	0.0204	255	0.0158	40	0.0180	49	0.0170	52	0.0134	50	0.0181	52	0.0225	48	1.324
S2C4F016	4.347	0.0211	245	0.0154	34	0.0177	48	0.0174	52	0.0138	49	0.0183	50	0.0196	42	1.327
S2C4F020	5.130	0.0206	245	0.0152	34	0.0172	48	0.0174	52	0.0139	49	0.0181	50	0.0195	42	1.330
S2C4F024	6.191	0.0202	244	0.0152	34	0.0175	48	0.0180	51	0.0142	49	0.0172	50	0.0201	42	1.334
S2C4F025	6.454	0.0187	243	0.0151	34	0.0168	48	0.0177	51	0.0135	49	0.0155	49	0.0196	42	1.334
S2C4F030	7.754	0.0175	241	0.0130	32	0.0175	48	0.0132	49	0.0147	48	0.0174	50	0.0193	42	1.339
S2C4F032	8.273	0.0187	241	0.0128	32	0.0181	48	0.0132	49	0.0143	48	0.0176	50	0.0199	42	1.341
S2C4F039	10.009	0.0170	249	0.0126	37	0.0191	49	0.0140	49	0.0126	48	0.0138	52	0.0182	47	1.344
S2C4F043	10.983	0.0183	250	0.0133	37	0.0186	49	0.0143	49	0.0136	48	0.0170	53	0.0193	47	1.344
POOLED		0.0187	10379	0.0116	1750	0.0149	2037	0.0134	2069	0.0117	2053	0.0147	2103	0.0174	1957	

* DF: Degrees-of-Freedom

Table 4.31

SONGS 3 Incore Detector Statistics

SNAPSHOT	BURNUP GWD/T	TOTAL S	TOTAL DF	SHARING S	SHARING DF	LEVEL - 5 S	LEVEL - 5 DF	LEVEL - 4 S	LEVEL - 4 DF	LEVEL - 3 S	LEVEL - 3 DF	LEVEL - 2 S	LEVEL - 2 DF	LEVEL - 1 S	LEVEL - 1 DF	RADIAL PEAKING
S3C1F013	4.051	0.0226	277	0.0065	53	0.0103	54	0.0067	55	0.0028	55	0.0051	55	0.0172	54	1.235
S3C1F039	10.736	0.0207	274	0.0069	51	0.0108	54	0.0058	54	0.0107	53	0.0109	55	0.0137	54	1.194
S3C2F019	2.779	0.0239	270	0.0190	50	0.0175	52	0.0164	52	0.0174	54	0.0221	54	0.0280	54	1.279
S3C2F020	3.035	0.0241	268	0.0163	48	0.0152	51	0.0153	52	0.0154	54	0.0190	54	0.0253	53	1.276
S3C2F022	3.531	0.0224	268	0.0160	48	0.0141	52	0.0136	51	0.0140	54	0.0196	54	0.0246	53	1.272
S3C2F023	3.829	0.0191	268	0.0142	48	0.0128	52	0.0129	51	0.0126	54	0.0156	54	0.0231	53	1.267
S3C2F027	5.122	0.0157	268	0.0114	48	0.0103	52	0.0109	51	0.0102	54	0.0124	54	0.0210	53	1.257
S3C2F028	5.305	0.0195	268	0.0103	48	0.0091	52	0.0106	51	0.0087	54	0.0118	54	0.0204	53	1.255
S3C2F032	6.433	0.0237	268	0.0097	48	0.0093	51	0.0110	51	0.0092	54	0.0109	54	0.0194	54	1.246
S3C2F039	8.167	0.0172	271	0.0114	51	0.0133	53	0.0119	52	0.0104	54	0.0130	54	0.0211	54	1.232
S3C2F040	8.411	0.0192	271	0.0109	51	0.0111	53	0.0088	52	0.0103	54	0.0113	54	0.0187	54	1.227
S3C2F043	9.029	0.0180	271	0.0122	51	0.0134	53	0.0118	52	0.0117	54	0.0116	54	0.0186	54	1.223
S3C2F044	9.319	0.0181	270	0.0111	50	0.0117	52	0.0102	52	0.0107	54	0.0114	54	0.0189	54	1.221
S3C2F046	9.913	0.0163	271	0.0119	51	0.0144	53	0.0106	52	0.0118	54	0.0120	54	0.0188	54	1.212
S3C3F007	1.963	0.0241	261	0.0137	45	0.0163	51	0.0082	51	0.0104	53	0.0186	51	0.0246	51	1.248
S3C3F010	2.981	0.0196	260	0.0093	45	0.0132	51	0.0029	50	0.0049	53	0.0131	51	0.0237	51	1.247
S3C3F011	3.481	0.0164	260	0.0066	44	0.0115	51	0.0002	51	0.0045	53	0.0104	51	0.0176	50	1.247
S3C3F017	5.801	0.0253	261	0.0049	45	0.0086	51	0.0078	51	0.0084	53	0.0078	51	0.0131	51	1.244
S3C3F021	6.911	0.0247	260	0.0051	44	0.0085	51	0.0092	50	0.0094	53	0.0074	51	0.0123	51	1.248
S3C3F023	7.884	0.0187	259	0.0045	43	0.0081	51	0.0090	50	0.0081	53	0.0065	51	0.0107	50	1.253
S3C3F026	8.398	0.0144	259	0.0070	43	0.0087	51	0.0119	50	0.0109	52	0.0088	51	0.0112	51	1.261
S3C3F030	9.431	0.0210	260	0.0083	44	0.0099	51	0.0128	50	0.0123	53	0.0099	51	0.0115	51	1.275
S3C3F032	10.373	0.0144	259	0.0082	43	0.0096	51	0.0140	50	0.0116	52	0.0091	50	0.0121	52	1.286
S3C3F034	10.891	0.0233	260	0.0092	44	0.0101	51	0.0142	50	0.0132	53	0.0100	51	0.0118	51	1.291
S3C3F035	11.527	0.0210	260	0.0084	44	0.0094	51	0.0137	50	0.0120	52	0.0100	51	0.0121	52	1.291
S3C3F039	12.043	0.0167	260	0.0109	44	0.0140	51	0.0165	50	0.0141	53	0.0109	51	0.0122	51	1.294
S3C3F041	12.455	0.0195	260	0.0111	44	0.0143	51	0.0159	50	0.0141	53	0.0112	51	0.0125	51	1.295
S3C3F043	12.963	0.0193	261	0.0111	45	0.0148	51	0.0166	50	0.0146	53	0.0110	51	0.0133	52	1.302
S3C3F046	13.497	0.0234	261	0.0117	45	0.0133	51	0.0167	50	0.0147	53	0.0121	51	0.0145	52	1.302
S3C4F005	1.035	0.0275	258	0.0181	44	0.0261	52	0.0195	50	0.0181	51	0.0186	50	0.0171	51	1.305
S3C4F006	1.299	0.0262	258	0.0184	44	0.0265	52	0.0198	50	0.0179	51	0.0187	50	0.0165	51	1.307
S3C4F007	1.564	0.0249	258	0.0181	44	0.0260	52	0.0199	50	0.0181	51	0.0185	50	0.0166	51	1.308
POOLED		0.0209	8458	0.0117	1490	0.0141	1655	0.0128	1631	0.0122	1701	0.0132	1672	0.0180	1671	

* DF: Degrees-of-Freedom

Table 4.32

Bartlett's Test Results for Assembly Peaking Factors

SONGS 2

	Total	Sharing	Level-5	Level-4	Level-3	Level-2	Level-1
b-value	447.6	528.5	192.0	412.8	413.2	512.5	208.2
DF*	39	39	39	39	39	39	39
$\chi^2_{0.05}$	55.6	55.6	55.6	55.6	55.6	55.6	55.6
Conclusion	Fail	Fail	Fail	Fail	Fail	Fail	Fail

SONGS 3

	Total	Sharing	Level-5	Level-4	Level-3	Level-2	Level-1
b-value	487.5	380.1	384.4	745.2	386.2	354.3	250.0
DF*	31	31	31	31	31	31	31
$\chi^2_{0.05}$	40.3	40.3	40.3	40.3	40.3	40.3	40.3
Conclusion	Fail	Fail	Fail	Fail	Fail	Fail	Fail

* DF: Degrees-of-Freedom

Table 4.33

The Least Favorable Standard Deviations

for Assembly Peaking Factors

	SONGS-2	SONGS-3
S^{S}_{FXY}	0.0248	0.0280
Degrees-of-Freedom	50	54
S^{S}_{FQ}	0.0234	0.0275
Degrees-of-Freedom	259	258
S^{S}_{FR}	0.0188	0.0190
Degrees-of-Freedom	41	50

Table 4.34

Calculation of Maximum Standard Deviations

in Terms of Percent

	SONGS-2	SONGS-3	MAXIMUM
S^{S}_{FXY} (Absolute)	0.0248	0.0280	
Minimum F^{R}	1.187	1.194	
S^{S}_{FXY} (%)	2.09	2.35	2.35
Degrees-of-Freedom	50	54	
S^{S}_{FQ} (Absolute)	0.0234	0.0275	
Minimum F_{R}	1.187	1.194	
S^{S}_{FQ} (%)	1.97	2.30	2.30
Degrees-of-Freedom	259	258	
S^{S}_{FR} (Absolute)	0.0188	0.0190	
Minimum F_{R}	1.187	1.194	
S^{S}_{FR} (%)	1.58	1.59	1.59
Degrees-of-Freedom	41	50	

Table 4.35

Calculation of 95/95 Tolerance Limits

for Assembly Power Peaking

	SONGS-2	SONGS-3	MAXIMUM
S^{S}_{FXY} (%)	2.09	2.35	2.35
Degrees-of-Freedom	50	54	
$K_{95/95}$	2.060	2.042	
$K_{95/95}S$ (%)	4.30	4.80	4.80
S^{S}_{FQ} (%)	1.97	2.30	2.30
Degrees-of Freedom	259	258	
$K_{95/95}$	1.812	1.813	
$K_{95/95}S$ (%)	3.57	4.17	4.17
S^{S}_{FR} (%)	1.58	1.59	1.59
Degrees-of-Freedom	41	50	
$K_{95/95}$	2.111	2.060	
$K_{95/95}S$ (%)	3.34	3.28	3.34

SECTION 5

PIN PEAKING FACTOR UNCERTAINTIES

5.0 INTRODUCTION

The SIMULATE-3 pin peaking factor uncertainties for the Planar Radial Peaking Factor (F_{XY}), One-Pin Peaking Factor (F_Q), and Integrated Radial Peaking Factor (F_R, $F_{\Delta H}$) were determined by combining the assembly power peaking uncertainties (S^S_{FXY}, S^S_{FQ}, and S^S_{FR}) from Section 4.7.3 with an appropriate uncertainty factor for the pin power reconstruction.

Yankee Atomic Electric Company verified the pin power reconstruction capabilities of SIMULATE-3 in extensive benchmarking (Reference 8). Three of the benchmark problems, B&W critical experiments: Core 01, Core 12, and Core 18; were lattice configurations (pin dimensions, water hole, etc.) similar to the SONGS lattices.

Section 5.1 describes the three B&W cases and the results which were used as an estimate of the pin power reconstruction uncertainty. Since the lattice configurations are explicitly represented in the model, the pin power reconstruction uncertainty is applicable to lattices with small water holes (W) and large water holes (CE).

In Section 5.2 the uncertainties for pin peaking factors were calculated by combining the assembly power peaking uncertainties (Section 4.7.3) with the pin power reconstruction uncertainty (Section 5.1).

5.1 PIN POWER RECONSTRUCTION UNCERTAINTY

This section compares the SIMULATE-3 predicted pin-by-pin power distributions with the measured data from B&W critical core configurations 01, 12, and 18 described in Reference 19.

Figures 5.1 through 5.3 show the SIMULATE-3 pin power distributions and the measurements. The differences, (Calculated - Measured)/Calculated, are also shown for each pin location. The SIMULATE-3 results agree well with the measurements. The Root-Mean-Squares (RMS) are all within one percent. Table 5.1 summarizes the mean ($\bar{x}$), standard deviation (S), and RMS for each case.

The standard deviations from these cases were tested for poolability with the Bartlett's test (Reference 20). Table 5.2 summarizes the parameters. The test confirms that the samples are poolable. Table 5.3 provides the pooled mean ($\bar{x}$), standard deviation (S), as well as the K*S value for the 95/95 tolerance limit.

The tolerance limit ($\bar{x} - K_{95/95}S$) was calculated by subtracting the mean from the $K_{95/95}S_{pooled}$. Since the sample mean was very small and positive, it was assumed zero. The resulting tolerance limit was 1.608%. For conservatism, the 95/95 tolerance limit for pin power reconstruction, $K_{95/95}S(pin)$, was set to 2.00%.

Figure 5.1

Pin Power Distribution Comparison

B&W Core 01

Measured	----	1.018	1.011	0.987	0.981	0.997	0.966	0.945
SIM-3	----	1.037	1.003	0.989	0.985	0.982	0.963	0.943
Diff (%)	----	1.83	-0.80	0.20	0.41	-1.53	-0.31	-0.21
		1.019	1.067	1.012	1.009	1.058	0.999	0.945
		1.030	1.068	1.014	1.011	1.050	0.984	0.947
		1.07	0.09	0.20	0.20	-0.76	-1.52	0.21
			----	1.081	1.090	----	1.032	0.953
			----	1.083	1.085	----	1.040	0.952
			----	0.18	-0.46	----	0.77	-0.11
				1.054	1.104	1.086	0.989	0.945
				1.060	1.105	1.087	0.990	0.946
				0.57	0.09	0.09	0.10	0.11
					----	1.059	0.965	0.934
					----	1.057	0.962	0.934
					----	-0.19	-0.31	0.00
AVG. (%)		0.012				0.988	0.938	0.923
						0.983	0.942	0.924
RMS (%)		0.631				-0.51	0.42	0.11
S.D. (%)		0.641					0.925	0.914
							0.927	0.914
							0.22	0.00
								0.903
								0.905
								0.22

Figure 5.2

Pin Power Distribution Comparison

B&W Core 12

Measured	----	1.075	1.041	1.006	1.019	1.000	0.960	0.923
SIM-3	----	1.095	1.033	1.012	0.999	0.987	0.956	0.920
Diff (%)	----	1.83	-0.77	0.59	-2.00	-1.32	-0.42	-0.33
		1.067	1.125	1.044	1.034	1.075	0.987	0.927
		1.073	1.123	1.040	1.028	1.079	0.979	0.923
		0.56	-0.18	-0.38	-0.58	0.37	-0.82	-0.43
			----	1.114	1.118	----	1.034	0.942
			----	1.127	1.119	----	1.052	0.924
			----	1.15	0.09	----	1.71	-1.95
				1.083	1.137	1.102	0.979	0.908
				1.078	1.138	1.108	0.977	0.913
				-0.46	0.09	0.54	-0.20	0.55
					----	1.071	0.939	0.895
					----	1.067	0.938	0.896
					----	-0.37	-0.11	0.11
AVG (%)		-0.048				0.958	0.900	0.883
						0.965	0.911	0.879
RMS (%)		0.872				0.73	1.21	-0.46
S.D. (%)		0.885					0.884	0.856
							0.885	0.860
							0.11	0.47
								0.845
								0.838
								-0.84

Figure 5.3

Pin Power Distribution Comparison

B&W Core 18

Measured	----	1.205	1.033	0.997	0.977	0.959	0.941	0.909
SIM-3	----	1.217	1.035	1.002	0.988	0.970	0.948	0.922
Diff (%)	----	0.99	0.19	0.50	1.11	1.13	0.74	1.41
		1.076	1.021	1.012	1.010	0.982	0.946	0.912
		1.082	1.033	1.028	1.014	0.983	0.951	0.920
		0.55	1.16	1.56	0.39	0.10	0.53	0.87
			1.065	1.228	1.203	1.043	0.957	0.928
			1.079	1.211	1.197	1.038	0.958	0.919
			1.30	-1.40	-0.50	-0.48	0.10	-0.98
				----	----	1.183	0.974	0.924
				----	----	1.168	0.966	0.913
				----	----	-1.28	-0.83	-1.20
					----	1.170	0.970	0.909
					----	1.154	0.953	0.901
					----	-1.39	-1.78	-0.89
AVG. (%)		0.048				0.995	0.924	0.886
						0.999	0.922	0.883
RMS (%)		0.925				0.40	-0.22	-0.34
S.D. (%)		0.939					0.893	0.866
							0.890	0.862
							-0.34	-0.46
								0.833
								0.838
								0.60

Table 5.1

SIMULATE-3 Pin Power Distribution

Benchmark Results

CASE	$\bar{x}$ (%)	S (%)	RMS (%)	N
Core 01	0.012	0.641	0.631	32
Core 12	-0.048	0.885	0.872	32
Core 18	0.048	0.939	0.925	32

Table 5.2

Bartlett's Test Results for Pin Power Distributions

b-value	4.773
Degrees-of-Freedom	2
$\chi^2_{0.05}$	5.991
Conclusion	Poolable
S_{pooled} (%)	0.832

Table 5.3

Pooled Statistics for SIMULATE-3

Pin Power Distribution

Benchmark Results

$\bar{X}$ (%)	S_{pooled} (%)	N	$K_{95/95}$	$K_{95/95}S_{POOLED}$ (%)
0.004	0.832	96	1.933	1.608

For conservatism, the tolerance limit is set to 2.00%

5.2 CALCULATION OF PIN PEAKING FACTOR UNCERTAINTIES

The 95/95 tolerance limits for Planar Radial Peaking Factor (F_{XY}), One-Pin Peaking Factor (F_Q), and the Integrated Radial Peaking Factor (F_R, $F_{\Delta H}$) can be calculated by using:

$$K_{95/95}S(\text{combined}) = ((K_{95/95}S(\text{assembly}))^2 + (K_{95/95}S(\text{pin}))^2)^{1/2} \quad \text{(Eq. 5.2.1)}$$

where,

$K_{95/95}S$(assembly) are the 95/95 tolerance limits for assembly power peaking. From Section 4.7.3, the 95/95 tolerance limits for F^S_{XY}, F^S_Q, and F^S_R are 4.80%, 4.17%, and 3.34%, respectively.

$K_{95/95}S$(pin) is the 95/95 tolerance limit for the pin power reconstitution. From Section 5.1, this uncertainty component is 2%.

Table 5.4 summarizes the calculation of the tolerance limits for F_{XY}, F_Q, and F_R ($F_{\Delta H}$) of 5.20%, 4.62%, and 3.89%, respectively.

The tolerance limits are applied to the SIMULATE-3 calculated peaking factors at all power levels and for all rodded and unrodded cases using:

Adjusted Peaking Factor = (SIMULATE-3 results) * (1 + Tolerance Limit/100)

(Eq. 5.2.2)

Table 5.4

Calculation of Peaking Factor Tolerance Limits

	$K_{95/95}S$ (Assembly) (%)	$K_{95/95}S$ (Pin) (%)	$K_{95/95}S$ (Combined) (%)
F_{XY}	4.780	2.000	5.20
F_Q	4.170	2.000	4.62
F_R	3.340	2.000	3.89

SECTION 6

CONCLUSIONS

Southern California Edison Company (SCE) has performed extensive benchmarking using the CASMO-3/SIMULATE-3 methodology. This effort consisted of comparisons of calculated physics parameters to measurements from both Pressurized Water Reactors (PWR) and Critical Experiments. The results were used to determine a set of 95/95 (probability/confidence) tolerance limits for application in the calculation of key PWR physics parameters. This effort has also successfully demonstrated SCE's ability to use the CASMO-3/SIMULATE-3 computer program package.

Based on the analyses and results contained in this report, SCE concludes that the CASMO-3/SIMULATE-3 methodology applies to all steady-state PWR reactor physics calculations. The accuracy of this methodology is sufficient for use in licensing applications, PWR reload physics analysis, safety analysis inputs, startup predictions, core physics databooks, and, reactor protection system and monitoring system setpoint updates.

SECTION 7

REFERENCES

1. Malte Edenius, Ake Ahlin, Bengt H. Forssen, "CASMO-3, A Fuel Assembly Burnup Program, User's Manual, Version 4.4" STUDSVIK/NFA - 89/3, Studsvik Energiteknik AB, Sweden, November 1989.

2. Malte Edenius, Clas Gragg, "CASLIB User's Manual, Version 1.3, STUDSVIK/NFA - 89/13, Studsvik Energiteknik AB, Sweden, November 1989.

3. Malte Edenius, Ake Ahlin, "MCBURN-3, Microscopic Burnup in Burnable Absorber Rods, User's Manual" STUDSVIK/NFA - 86/26, Studsvik Energiteknik AB, Sweden, November 1989.

4. Malte Edenius, Bengt H. Forssen, "MOVEROD-3 User's Manual," STUDSVIK/NFA - 89/14, Studsvik Energiteknik AB, Sweden, November 1989.

5. K. S. Smith, J. A. Umbarger, D. M. Ver Planck, "TABLES-3, Library Preparation Code for SIMULATE-3, User's Manual, Version 3.0," STUDSVIK/SOA - 89/05, Studsvik of America,Inc., November 1989.

6. K. S. Smith, J. A. Umbarger, D. M. Ver Planck, "SIMULATE-3, Advanced Three-Dimensional Two-Group Reactor Analysis Code, User's Manual, Version 3.0," STUDSVIK/SOA - 89/03, Studsvik of America, Inc., November 1989.

7. "CASMO-3G Validation," YAEC-1363A, Yankee Atomic Electric Company, 1988.

8. "SIMULATE-3 Validation and Verification," YAEC-1659A, Yankee Atomic Electric Company, 1988.

9. "ESCORE: The EPRI Steady-State Core Reload Evaluator Code; General Description," EPRI NP-5100-A, May 1990.

10. Updated Final Safety Analysis Report, San Onofre Nuclear Generating Station, Unit 1, Revision 1.

11. Updated Final Safety Analysis Report, San Onofre Nuclear Generating Station, Units 2&3, Revision 6.

12. Final Safety Analysis Report, Arkansas Nuclear One - Unit 2, Revision 0.

13. "INCORE3 User's Manual," Westinghouse Electric Corporation, October 1988.

14. "CECOR 2.0 General Description, Methods, and Algorithms," NPSD-103-P, Combustion Engineering, Inc., June 1980.

15. ANSI N15.15-1974, "American National Standard: Assessment of the Assumption of Normality (Employing Individual Observed Values)," October 1973.

16. Factors for One-Sided Tolerance Limits and for Variables Sampling Plans, D. B. Owen, Sandia Corporation Monograph, SCR-607, March 1963.

17. "Statistical Combination of Uncertainties, Part II," CEN-283(S)-P, Combustion Engineering, Inc., October 1984.

18. Probability and Statistics for Engineers and Scientists, Walpole and Myers, Macmillan Publishing Company, pp. 358-361, 1972.

19. "Urania-Gadolinia: Nuclear Model Development and Critical Experiment Benchmark," DOE/ET/34212-41, April 1984.

20. Reference 18, pp. 154-158.

21. Letter, USNRC to G. Papanic, Jr. (YAEC), "Acceptance for Referencing of Topical Report YAEC-1363, CASMO-3G Validation," March 21, 1990.

22. Letter, USNRC to G. Papanic, Jr. (YAEC), "Acceptance for Referencing of Topical Report YAEC-1659, SIMULATE-3, Validation and Verification," February 20, 1990.

23. Letter, USNRC to C. R. Lehmann (PP&L), "Acceptance for Referencing of Licensing Topical Report EPRI-NP-5100, ESCORE - The EPRI Steady-State Core Reload Evaluation Code: General Description," May 23, 1990.